Control and Stability of DFIG-based Wind Turbine Systsm

Chao Wu

Postdoc
Email: cwu@et.aau.dk

AALBORG UNIVERSITY
DENMARK

WinGrid

Outline

1. Research background
2. Stability analysis of DFIG-AC system
3. Stability enhancement of DFIG-AC system
4. Control of DFIG-DC system
5. Conclusion

Research Background

- **Reported statility issues of DFIG based wind farm**

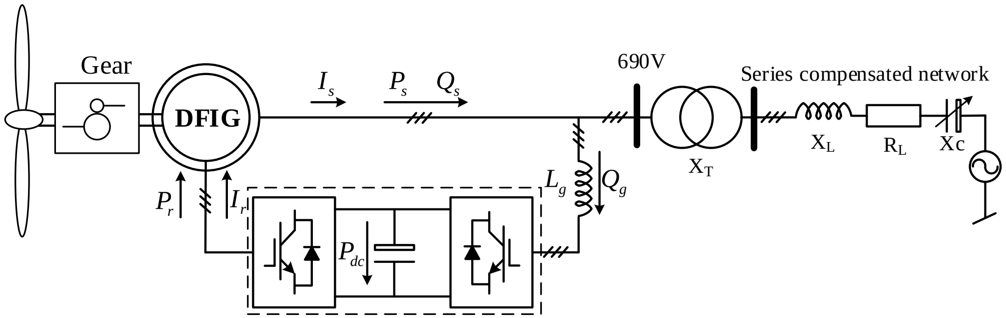

DFIG system connected to the series compensated weak network.

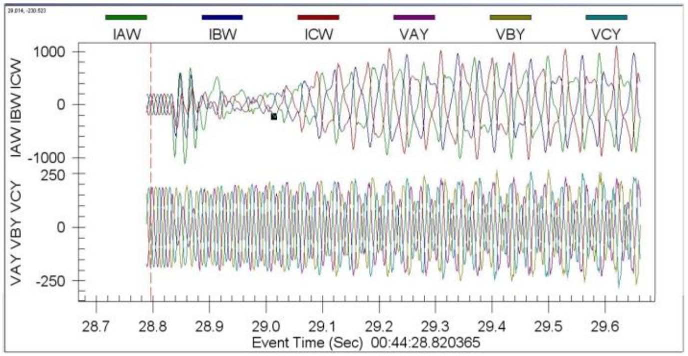

2009, South Texas[1], **20 Hz**, DFIG wind farm.

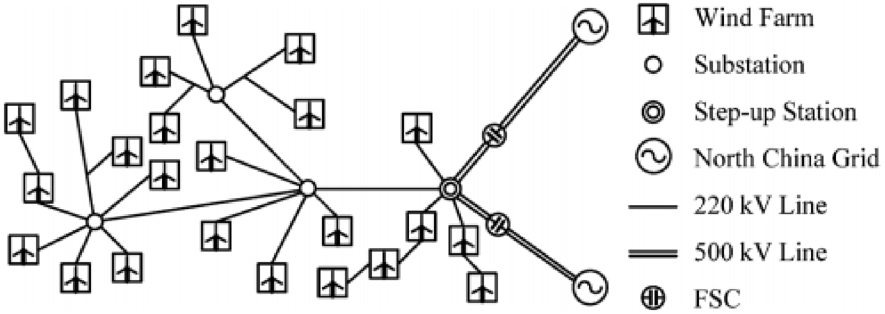

Wind farms and the series-compensated system [2].

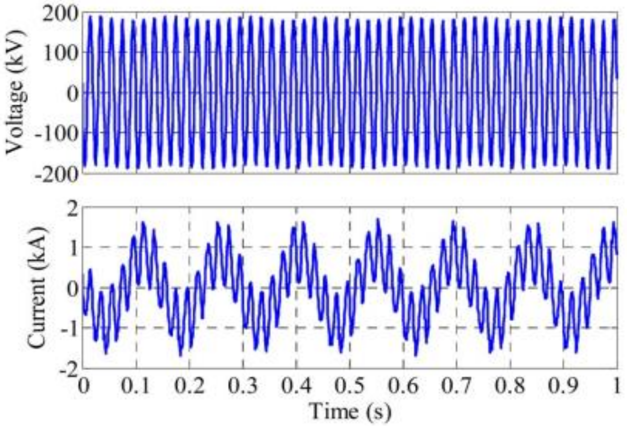

2012, North China[2], **6~8 Hz**, DFIG wind farm.

[1] J. Adams, C. Carter and S. Huang, "ERCOT experience with Sub-synchronous Control Interaction and proposed remediation," *PES T&D 2012*, Orlando, FL, 2012, pp. 1-5

[2] L. Wang,et al, "Investigation of SSR in practical DFIG-based wind farms connected to a series-compensated power system," *IEEE Trans. Power Systems*, vol. 30, no. 5, pp. 2772-2779, Sept. 2015

Stability analysis of DFIG-AC system

Stability analysis of DFIG-AC system

◆ Overview of stability analysis methods

Stability analysis methods

- **EMT simulation** → Cannot reflect the internal characteristics of the system; Unable to provide basis for system design.
- **State space model** → Widely used in current system stability analysis; All the specific information are necessary in the system; The entire system needs to be re-analyzed when the system changes.
- **Impedance model** → Only need the impedance characteristics of the input/output of each link of the system; It can be obtained through analytical models, simulation or experiments, etc.

[1] J. Sun, "Small-Signal Methods for AC Distributed Power Systems–A Review," in IEEE Transactions on Power Electronics, vol. 24, no. 11, pp. 2545-2554, Nov. 2009.
[2] J. Sun, etc. Renewable Energy Transmission by HVDC Across The Continent: System Challenges and Opportunities, CSEE JOURNAL OF POWER AND ENERGY SYSTEMS, VOL. 3, NO. 4, DECEMBER 2017

Stability analysis of DFIG-AC system

◆ Impedance model of single DFIG

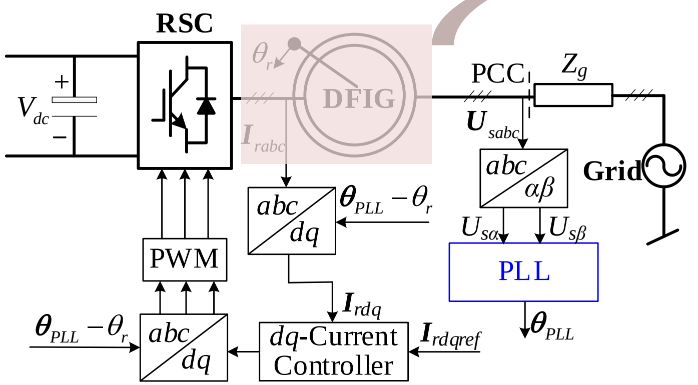

Topology of DFIG connected to three phase AC grid.

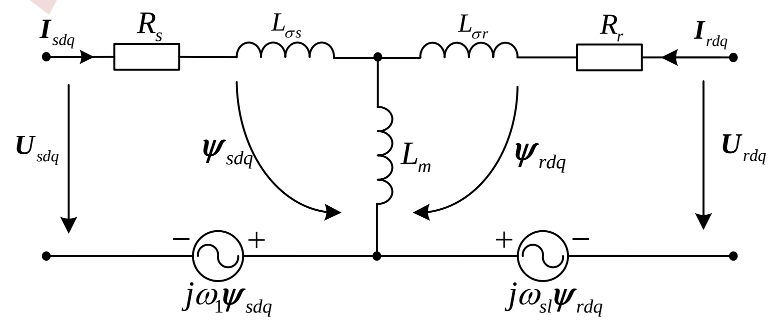

Equivalent circuit of DFIG in the synchronous *dq* frame.

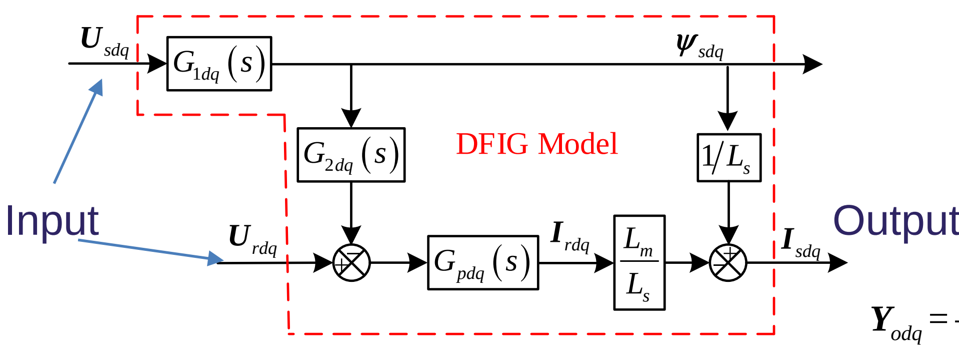

Model of DFIG in synchronous *dq* frame.

$$G_{1dq}(s)=\frac{1}{s+j\omega_1},\ G_{2dq}(s)=\frac{L_m}{L_s}(s+j\omega_{sl})$$

$$G_{pdq}(s)=\frac{1}{\sigma L_r s+R_r+j\omega_{sl}\sigma L_r}$$

$$I_{sdq}=Y_{odq}U_{sdq}-\frac{L_m}{L_s}G_{pdq}(s)U_{rdq}$$

$$Y_{odq}=\frac{1}{L_s}G_{1dq}(s)+\frac{L_m}{L_s}G_{1dq}(s)G_{2dq}(s)G_{pdq}(s) \qquad Y_{o\alpha\beta}=Y_{odq}(s-j\omega_1)$$

❑ **The single DFIG is a symmetrical plant, which shows the inductive-resistive characteristic in the high frequency.**

Stability analysis of DFIG-AC system

◆ Impedance model of RSC+DFIG

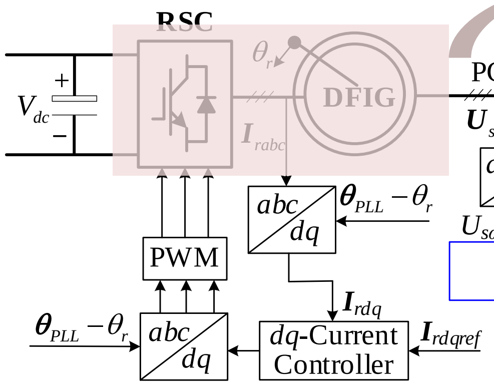

Topology of DFIG connected to three phase AC grid.

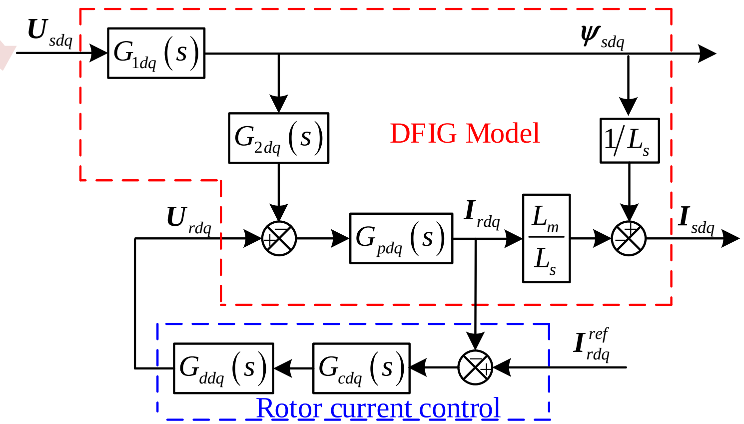

Model of RSC+DFIG in dq frame without considering PLL effect.

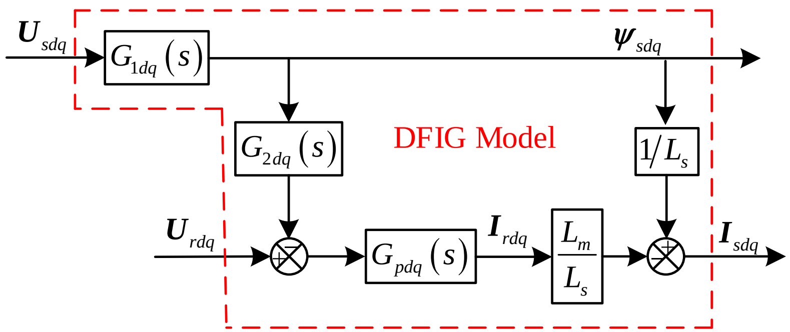

Model of DFIG in synchronous dq frame.

$$G_{cdq}(s)=\frac{k_{pi}s+k_{ii}}{s} \qquad G_{ddq}(s)=e^{-T_d s}$$

$$\boldsymbol{I}_{sdq}=\boldsymbol{Y}_{cdq}\boldsymbol{U}_{sdq}-\boldsymbol{G}_{ircdq}(s)\boldsymbol{I}_{rdq}^{ref}$$

$$\boldsymbol{Y}_{cdq}=G_{1dq}(s)/L_s+\frac{L_m}{L_s}\frac{G_{1dq}(s)G_{2dq}(s)G_{pdq}(s)}{1+G_{cdq}(s)G_{ddq}(s)G_{pdq}(s)}$$

$$\boldsymbol{Y}_{c\alpha\beta}=\boldsymbol{Y}_{cdq}(s-j\omega_1)$$

❑ **The RSC+DFIG is still a symmetrical plant, which can be analyzed as SISO system.**

Stability analysis of DFIG-AC system

◆ Impedance model considering PLL effect

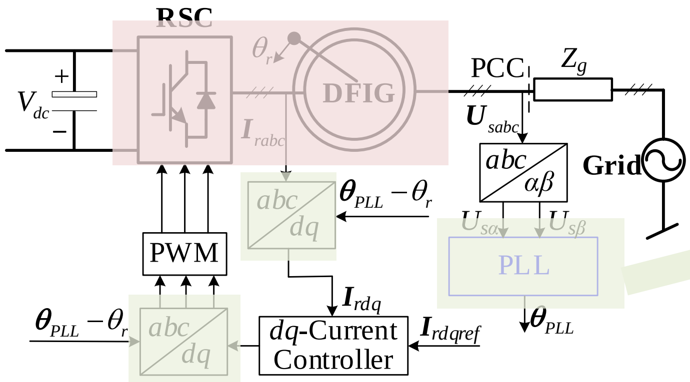

Topology of DFIG connected to three phase AC grid.

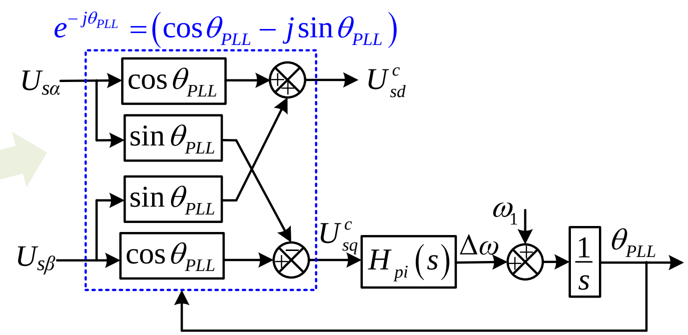

Conventional SRF-PLL.

Control frame → $\boldsymbol{U}_{sdq}^{c}=e^{-j\theta_{PLL}}\boldsymbol{U}_{s\alpha\beta}$ ← **Real frame**

Transformation formula: $\begin{bmatrix}U_{sd}^c\\U_{sq}^c\end{bmatrix}=\begin{bmatrix}\cos\theta_{PLL} & \sin\theta_{PLL}\\-\sin\theta_{PLL} & \cos\theta_{PLL}\end{bmatrix}\begin{bmatrix}U_{s\alpha}\\U_{s\beta}\end{bmatrix}$

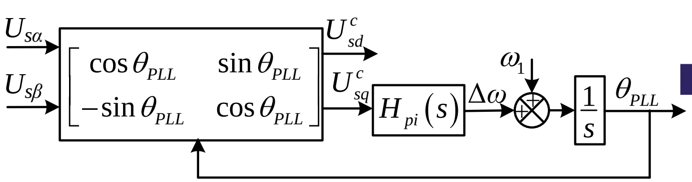

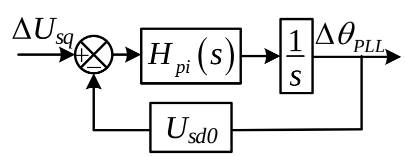

Scalar

$$\Delta\theta_{PLL}=H_{PLL}(s)\Delta U_{sq}$$

$$H_{PLL}(s)=\frac{H_{pi}(s)}{s+U_{sd0}H_{pi}(s)}$$

❑ **The small signal model of SRF-PLL is asymmetrical and the complex vector model can not be applied directly.**

Stability analysis of DFIG-AC system

◆ Impedance model considering PLL effect

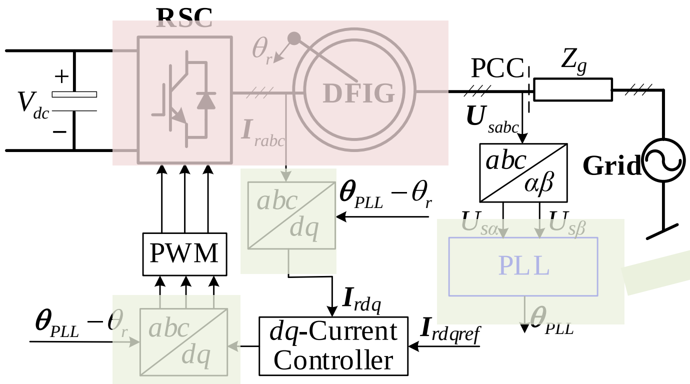

Topology of DFIG connected to three phase AC grid.

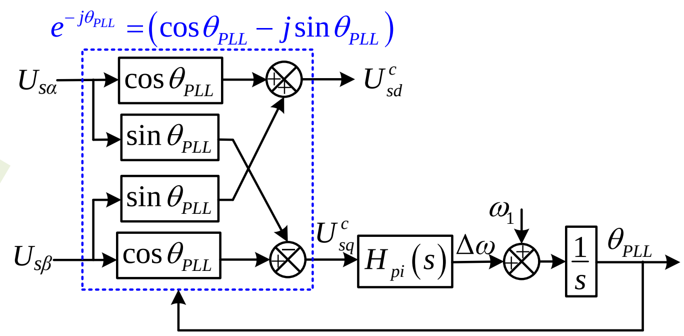

Conventional SRF-PLL.

Effect on current Park transformation

$$\boldsymbol{I}^c_{rdq} = e^{-j(\theta_{PLL}-\theta_r)}\boldsymbol{I}_{r\alpha\beta} = \left(\boldsymbol{I}_{rdq0} + \Delta\boldsymbol{I}_{rdq}\right)e^{-j\Delta\theta_{PLL}}$$

$$\approx \left(\boldsymbol{I}_{rdq0} + \Delta\boldsymbol{I}_{rdq}\right)(1 - j\Delta\theta) = \boldsymbol{I}_{rdq0} + \Delta\boldsymbol{I}_{rdq} - j\boldsymbol{I}_{rdq0}\Delta\theta_{PLL}$$

$$\Delta\boldsymbol{I}^c_{rdq} = -j\boldsymbol{I}_{rdq0}\Delta\theta + \Delta\boldsymbol{I}_{rdq} = -G^i_{PLL}(s)\Delta\boldsymbol{U}_{dq} + \Delta\boldsymbol{I}_{rdq}$$

$$G^i_{PLL}(s) = \begin{bmatrix} 0 & -I_{rq0}H_{PLL}(s) \\ 0 & I_{rd0}H_{PLL}(s) \end{bmatrix}$$

Effect on voltage Inverse Park transformation

$$\boldsymbol{U}^c_{rdq} = e^{j(\theta_{PLL}-\theta_r)}\boldsymbol{U}_{r\alpha\beta} = \left(\boldsymbol{U}_{rdq0} + \Delta\boldsymbol{U}_{rdq}\right)e^{j\Delta\theta_{PLL}}$$

$$\approx \left(\boldsymbol{U}_{rdq0} + \Delta\boldsymbol{U}_{rdq}\right)(1 + j\Delta\theta_{PLL}) = \boldsymbol{U}_{rdq0} + \Delta\boldsymbol{U}_{rdq} + j\boldsymbol{U}_{rdq0}\Delta\theta_{PLL}$$

$$\Delta\boldsymbol{U}^c_{rdq} = j\boldsymbol{U}_{rdq0}\Delta\theta + \Delta\boldsymbol{U}_{rdq} = G^d_{PLL}(s)\Delta\boldsymbol{U}_{sdq} + \Delta\boldsymbol{U}_{rdq}$$

$$G^d_{PLL}(s) = \begin{bmatrix} 0 & -U_{rq0}H_{PLL}(s) \\ 0 & U_{rd0}H_{PLL}(s) \end{bmatrix}$$

- ❑ **The small signal model of SRF-PLL is asymmetrical and the complex vector model can not be applied directly.**

Stability analysis of DFIG-AC system

◆ Impedance model considering PLL effect

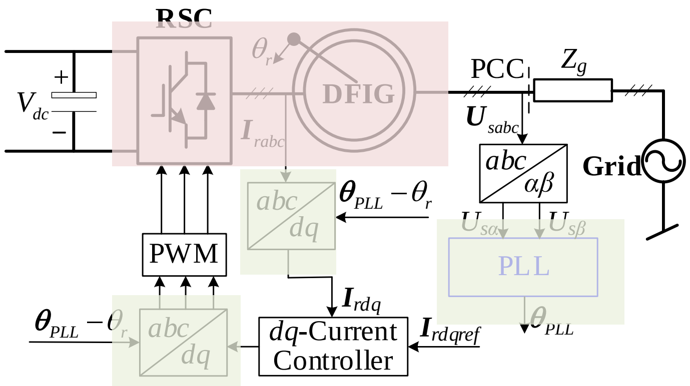

Topology of DFIG connected to three phase AC grid.

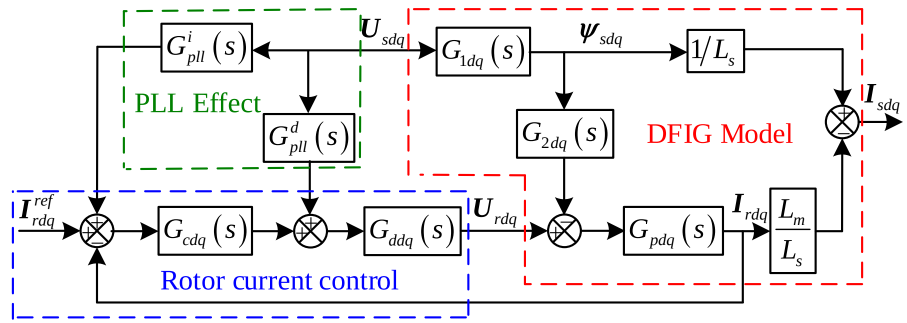

Model of RSC+DFIG in *dq* frame considering PLL effect.

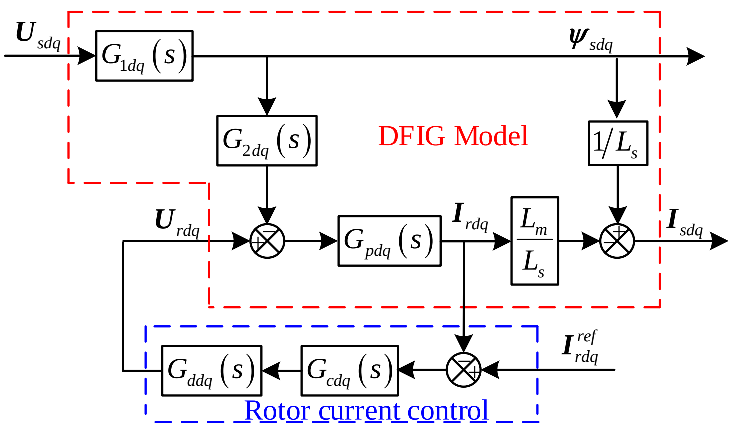

Model of RSC+DFIG in dq frame without considering PLL effect.

$$I_{sdq} = Y_{cpdq} U_{sdq} - G_{ircpdq}(s) I_{rdq}^{ref}$$

$$Y_{cpdq} = G_{1dq}(s)/L_s + \frac{L_m}{L_s}\frac{G_{pdq}(s)G_{2dq}(s)G_{1dq}(s)}{1+G_{cdq}(s)G_{ddq}(s)G_{pdq}(s)}$$

$$-\frac{L_m}{L_s}\frac{G_{pdq}(s)G_{ddq}(s)\left(G_{cdq}(s)G_{pll}^{i}(s)+G_{pll}^{d}(s)\right)}{1+G_{cdq}(s)G_{ddq}(s)G_{pdq}(s)}$$

$$Y_{cpdq} = \begin{bmatrix} Y_{cp11} & Y_{cp12} \\ 0 & Y_{cp22} \end{bmatrix}$$

❑ **The RSC+DFIG becomes asymmetrical plant due to the PLL effect, which should be analyzed by MIMO method.**

Stability analysis of DFIG-AC system

◆ **Relationship between different impedance models**

dq scalar impedance → dq sequence impedance → αβ sequence impedance

dq scalar impedance model

$$\begin{bmatrix} U_d(s) \\ U_q(s) \end{bmatrix} = \begin{bmatrix} Z_{dd} & Z_{dq} \\ Z_{qd} & Z_{qq} \end{bmatrix} \begin{bmatrix} I_d(s) \\ I_q(s) \end{bmatrix}$$

$$\boldsymbol{U}_{dq}(s) = U_d(s) + jU_q(s)$$
$$\boldsymbol{I}_{dq}(s) = I_d(s) + jI_q(s)$$

$$\boldsymbol{Z}_{dq}(s) = \frac{\boldsymbol{U}_{dq}(s)}{\boldsymbol{I}_{dq}(s)}$$

If the impedance is symmetric

$$\boldsymbol{Z}_{dq}(s) = Z_{dd} - jZ_{dq}$$

→

$\alpha\beta$(phase) sequence impedance model

$$\boldsymbol{Z}_{\alpha\beta}(s) = \boldsymbol{Z}_{dq}(s - j\omega_1) = \frac{u_a}{i_a}$$

Stability analysis of DFIG-AC system

◆ **Relationship between different impedance models**

If the impedance is asymmetric, how to transfer the *dq* scalar impedance to sequence impedance?

$$\begin{bmatrix} U_d(s) \\ U_q(s) \end{bmatrix} = \begin{bmatrix} 1 & 1 \\ -j & j \end{bmatrix} \begin{bmatrix} \boldsymbol{U}_p(s) \\ \boldsymbol{U}_n(s) \end{bmatrix} \quad \begin{bmatrix} \boldsymbol{U}_p(s) \\ \boldsymbol{U}_n(s) \end{bmatrix} = \frac{1}{2} \begin{bmatrix} 1 & j \\ 1 & -j \end{bmatrix} \begin{bmatrix} U_d(s) \\ U_q(s) \end{bmatrix} \quad \begin{bmatrix} I_d(s) \\ I_q(s) \end{bmatrix} = \begin{bmatrix} 1 & 1 \\ -j & j \end{bmatrix} \begin{bmatrix} \boldsymbol{I}_p(s) \\ \boldsymbol{I}_n(s) \end{bmatrix}$$

$$\begin{bmatrix} \boldsymbol{U}_p(s) \\ \boldsymbol{U}_n(s) \end{bmatrix} = \frac{1}{2} \begin{bmatrix} 1 & j \\ 1 & -j \end{bmatrix} \begin{bmatrix} Z_{dd} & Z_{dq} \\ Z_{qd} & Z_{qq} \end{bmatrix} \begin{bmatrix} 1 & 1 \\ -j & j \end{bmatrix} \begin{bmatrix} \boldsymbol{I}_p(s) \\ \boldsymbol{I}_n(s) \end{bmatrix} \longrightarrow \begin{bmatrix} \boldsymbol{U}_p(s) \\ \boldsymbol{U}_n(s) \end{bmatrix} = \begin{bmatrix} \boldsymbol{Z}_{dd} & \boldsymbol{Z}_{dq} \\ \boldsymbol{Z}_{qd} & \boldsymbol{Z}_{qq} \end{bmatrix} \begin{bmatrix} \boldsymbol{I}_p(s) \\ \boldsymbol{I}_n(s) \end{bmatrix}$$

dq sequence impedance model

Transformation from *dq* sequence to phase sequence model

$$\begin{bmatrix} \boldsymbol{U}_p(s) \\ \boldsymbol{U}_n(s) \end{bmatrix} = \begin{bmatrix} \boldsymbol{Z}_{dd} & \boldsymbol{Z}_{dq} \\ \boldsymbol{Z}_{qd} & \boldsymbol{Z}_{qq} \end{bmatrix} \begin{bmatrix} \boldsymbol{I}_p(s) \\ \boldsymbol{I}_n(s) \end{bmatrix} \xrightarrow[\boldsymbol{I}_p = e^{-j\theta}\boldsymbol{I}_{\alpha\beta},\ \boldsymbol{I}_n = e^{j\theta}\boldsymbol{I}^*_{\alpha\beta}]{\boldsymbol{U}_p = e^{-j\theta}\boldsymbol{U}_{\alpha\beta},\ \boldsymbol{U}_n = e^{j\theta}\boldsymbol{U}^*_{\alpha\beta}} \begin{bmatrix} \boldsymbol{U}_{\alpha\beta} \\ e^{j2\theta}\boldsymbol{U}^*_{\alpha\beta} \end{bmatrix} = \begin{bmatrix} \boldsymbol{Z}_{dd}(s-j\omega_1) & \boldsymbol{Z}_{dq}(s-j\omega_1) \\ \boldsymbol{Z}_{qd}(s-j\omega_1) & \boldsymbol{Z}_{qq}(s-j\omega_1) \end{bmatrix} \begin{bmatrix} \boldsymbol{I}_{\alpha\beta} \\ e^{j2\theta}\boldsymbol{I}^*_{\alpha\beta} \end{bmatrix}$$

A. Rygg, M. Molinas, C. Zhang, and X. Cai, “A modified sequence domain impedance definition and its equivalence to the *dq*-domain impedance definition for the stability analysis of ac power electronic systems,” *IEEE J. Emerg. Sel. Topics Power Electron.*, vol. 4, no. 4, pp. 1382–1396, Dec.2016.

Stability analysis of DFIG-AC system

◆ Validation of impedance model

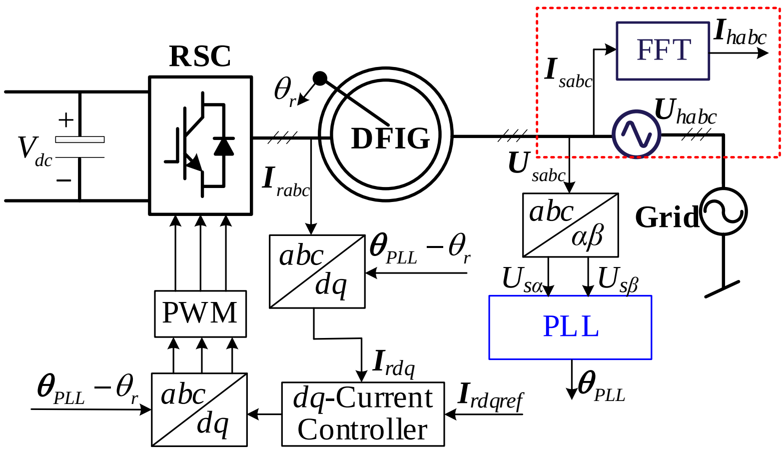

Topology of DFIG connected to three phase AC grid.

Table Parameters of DFIG used in simulation

Parameter	Symbol	Value
Rated Voltage	U_s	690 V
Rated Power	P_s	1.5 MW
Rtaed Frequency	f_1	50 Hz
Pole Pairs	n_p	2
Dc-link Voltage	V_{dc}	1150 V
Stator Leakage	L_{ls}	0.060 mH
Rotor Leakage	L_{lr}	0.083 mH
Mutual Inductance	L_{ms}	2.95 mH
Stator Resistance	R_s	0.0024 Ω
Rotor Resistance	R_r	0.0020 Ω
Sampling Period	T_s	0.1 ms
Turns Ratio	K_e	0.33
Base Inductance	L_{base}	1mH

Frequency scan results

$$Z_h = \frac{U_{ha}}{I_{ha}}$$

Control parameters

PLL parameters

$$H_{pi}(s)=k_{pp}+\frac{k_{pi}}{s}=1+\frac{10}{s}$$

Current control parameters

$$G_c(s)=k_{ip}+\frac{k_{ii}}{s}=5+\frac{500}{s}$$

Control delay

$$G_d(s)=e^{-0.00015s}$$

Stability analysis of DFIG-AC system

◆ Validation of admittance model

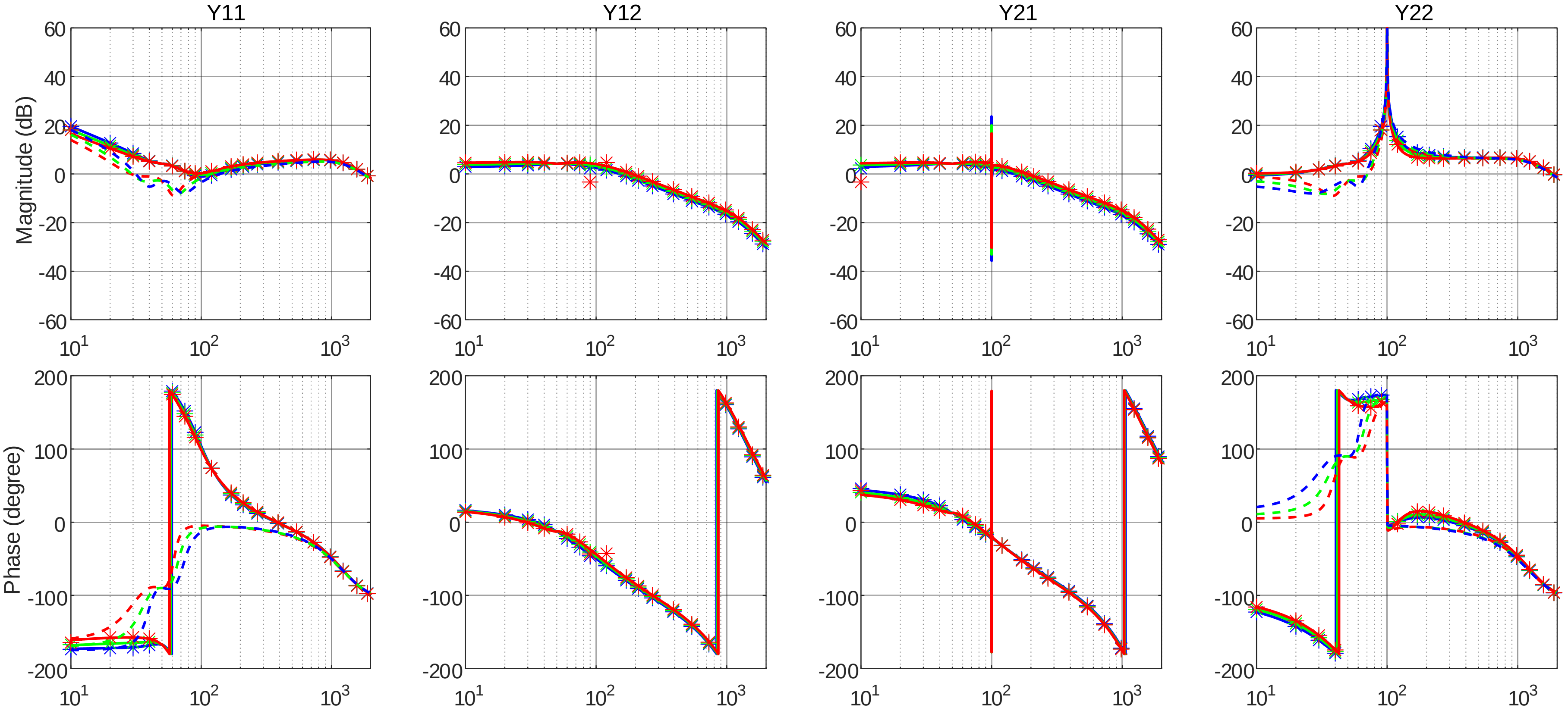

Model validation by frequency scan, the solid lines are calculated by the admittance matrix , the dotted lines are calculated by the simplified admittance matrix, the points are obtained by simulation results. Red represents ω_r=40Hz, green represents ω_r =50Hz, red represents ω_r =60Hz.

Stability analysis of DFIG-AC system

◆ Generalized Nyquist Criterion (GNC)

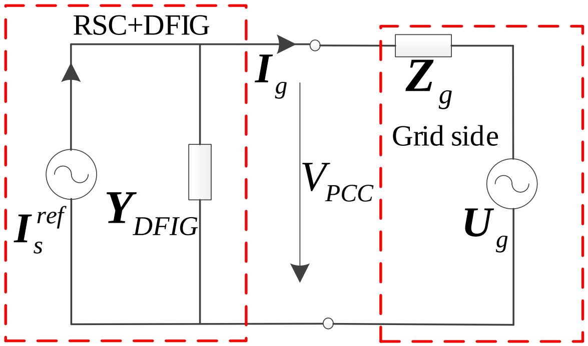

Grid impedance matrix $\boldsymbol{Z}_g = \begin{bmatrix} sL_g & 0 \\ 0 & (s - j2\omega_1)L_g \end{bmatrix}$

DFIG impedance matrix $\boldsymbol{Y}_{DFIG} = \begin{bmatrix} Y_{DFIG11} & Y_{DFIG12} \\ Y_{DFIG21} & Y_{DFIG22} \end{bmatrix}$

Current injected to grid $\boldsymbol{I}_g = \left(\boldsymbol{I}_s^{ref} - \boldsymbol{Y}_{DFIG}\boldsymbol{U}_g\right) \cdot \dfrac{1}{\boldsymbol{I} + \boldsymbol{Y}_{DFIG} \cdot \boldsymbol{Z}_g}$

To guarantee the stability of the system, all the poles of the denominator should be on the left half plan. In order to avoid the complicated process of solving the characteristic equation, the GNC is used.

GNC $\det\left(\boldsymbol{I} + \boldsymbol{Y}_{DFIG} \cdot \boldsymbol{Z}_g\right) = 0$

The two eigenvalues of the matrix can be used for assessing the stability by checking whether the eigenvalues will encircle (-1,0).

Stability analysis of DFIG-AC system

◆ Generalized Nyquist Criterion (GNC)

Grid impedance matrix $\boldsymbol{Z}_g = \begin{bmatrix} sL_g & 0 \\ 0 & (s - j2\omega_1)L_g \end{bmatrix}$ GNC $\det\left(\boldsymbol{I} + \boldsymbol{Y}_{DFIG} \cdot \boldsymbol{Z}_g\right) = 0$

◆ Control delay effect

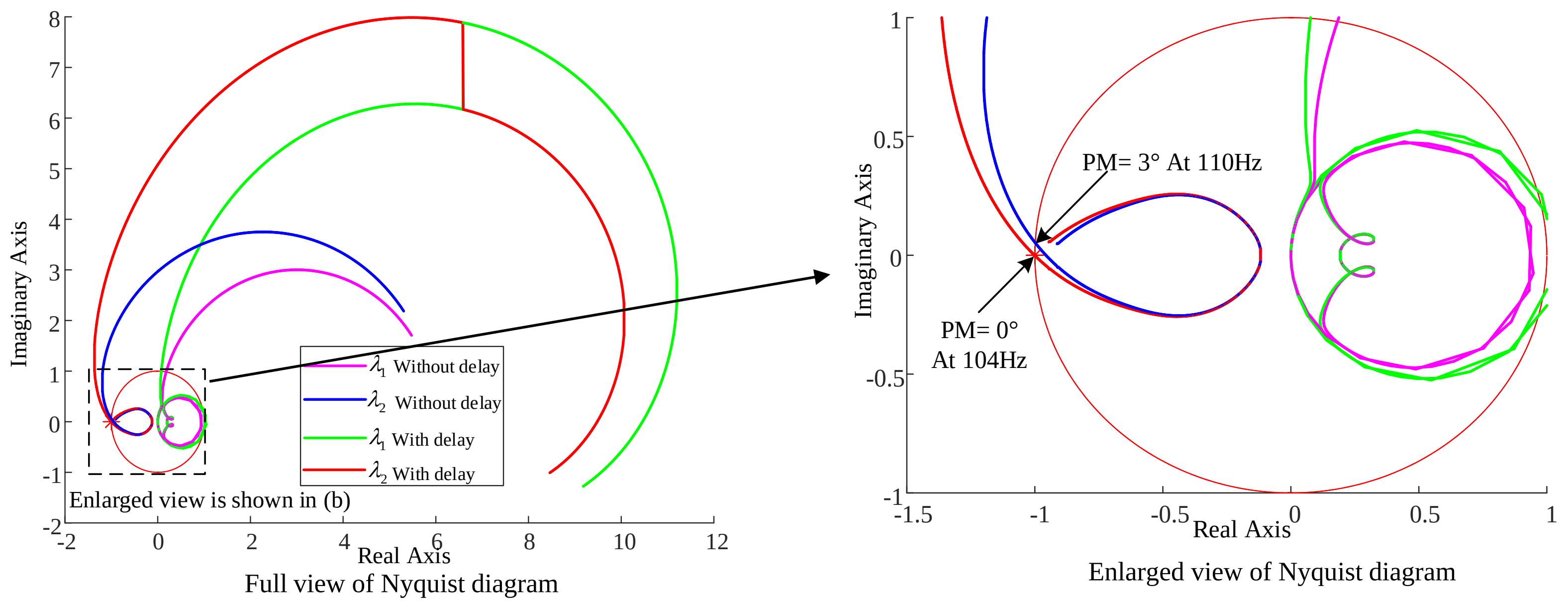

Nyquist diagram with or without control delay.

Remarks: The locus of eigenvalue λ_1 is always located at the right side of eigenvalue λ_2, which cannot encircle the (-1,0) point. Thus, the locus of eigenvalue λ_1 will be omitted in order to make the Nyquist diagram more simple and clear in the next Nyquist diagrams

Stability analysis of DFIG-AC system

◆ Generalized Nyquist Criterion (GNC)

Grid impedance matrix $\mathbf{Z}_g = \begin{bmatrix} sL_g & 0 \\ 0 & (s - j2\omega_1)L_g \end{bmatrix}$ GNC $\det\left(\mathbf{I} + \mathbf{Y}_{DFIG} \cdot \mathbf{Z}_g\right) = 0$

◆ PLL parameters

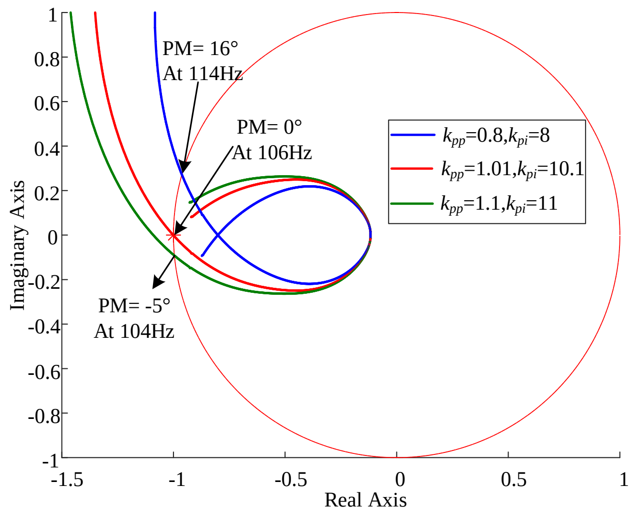

Nyquist diagram with different PLL parameters

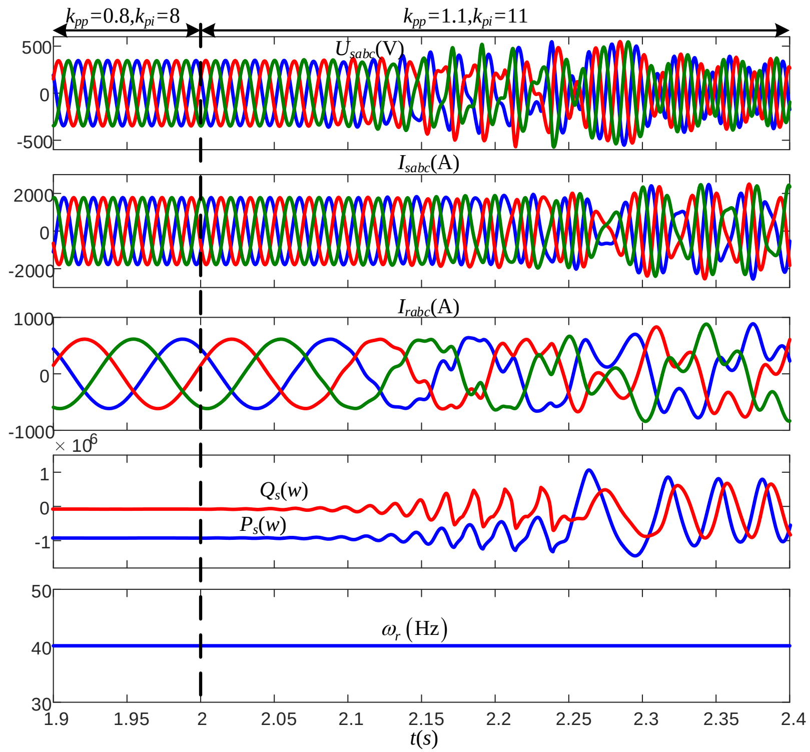

Simulation result of DFIG with k_{pp}=1.1,k_{pi}=11.

Remarks: High PLL bandwidth will cause instability of DFIG system under weak grid

Stability analysis of DFIG-AC system

◆ Generalized Nyquist Criterion (GNC)

Grid impedance matrix $\boldsymbol{Z}_g = \begin{bmatrix} sL_g & 0 \\ 0 & (s - j2\omega_1)L_g \end{bmatrix}$ GNC $\det\left(\boldsymbol{I} + \boldsymbol{Y}_{DFIG} \cdot \boldsymbol{Z}_g\right) = 0$

◆ Rotor speed

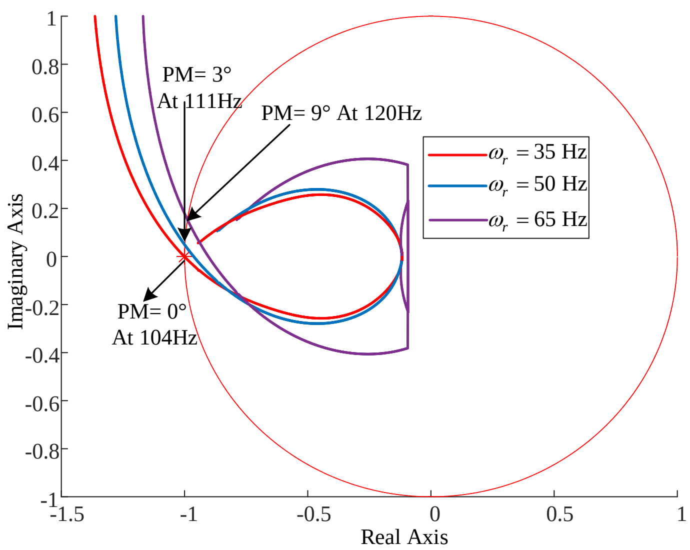

Generalized nyquist diagram with different rotor speed.

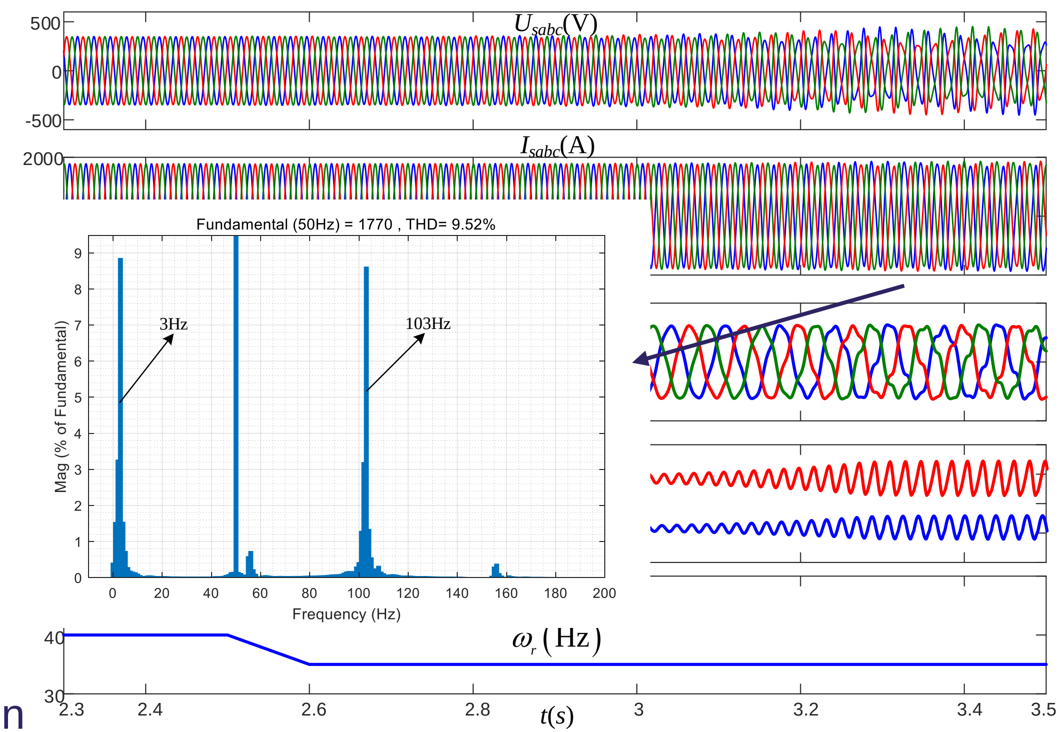

Simulation result of DFIG with rotor speed variation.

Remarks: rotor speed also has effect on the system stabilty

Stability analysis of DFIG-AC system

◆ **Conclusion**

❑ The conventional SRF-PLL will introduce a asymmetric matrix to the impedance, which will make DFIG system more complicated.

❑ The dq impedance and sequence impedance can be converted to each other, which are essentially equivalent.

❑ The impedance results would be wrong without considering the PLL effect, which might cause a wrong stability assessment.

❑ The Generalized Nyquist Criterion can be applied for accurate stability analysis. However, it is only based on the figure and difficult to guide the parameter design.

Stability enhancement of DFIG-AC system

Stability enhancement of DFIG-AC system

◆ Small signal of conventional SRF-PLL

$$e^{-j\theta_{PLL}} = \left(\cos\theta_{PLL} - j\sin\theta_{PLL}\right)$$

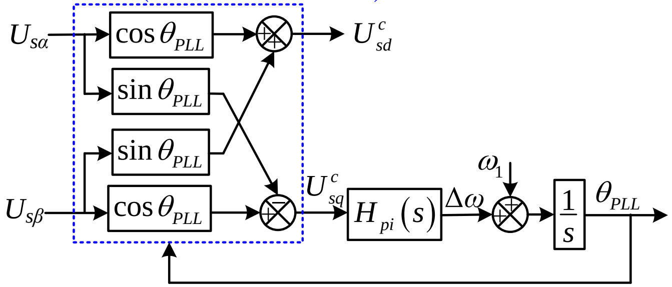

Conventional SRF-PLL.

Characteristic of SRF-PLL

- ❑ The obtained orientation angle θ is a real number.
- ❑ Only control the *q*-axis voltage to be zero, without controlling the *d*-axis voltage.

Control frame → $\boldsymbol{U}^c_{sdq} = e^{-j\theta_{PLL}}\boldsymbol{U}_{s\alpha\beta}$ ← **Real frame**

Transformation formula:

$$\begin{bmatrix} U^c_{sd} \\ U^c_{sq} \end{bmatrix} = \begin{bmatrix} \cos\theta_{PLL} & \sin\theta_{PLL} \\ -\sin\theta_{PLL} & \cos\theta_{PLL} \end{bmatrix} \begin{bmatrix} U_{s\alpha} \\ U_{s\beta} \end{bmatrix}$$

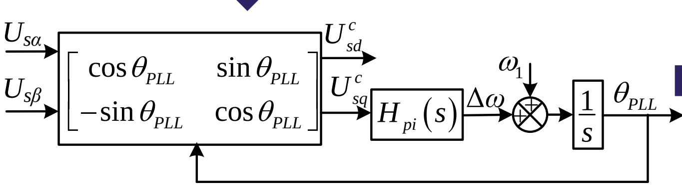

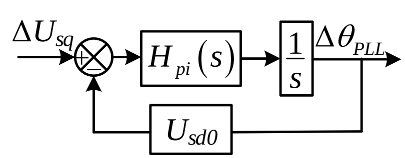

Scalar

$$\Delta\theta_{PLL} = H_{PLL}(s)\Delta U_{sq}$$

$$H_{PLL}(s) = \frac{H_{pi}(s)}{s + U_{sd0}H_{pi}(s)}$$

- ❑ **The small signal model of SRF-PLL is asymmetrical and the complex vector model can not be applied directly.**

Source: D. Yang, X. Wang, F. Blaabjerg, etc, "Complex-Vector PLL for Enhanced Synchronization with Weak Power Grids," *2018 IEEE 19th Workshop on Control and Modeling for Power Electronics (COMPEL)*, Padua, 2018, pp. 1-6.

Stability enhancement of DFIG-AC system

◆ Small signal of symmetrical PLL

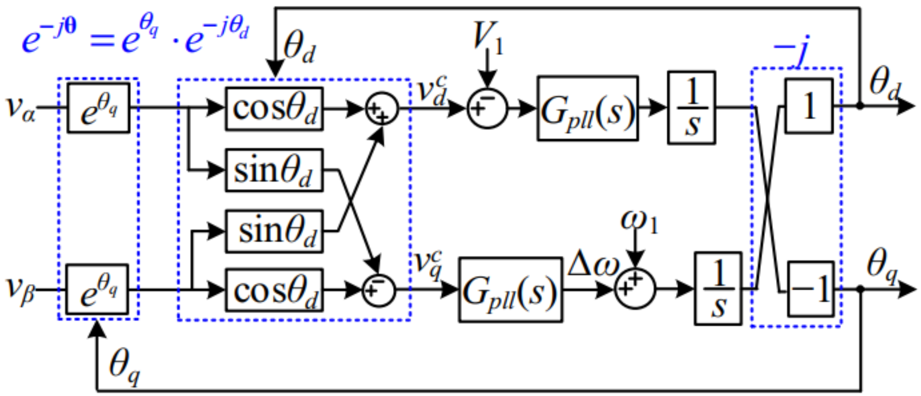

Structure of symmetrical PLL.

Characteristic of symmetrical PLL

- ❑ **The obtained orientation angle $\boldsymbol{\theta}$ is a complex number, which contains two terms θ_d *and* θ_q, $\boldsymbol{\theta} = \theta_d + j\theta_q$**
- ❑ **Not only control the *q*-axis voltage to be zero, but also control the *d*-axis voltage to a rated value.**

$$\boldsymbol{v}_{dq}^c = e^{-j\boldsymbol{\theta}} \cdot \boldsymbol{v}_{\alpha\beta} = e^{-j(\theta_d + j\theta_q)} \cdot \boldsymbol{v}_{\alpha\beta}$$

Transformation formula:

$$\begin{bmatrix} v_d^c \\ v_q^c \end{bmatrix} = e^{\theta_q} \begin{bmatrix} \cos\theta_d & \sin\theta_d \\ -\sin\theta_d & \cos\theta_d \end{bmatrix} \begin{bmatrix} v_\alpha \\ v_\beta \end{bmatrix}$$

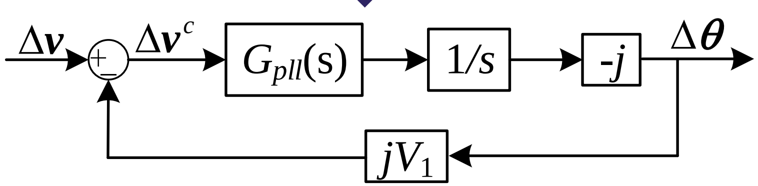

$$\Delta\boldsymbol{\theta} = -j\frac{G_{pll}(s)}{s + V_1 G_{pll}(s)} \Delta\boldsymbol{v}$$

Vector

- ❑ **The small signal of angle $\boldsymbol{\theta}$ is related to small signal of voltage vector, which means the small siganl model is symmetrical and the complex vector model can be applied.**

Source: D. Yang, X. Wang, F. Liu, K. Xin, Y. Liu and F. Blaabjerg, "Symmetrical PLL for SISO Impedance Modeling and Enhanced Stability in Weak Grids," in IEEE Transactions on Power Electronics, vol. 35, no. 2, pp. 1473-1483, Feb. 2020.

Stability enhancement of DFIG-AC system

◆ Small signal of symmetrical PLL

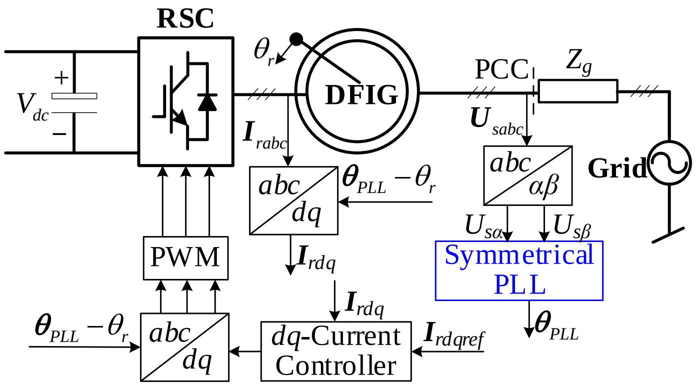

Control scheme of DFIG based on symmetrical PLL.

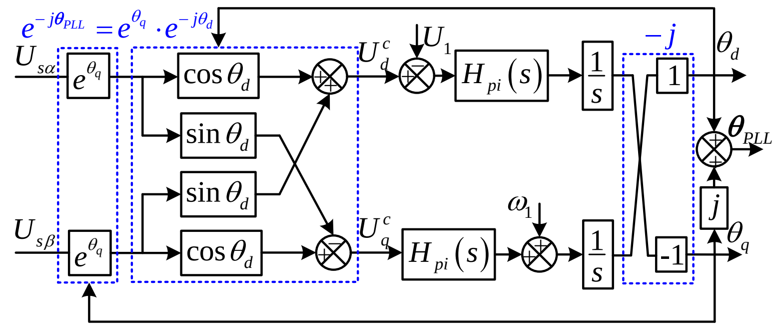

Block diagram of symmetrical PLL.

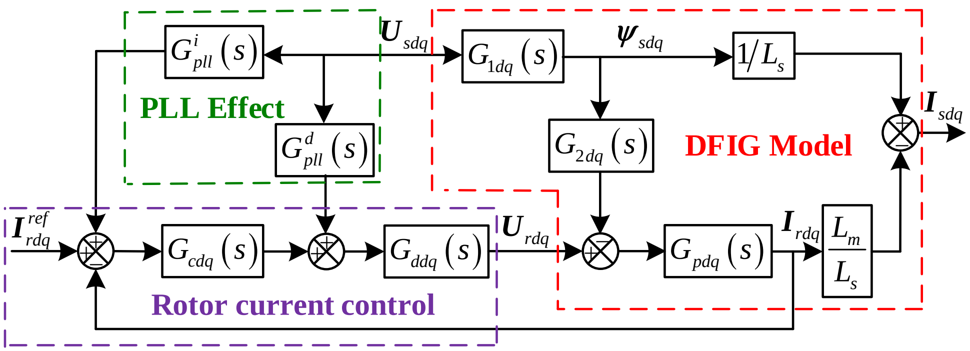

Complex transfer function of DFIG in *dq* frame considering PLL.

$$G_{1dq}(s)=\frac{1}{s+j\omega_1}$$

$$G_{2dq}(s)=\frac{L_m}{L_s}(s+j\omega_{sl})$$

$$G_{pdq}(s)=\frac{1}{\sigma L_r s+R_r+j\omega_{sl}\sigma L_r}$$

$$G_{pll}^{i}(s)=\frac{H_{pi}(s)\cdot I_{r1}}{s+U_1H_{pi}(s)}$$

$$G_{pll}^{d}(s)=\frac{H_{pi}(s)\cdot U_{r1}}{s+U_1H_{pi}(s)}$$

$$Y_{dq}=G_{1dq}(s)/L_s+\frac{L_m}{L_s}\frac{G_{pdq}(s)G_{2dq}(s)G_{1dq}(s)}{1+G_{cdq}(s)G_{ddq}(s)G_{pdq}(s)}-\frac{L_m}{L_s}\frac{G_{pdq}(s)G_{ddq}(s)\left(G_{cdq}(s)G_{pll}^{i}(s)+G_{pll}^{d}(s)\right)}{1+G_{cdq}(s)G_{ddq}(s)G_{pdq}(s)} \Rightarrow Y_{\alpha\beta}=Y_{dq}(s-j\omega_1)$$

Source: C. Wu, B. Hu, H. Nian, F.Blaabjerg, "Eliminating Frequency Coupling of DFIG System Using a Complex Vector PLL", APEC, 2020.

Stability enhancement of DFIG-AC system

- **Validation of admittance model**

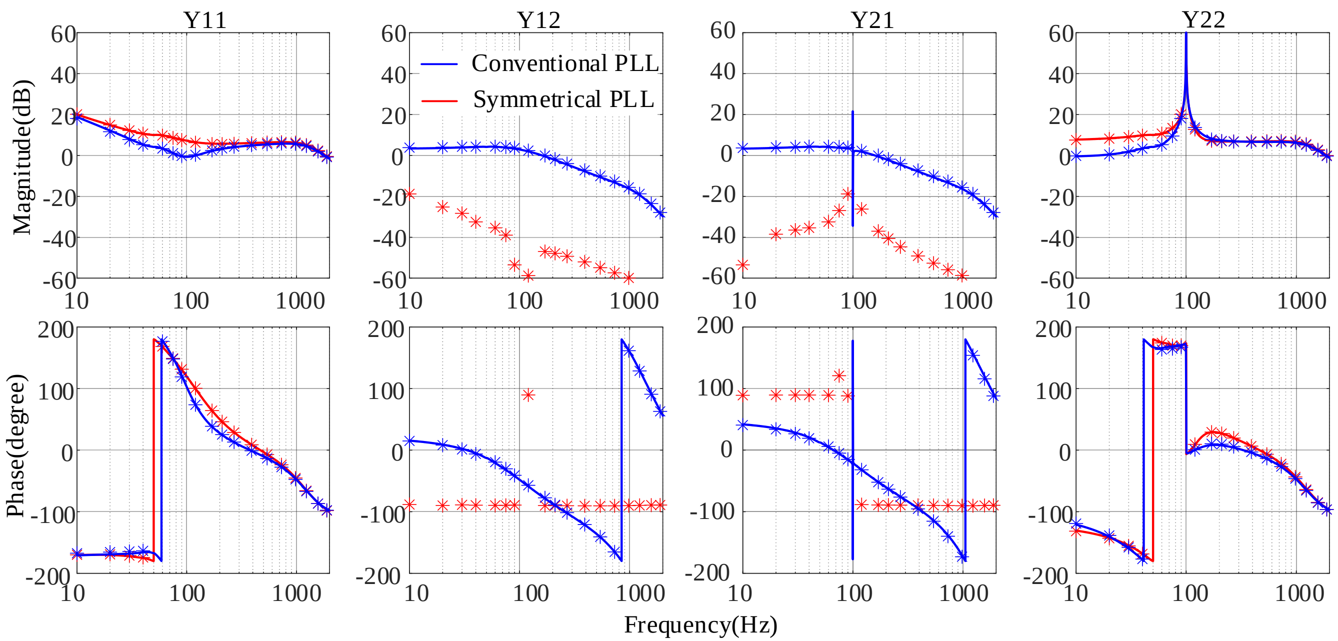

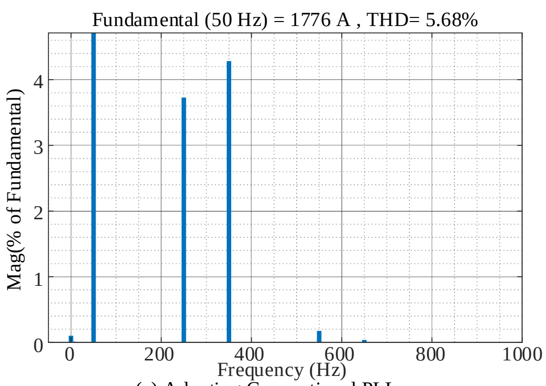

(a) Adopting Conventional PLL

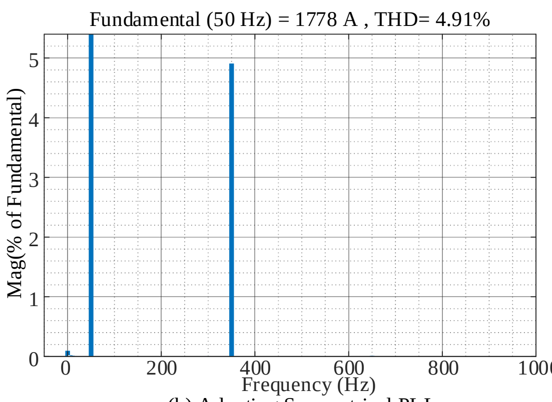

(b) Adopting Symmetrical PLL

Stability enhancement of DFIG-AC system

◆ Stability analysis of DFIG based on symmetrical PLL

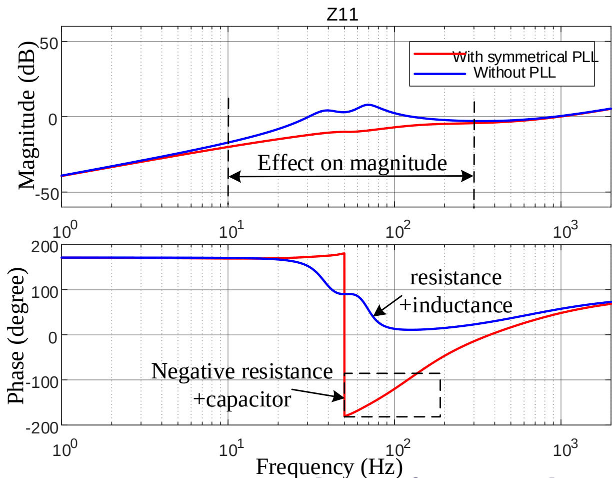

The positive sequence impedance of DFIG with symmetrical PLL and without considering PLL.

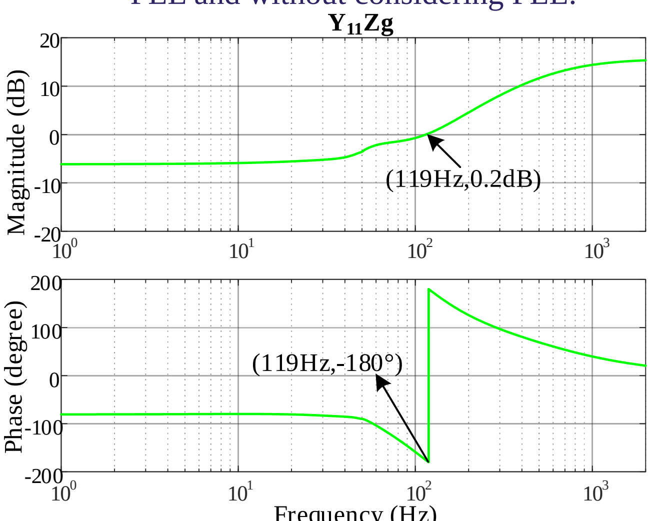

The bode diagram of $Y_{11}Z_g$.

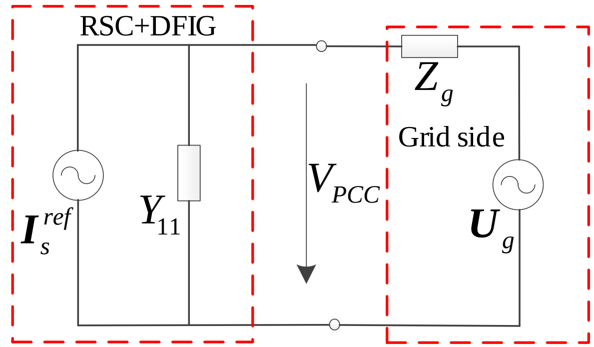

Equivalent impedance model of whole system.

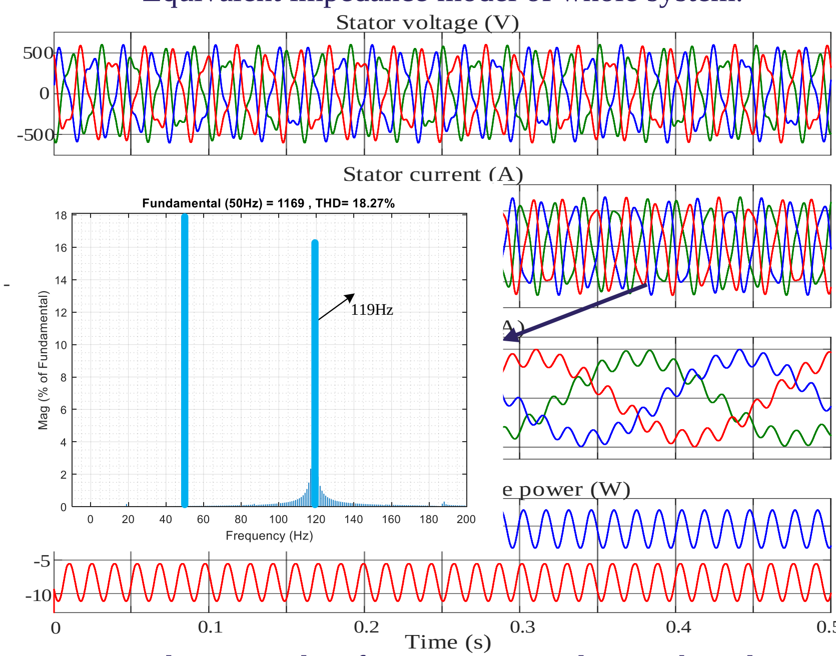

Simulation results of DFIG connected to weak grid.

Stability enhancement of DFIG-AC system

◆ Impedance model analysis

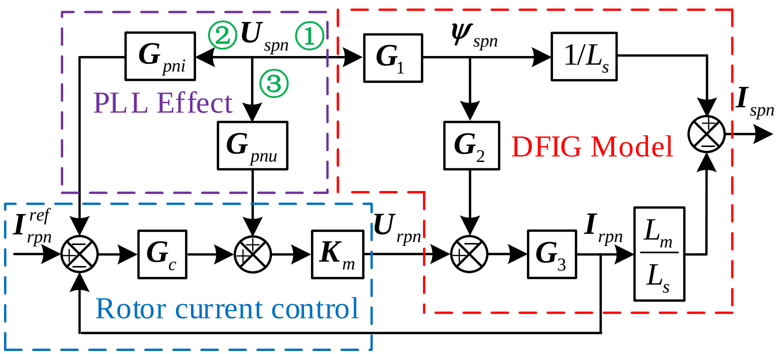

DFIG impedance model based on symmetrical PLL

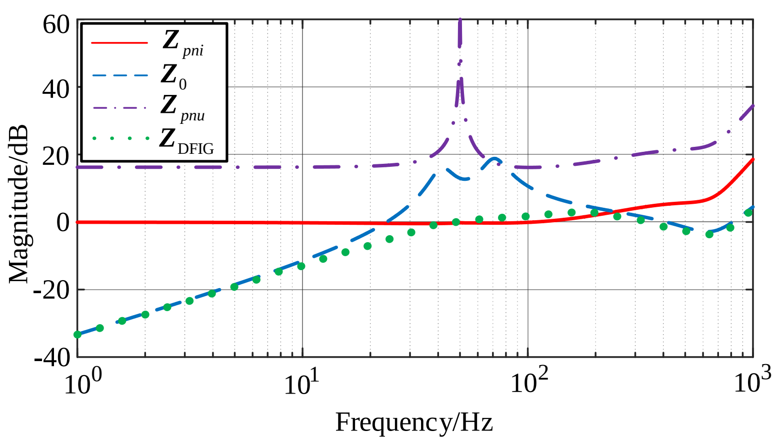

Amplitude-frequency characteristic curves of impedance subsystem

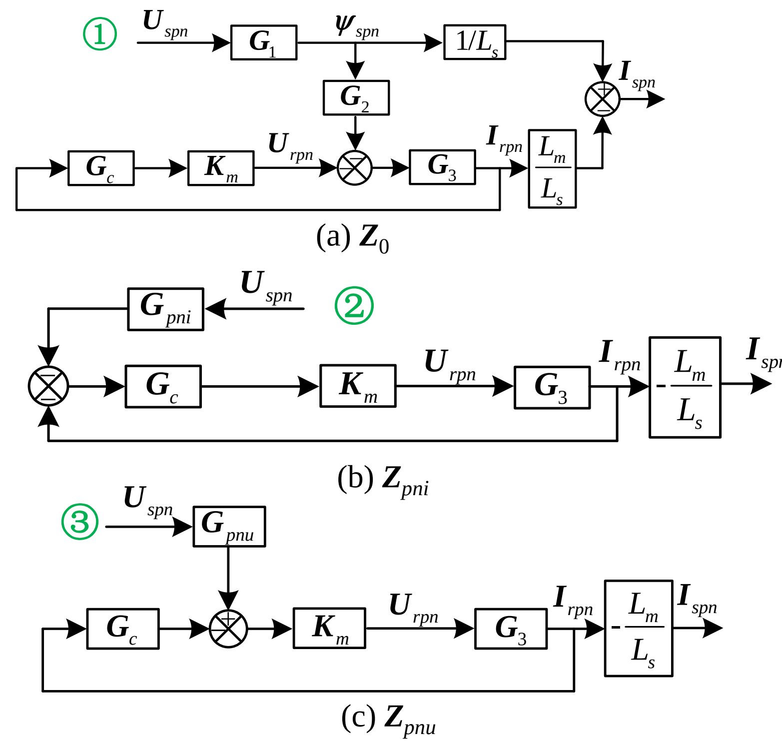

Block diagram of DFIG subsystem impedance.

$$Z_{DFIG} = \left(1/Z_0 + 1/Z_{pnu} + 1/Z_{pni}\right)^{-1}$$

Stability enhancement of DFIG-AC system

◆ Impedance model analysis

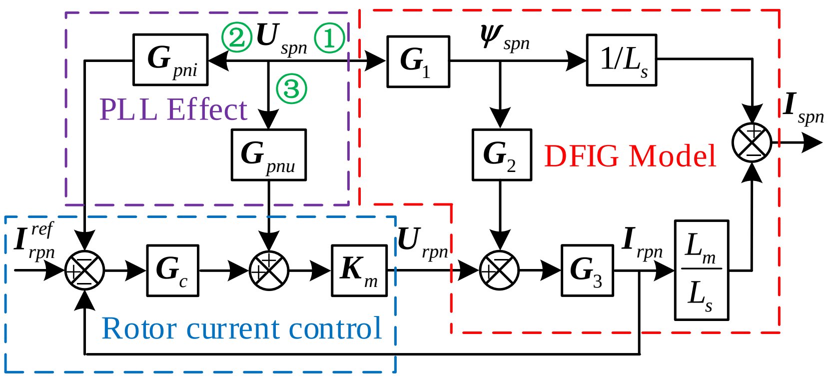

DFIG impedance model based on symmetrical PLL

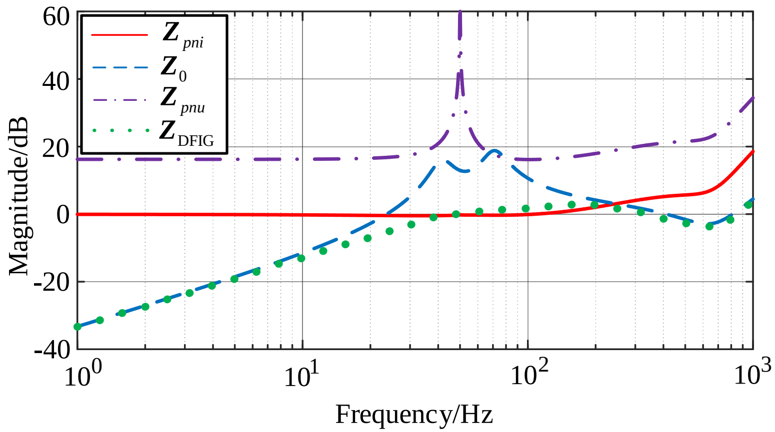

Amplitude-frequency characteristic curves of impedance subsystem

- ❑ **From 50-200Hz, the impedance is mainly detemined by Z_{pni}.**
- ❑ **Z_{pni} will introduce a negative resistance in this frequency range, which is the main reason that might cause instability under weak grid.**

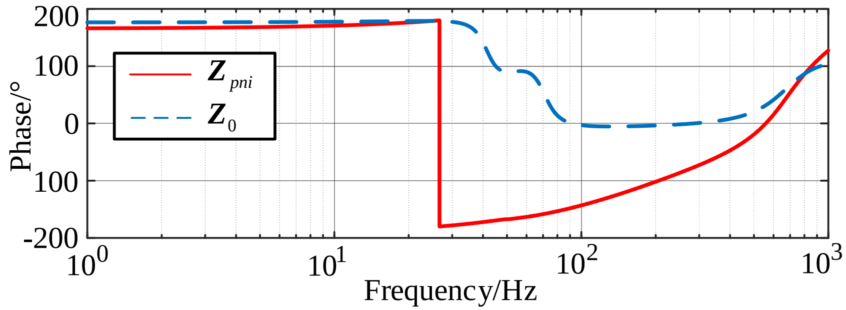

Phase-frequency characteristic curves of DFIG impedance subsystem

Stability enhancement of DFIG-AC system

◆ Impedance reshaping control strategy

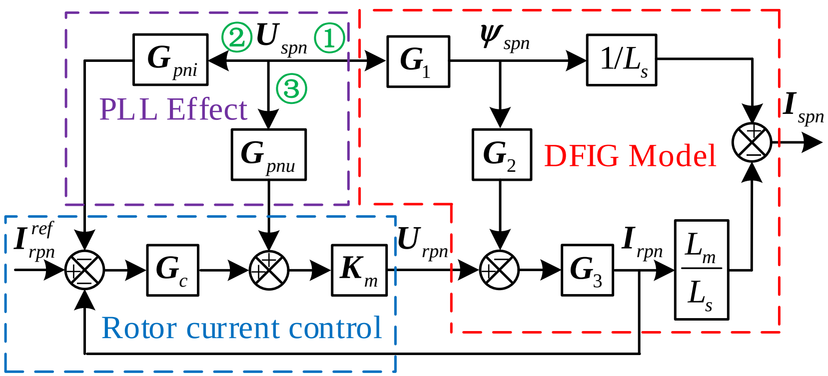

DFIG impedance model based on symmetrical PLL

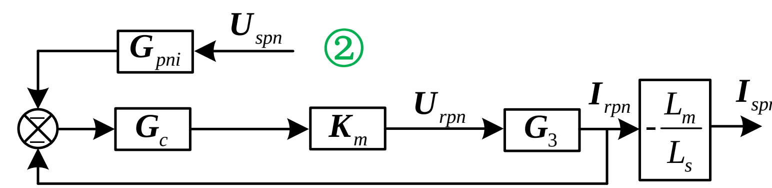

(b) Z_{pni}

$$Z'_{pni} \approx \frac{1+G'_c G'_3}{G'_{pni} G'_c G'_3} = \frac{1/G'_3 + G'_c}{G'_{pni} G'_c} \qquad 1/G'_3 = R_r + (s - j\omega_r) L_r \sigma \qquad G'_c = \frac{K_{pc}(s - j\omega_1) + K_{ic}}{s - j\omega_1}$$

$$Z'_{pni} \approx \frac{1}{G'_{pni}} = -\frac{1}{I_{rdq1}} \left(\frac{(s - j\omega_1)^2}{K_{pp}(s - j\omega_1) + K_{ip}} + 1 \right)$$

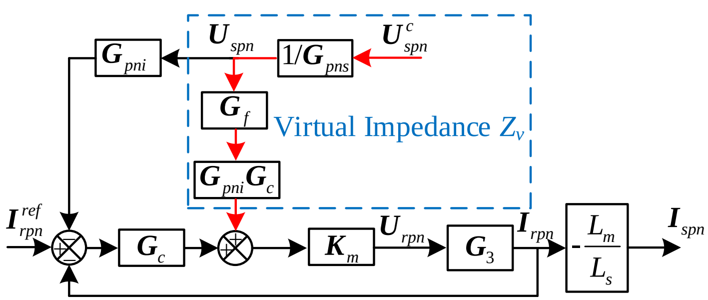

Virtual impedance implemented in control frame

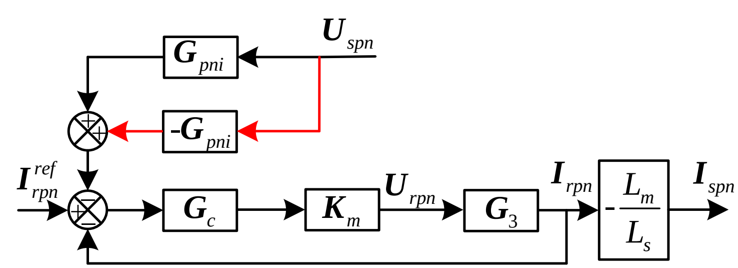

Block diagram of DFIG impedance based on the virtual impedance

Stability enhancement of DFIG-AC system

◆ Impedance reshaping control strategy

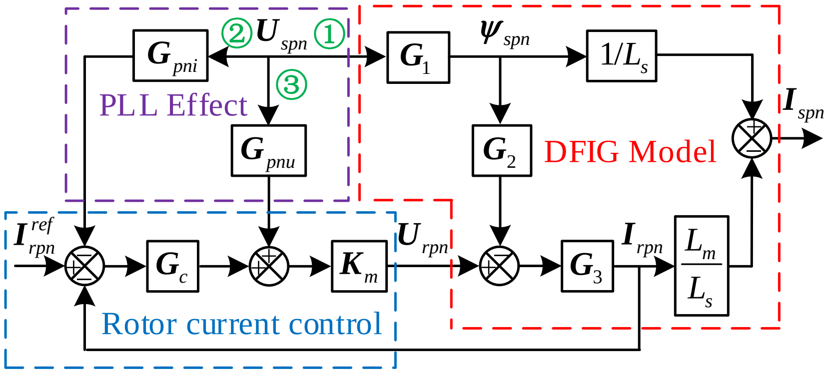

DFIG impedance model based on symmetrical PLL

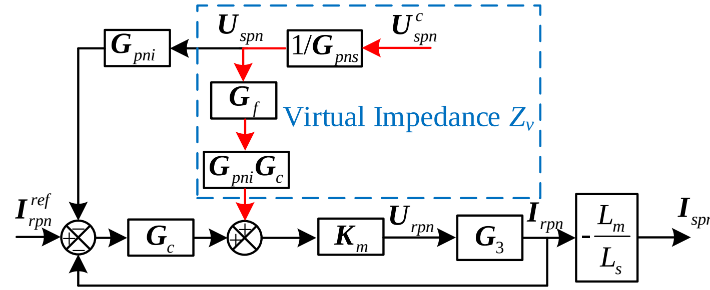

Virtual impedance implemented in control frame

$$\boldsymbol{G}_{pns}=\begin{bmatrix}1-U_{sd1}H_{PLL}(s) & 0\\ 0 & 1-U_{sd1}H_{PLL}(s)\end{bmatrix}$$

$$G_f'=\frac{s^3}{s^3+2\omega_L s^2+2\omega_L{}^2 s+\omega_L{}^3}$$

$$Z_v'\approx G_f' G_{pni}' G_c'/G_{pns}'$$

$$=-\boldsymbol{I}_{rdq1}\frac{\left(K_{pp}(s-\mathrm{j}\omega_1)+K_{ip}\right)\left(K_{pc}(s-\mathrm{j}\omega_1)+K_{ic}\right)}{(s-\mathrm{j}\omega_1)^3}G_f'$$

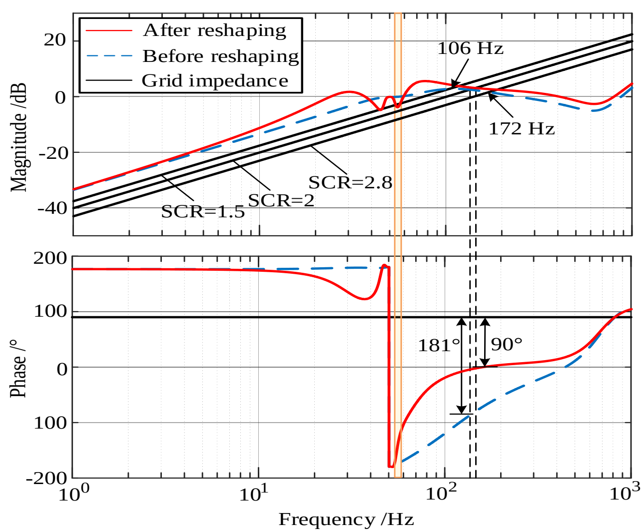

Impedance Bode diagram of DFIG system with virtual impedance

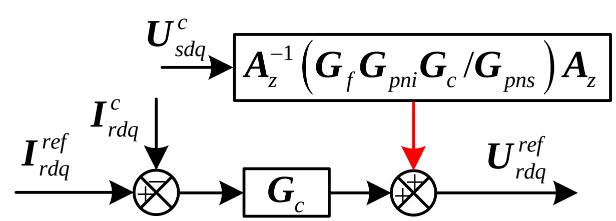

Control diagram of the proposed impedance reshaping control strategy in *dq*-domain

Stability enhancement of DFIG-AC system

◆ Experimental validations

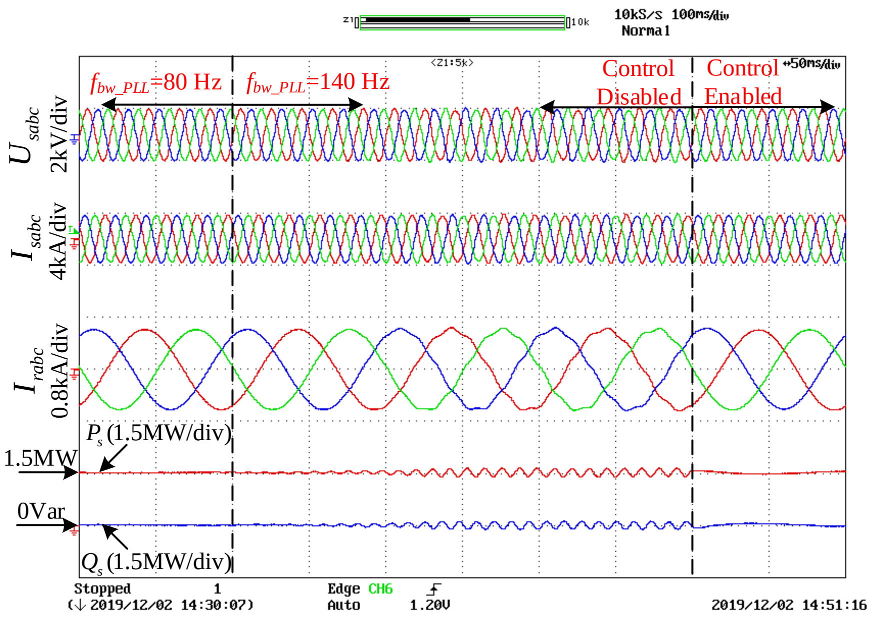

Experimental results of DFIG system with proposed control strategy

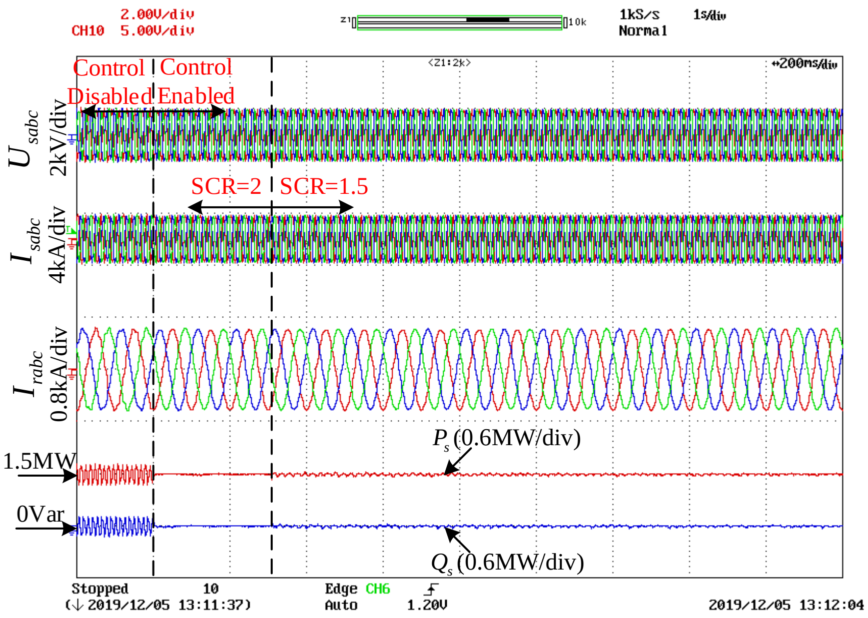

Experimental results of adaptability of the proposed control strategy for resonance frequency shifts due to the SCR changes

- ❑ **With the proposed impedance reshaping method, the negative resistance can be counteracted and the stability can be improved.**
- ❑ **Frequency coupling and system stability are two seperate issues, eliminating frequency coupling does not improve the system stability.**

Stability enhancement of DFIG-AC system

◆ **Conclusion**

- ❑ **The frequency coupling phenomenon of DFIG system caused PLL can be eliminated by using a symmetrical PLL.**

- ❑ **The sequence impedance model of DFIG system can easily be obtained based on complex transfer function, since it is simplified as a SISO system with the symmetrical PLL.**

- ❑ **SISO impedance reshaping method can be implemented to enhance the stability of DFIG system under the weak grid condition.**

[1] C. Wu, B. Hu, H. Nian, F.Blaabjerg, “Eliminating Frequency Coupling of DFIG System Using a Complex Vector PLL”, APEC, 2020.
[2] H. Nian, B. Hu, C. Wu, L. Chen, Y. Xu and F. Blaabjerg, "Analysis and Reshaping on Impedance Characteristic of DFIG System based on Symmetrical PLL," in IEEE Transactions on Power Electronics.doi: 10.1109/TPEL.2020.2982946

Control of DFIG-DC system

Research Background

◆ **The significance of dc grid connection for renewable energy**

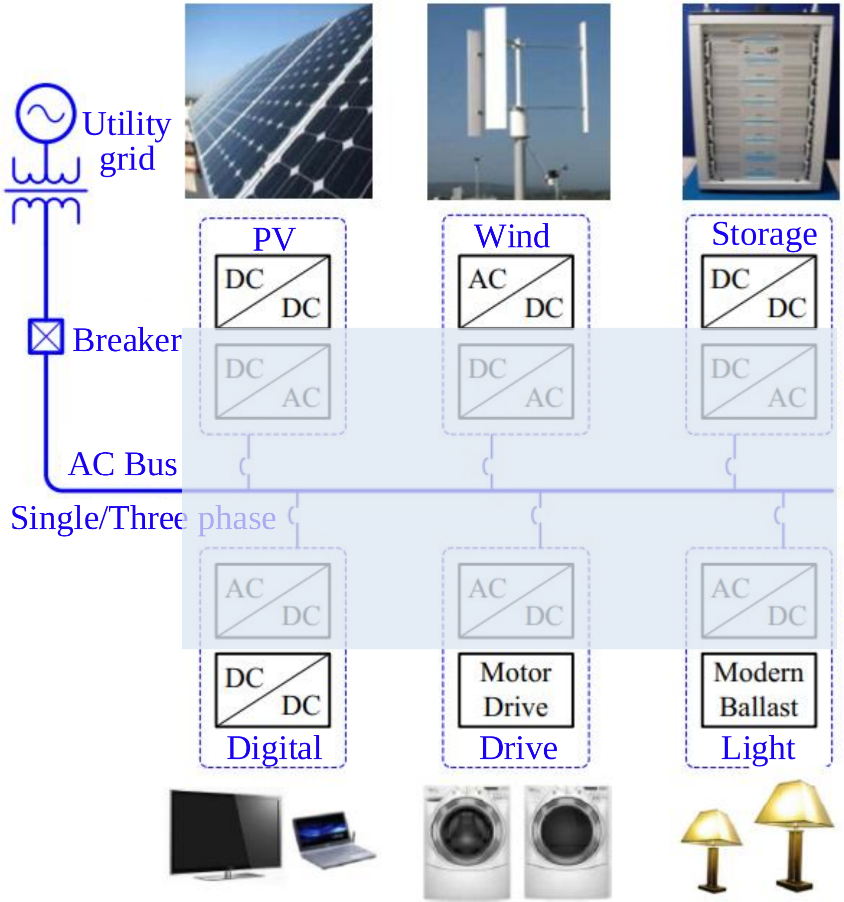

Structure of ac microgrid

◆ **Advantage of dc connection**

1. Avoid additional DC/AC block
2. Reduce the system cost and complexity
3. Increase the system efficiency

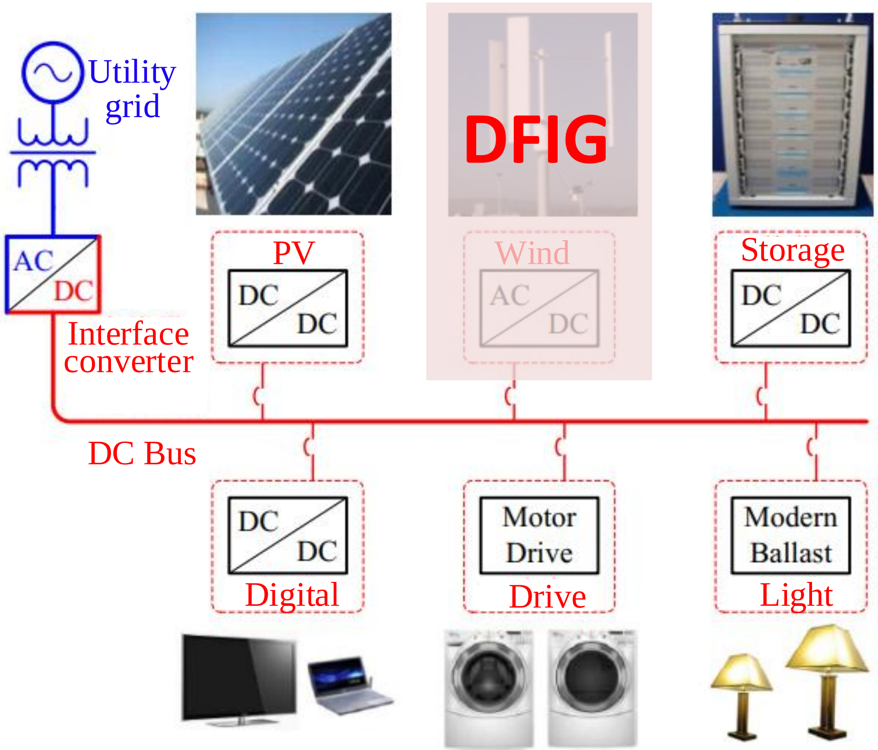

Structure of dc microgrid

Research Background

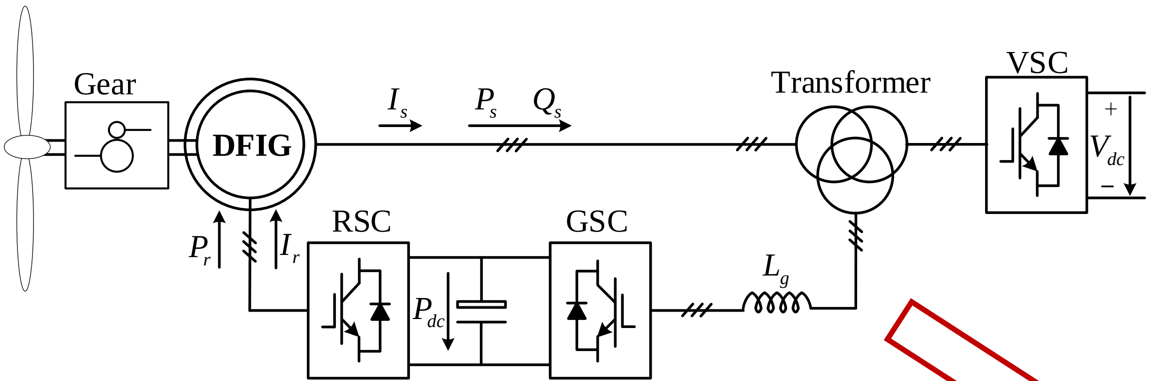

DFIG connected to dc link based on additional voltage source converter (VSC)

Pros : Control strategy is the same with DFIG-AC system, can be easily transplanted from existed DFIG-AC system
Cons: complex and too much energy converting block, the capacity of VSC is limited like weak grid which will cause some instability issue

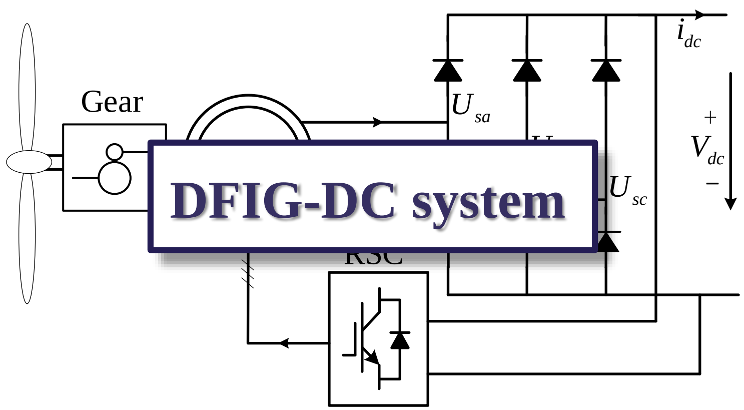

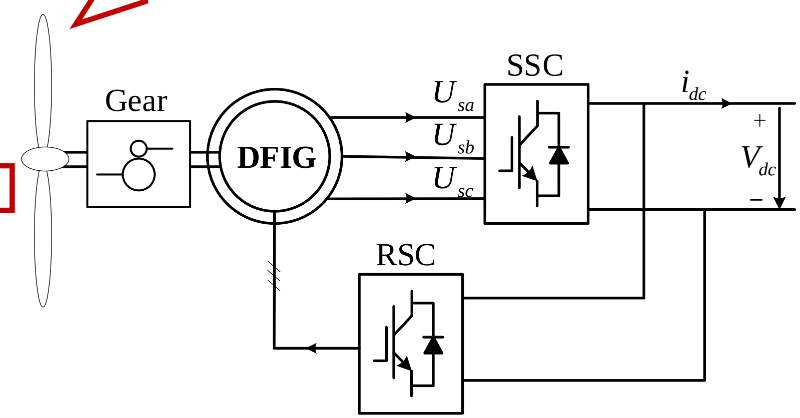

DFIG connected to dc link based on stator side converter (SSC)

Pros： cost effective and simpler control structure
Cons： distorted stator voltage and distorted currents cause power and torque ripples

Pros: the topology is simplified and the energy transition efficiency is improved
Cons： the capacity of SSC is high

Research Background

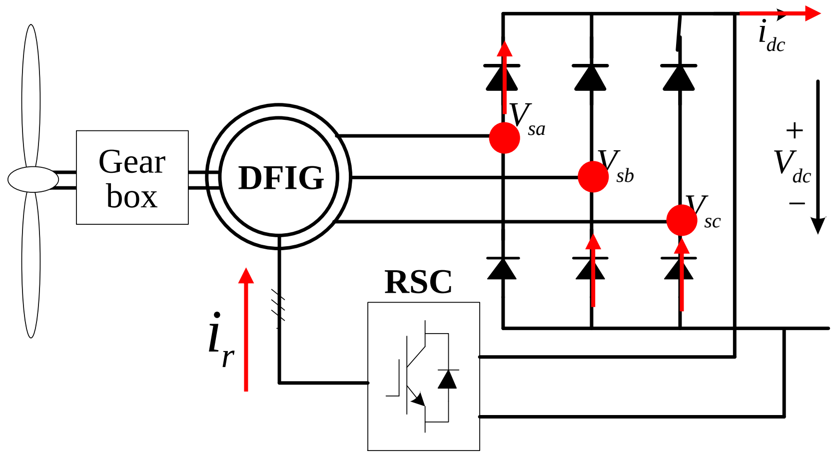

Equivalent circuit of DFIG-DC system

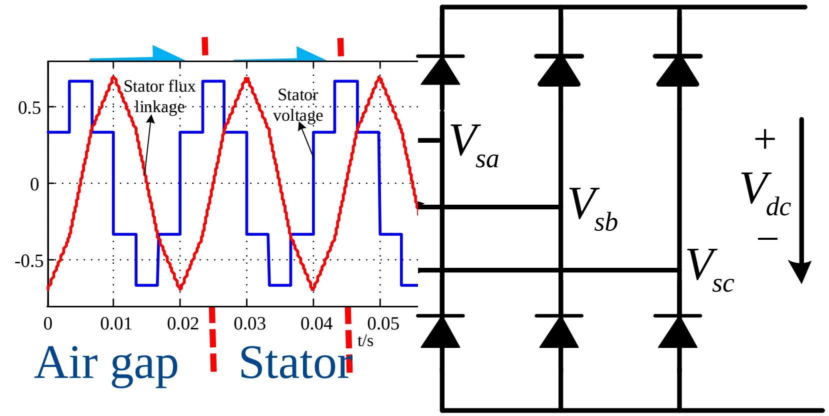

Equivalent circuit from stator side

Working principle

Building rotor exciting current → Building stator voltage → Diode bridge conducting → Output power to dc side

- ❑ How to achieve the orientation control and stator frequency control ?
- ❑ How to suppress the harmonic currents?
- ❑ How to suppress the torque ripple?

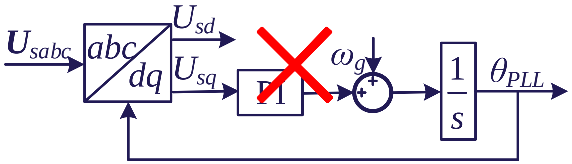

Conventional PLL based on stator voltage

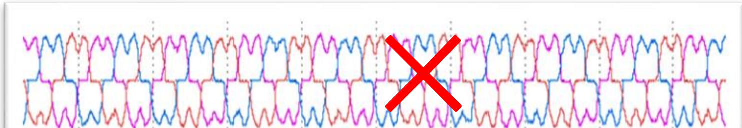
Stator current


Torque

Research Background

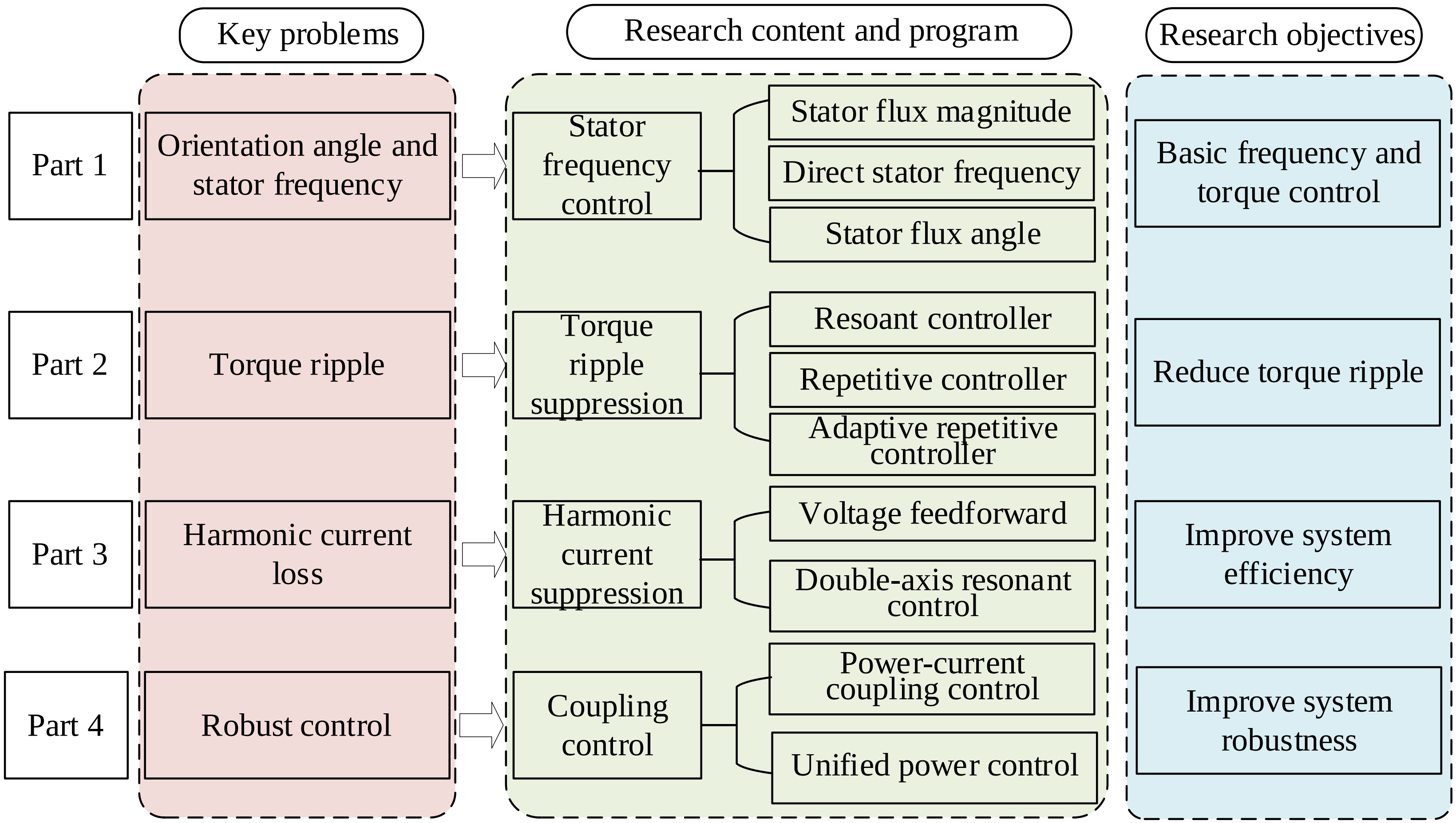

Objectives: Build good performance、high efficiency、low cost DFIG-DC system

Stator frequency control of DFIG-DC system

Stator frequency control of DFIG-DC system

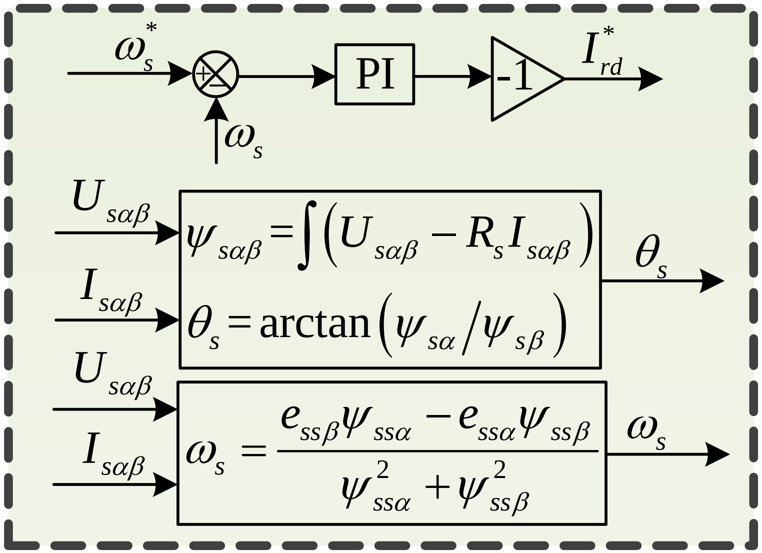

Directly calculating stator freqeuncy [1]

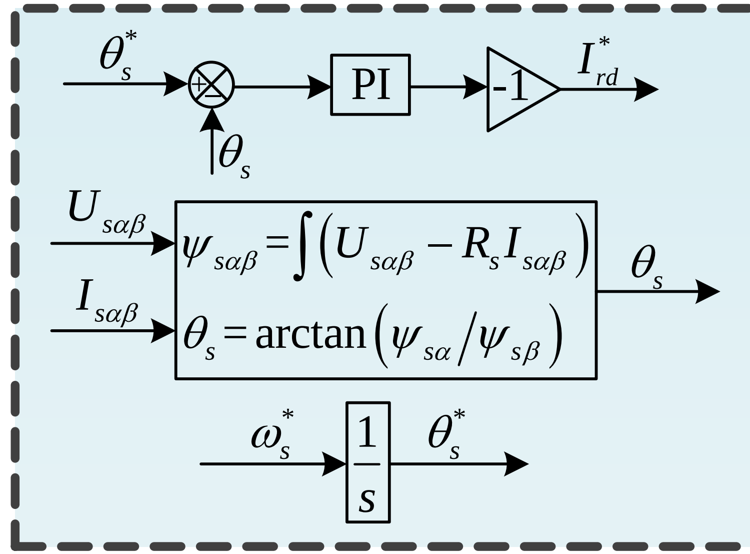

Directly calculating stator flux angle [2]

Existed problems

- Pure integral block is affected by dc offset
- Calculating stator frequency has a high parameter dependency

[1] Iacchetti, M.F., G.D. Marques and R. Perini, Torque Ripple Reduction in a DFIG-DC System by Resonant Current Controllers. *IEEE Transactions on Power Electronics*, 2015. 30(8): p. 4244-4254.

[2] Marques, G.D. and M.F. Iacchetti, Stator Frequency Regulation in a Field-Oriented Controlled DFIG Connected to a DC Link. *IEEE Transactions on Industrial Electronics*, 2014. 61(11): p. 5930-5939.

Stator frequency control of DFIG-DC system

◆ **Operation mode of diode bridge rectifier**

Conduction mode：the magnitude ratio between ac voltage and dc voltage

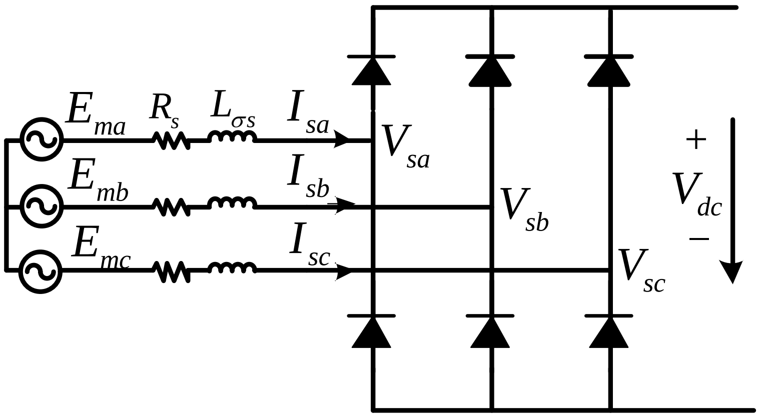

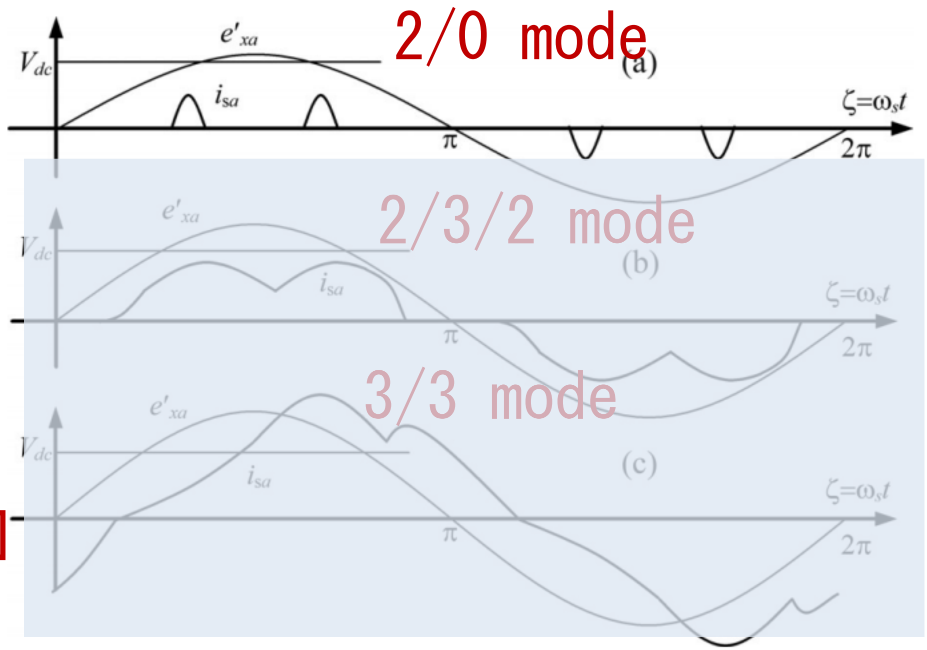

Fundamental voltage

$$V_{sa1} = \frac{2}{\pi} V_{dc}$$

Key property：The product of stator frequency and flux is a constant value

Stator frequency control of DFIG-DC system

◆ **Indirect stator frequency control based on stator flux magnitude**

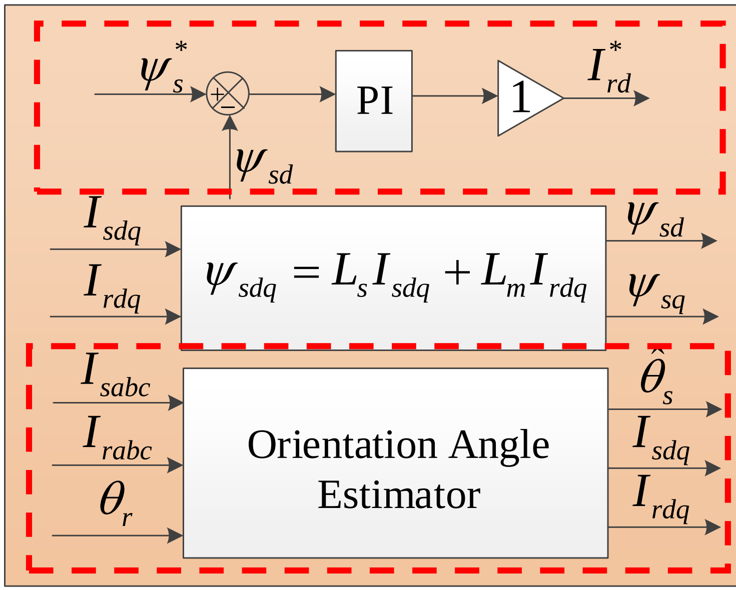

Stator flux magnitude control [1]

Control stator frequency by controlling stator flux linkage indirectly

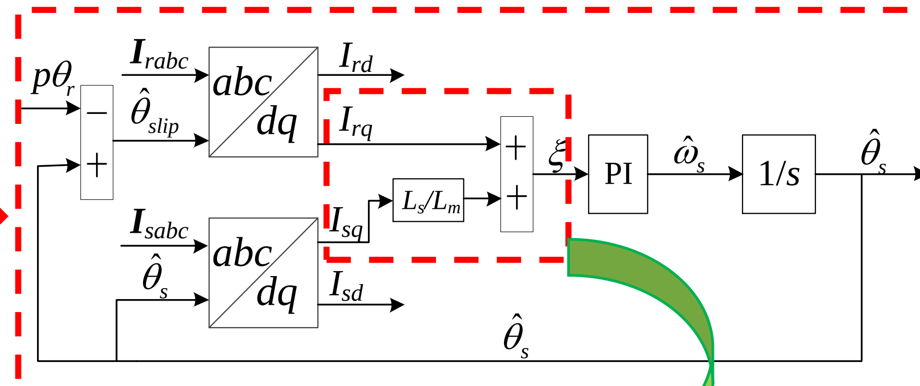

Indirectly stator flux orientation

$$\boldsymbol{\psi}_{sq} = L_s \boldsymbol{I}_{sq} + L_m \boldsymbol{I}_{rq} = 0$$

Pros

- Without calculating stator flux angle
- Without calculating stator frequency

[1] Nian Heng, **Wu Chao**, Cheng Peng. Direct resonant control strategy for torque ripple mitigation of DFIG connected to DC link through diode rectifier on stator[J]. IEEE Transactions on Power Electronics, 2017，32(9)：6936-6945.

Stator frequency control of DFIG-DC system

- **Indirect stator frequency control based on stator flux magnitude**

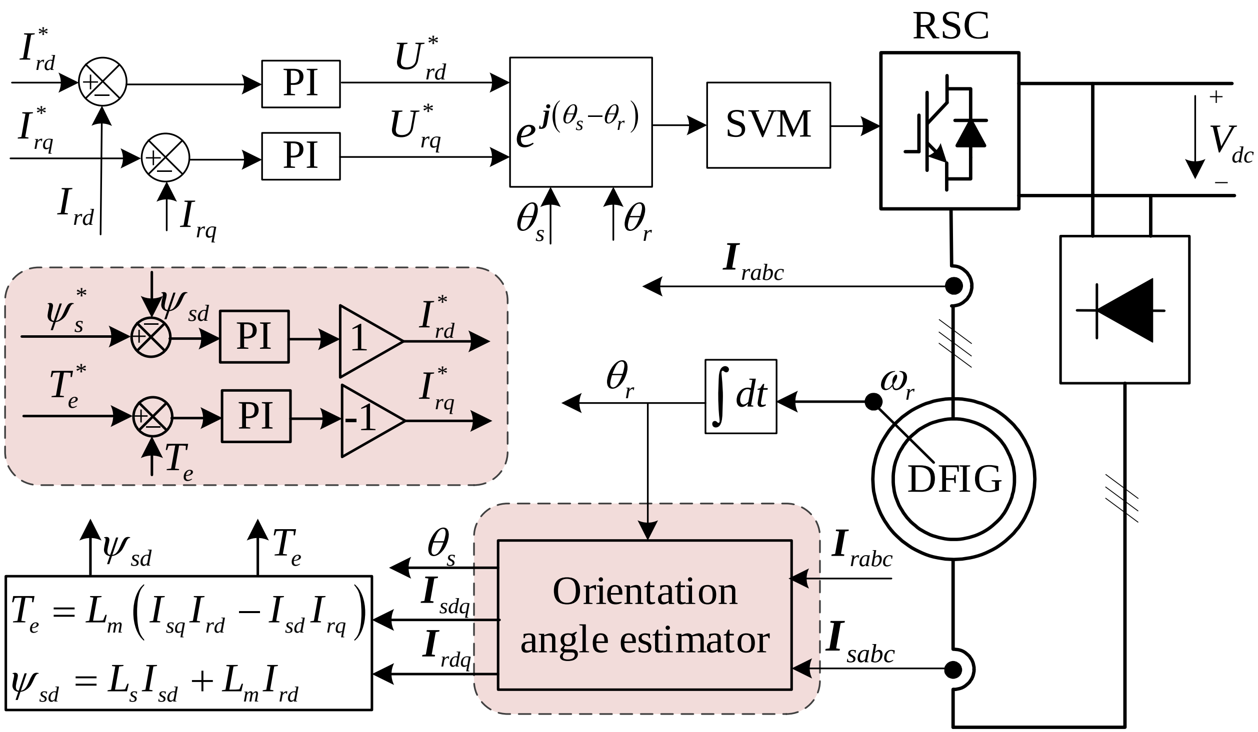

Drawbacks：

1.Dependent on the ratio between stator and mutual inductance

2.Control accuracy of stator frequency is dependent on stator flux accuracy

Heng Nian, **Chao Wu**, Peng Cheng. Direct resonant control strategy for torque ripple mitigation of DFIG connected to DC link through diode rectifier on stator[J]. IEEE Transactions on Power Electronics, 2017，32(9)：6936-6945.

Stator frequency control of DFIG-DC system

- **Direct stator frequency control method**

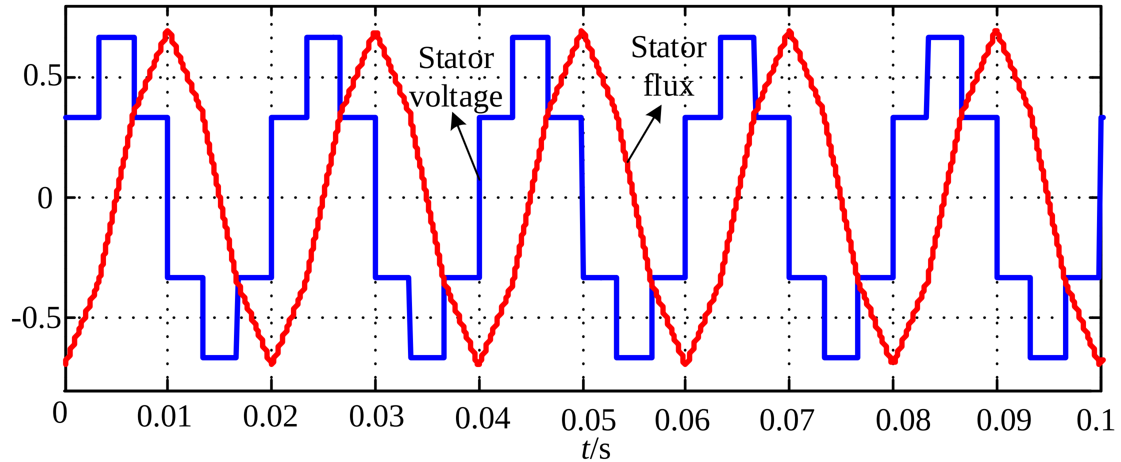

Waveforms of stator voltage and flux

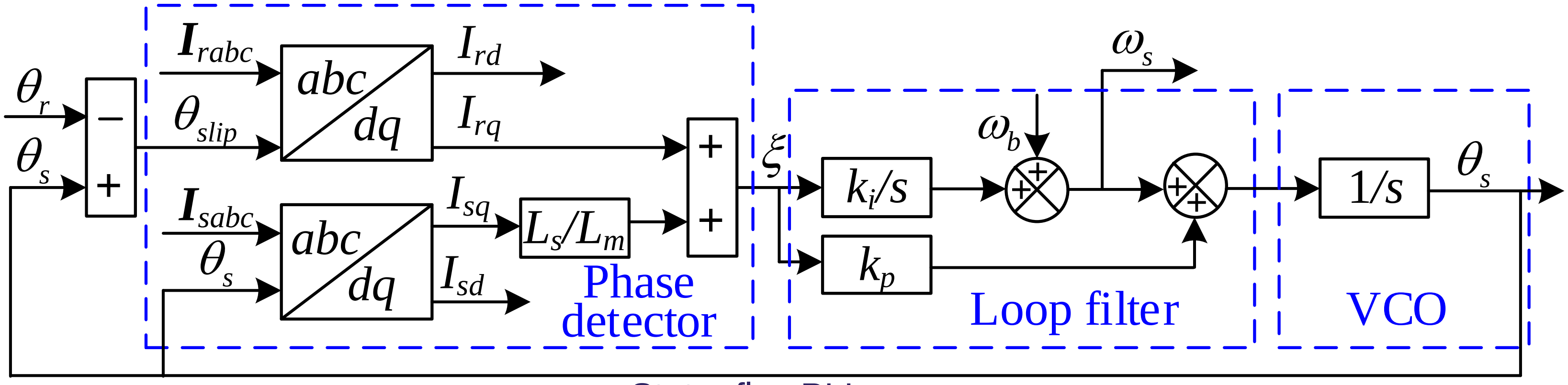

Stator flux PLL

Obtaining stator frequency and staor flux angle simultaneously

Stator frequency control of DFIG-DC system

◆ **Direct stator frequency control method**

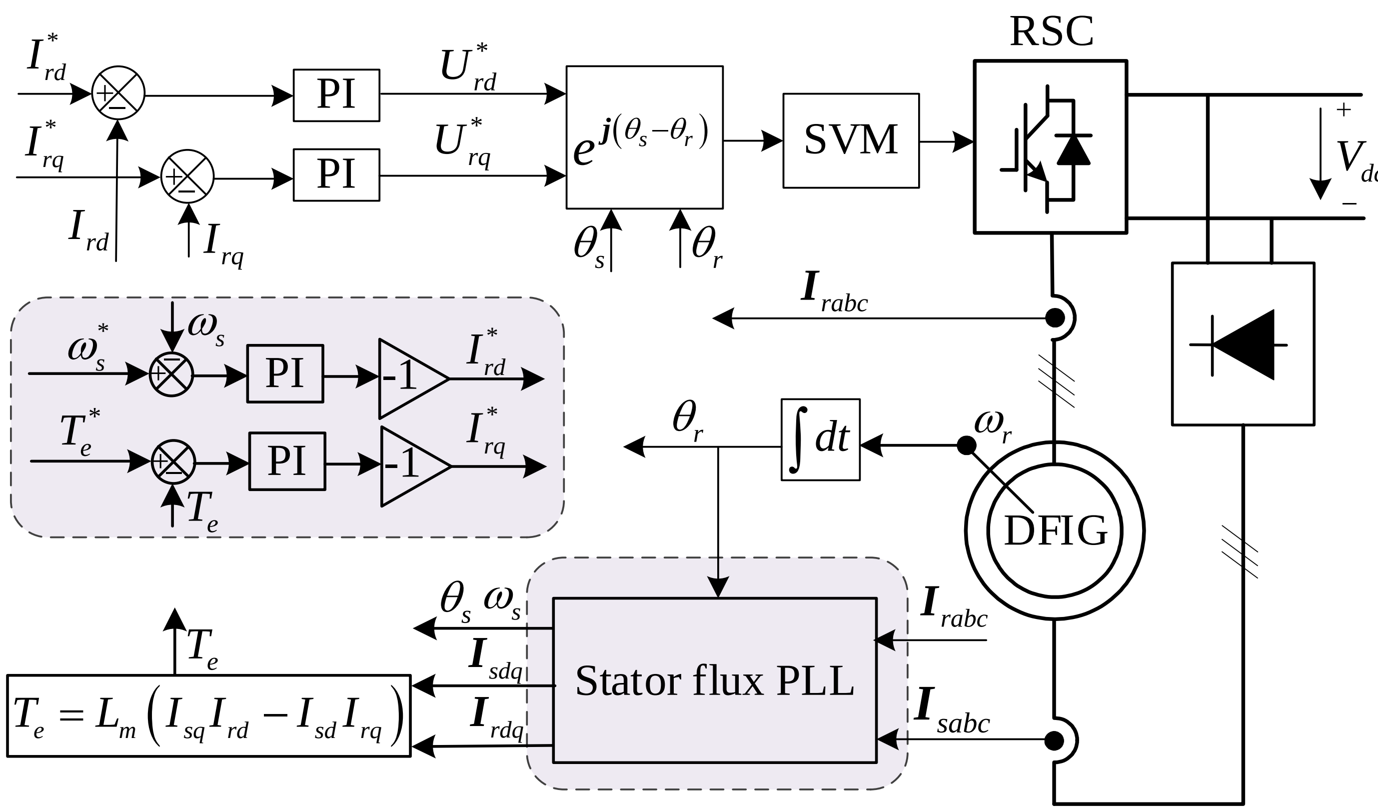

Cons：

1.The accuracy is dependent on ratio between stator and mutual inductance

Chao Wu, Heng Nian. An improved repetitive control of DFIG-DC system for torque ripple suppression[J]. IEEE Transactions on Power Electronics, 2018，33(9)：7634-7644.

Stator frequency control of DFIG-DC system

- **Acquiring stator flux angle**

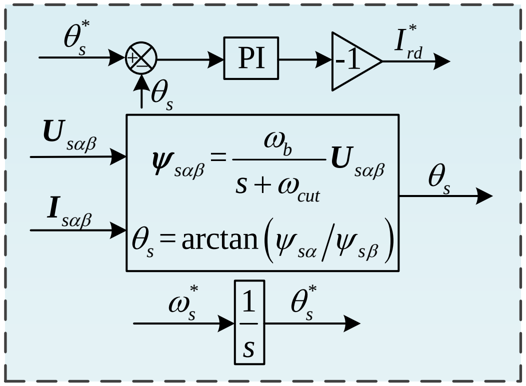

$$\psi_{s\alpha\beta} = \frac{\omega_b}{s+\omega_{cut}} U_{s\alpha\beta}$$

$$\theta_s = \arctan(\psi_{s\alpha}/\psi_{s\beta})$$

Acquiring stator flux angle based on inertia link

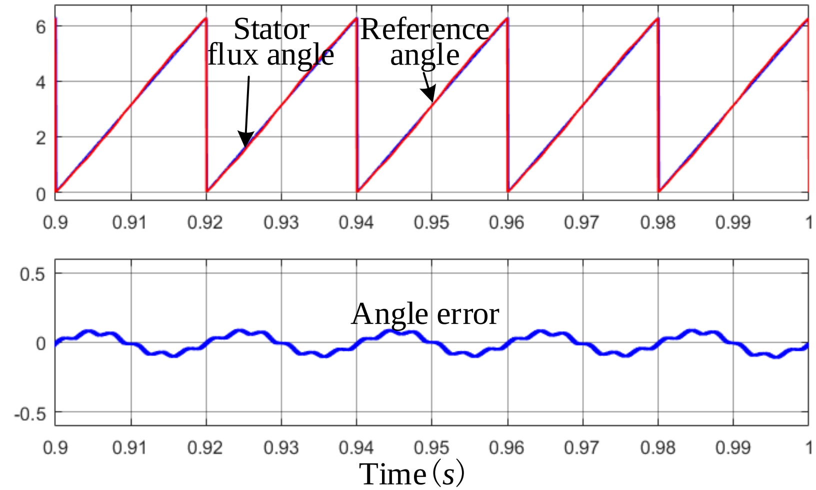

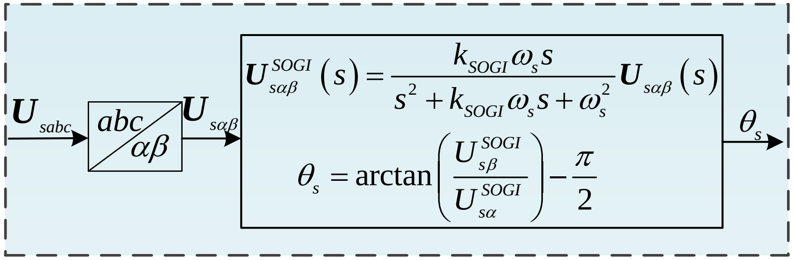

$$U_{s\alpha\beta}^{SOGI}(s) = \frac{k_{SOGI}\omega_s s}{s^2 + k_{SOGI}\omega_s s + \omega_s^2} U_{s\alpha\beta}(s)$$

$$\theta_s = \arctan\left(\frac{U_{s\beta}^{SOGI}}{U_{s\alpha}^{SOGI}}\right) - \frac{\pi}{2}$$

Acquiring stator flux angle based on SOGI

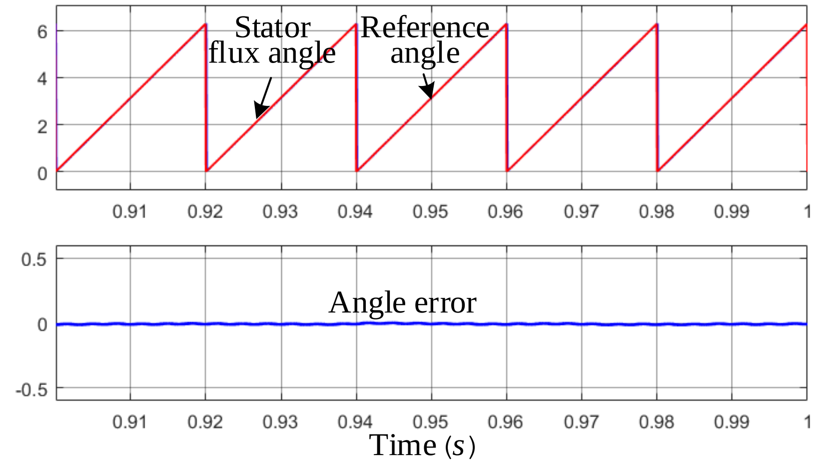

Stator frequency control of DFIG-DC system

- Indirect stator frequency control based on stator flux angle

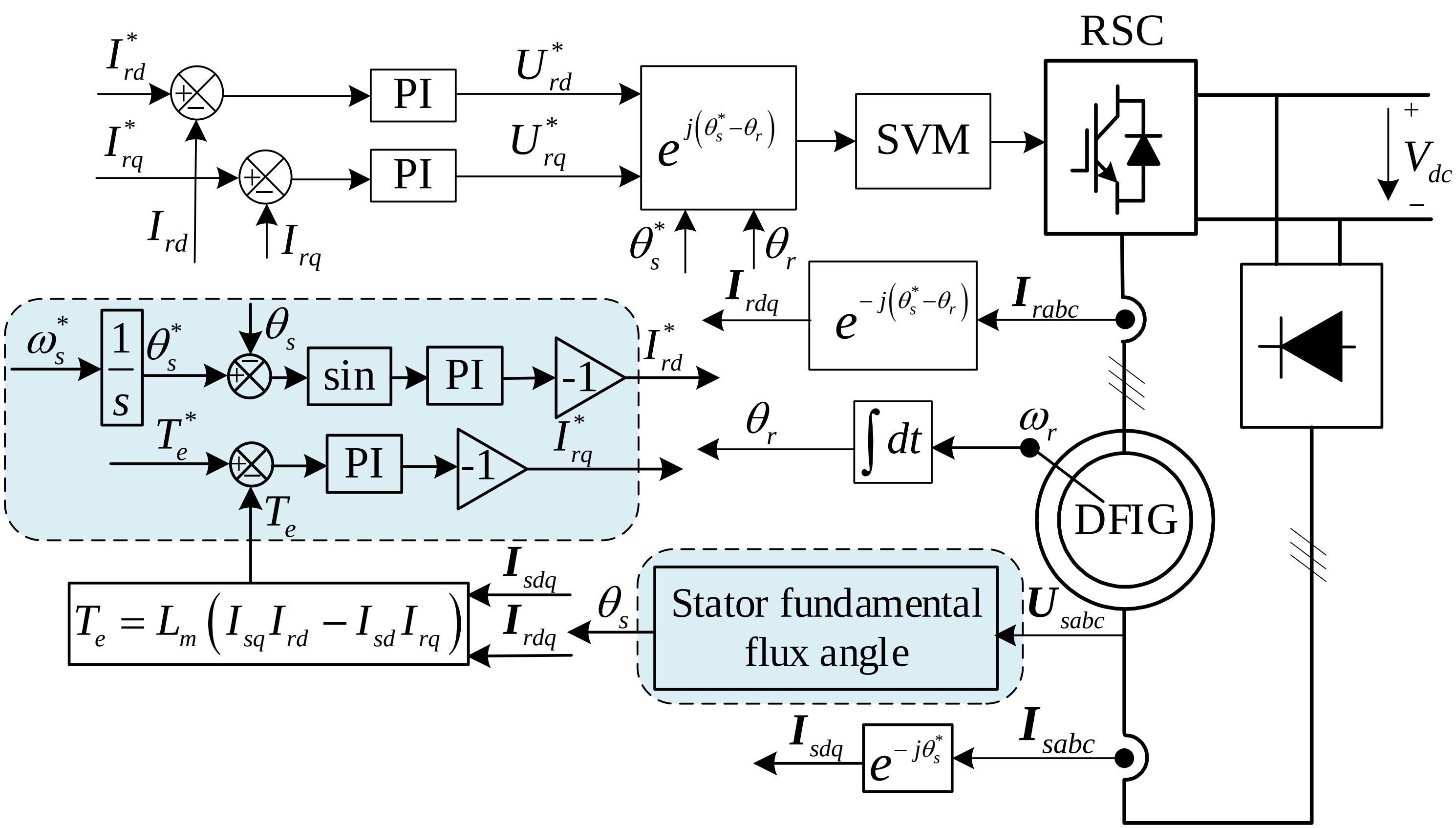

> Obtaining Stator flux angle based on SOGI can eliminate the bad effect of dc offset

Stator frequency control of DFIG-DC system

◆ Experimental setup

Parameters	*Value*	*Parameters*	*Value*
Rated power	1.0 kW	Rated voltage	110 V
Rated frequency	50 Hz	DC voltage	140 V
DC capacitance	780 μF	R_s	1.01 Ω
R_r	0.88 Ω	L_m	87.5 mH
$L_{\sigma s}$	5.6 mH	$L_{\sigma r}$	5.6 mH

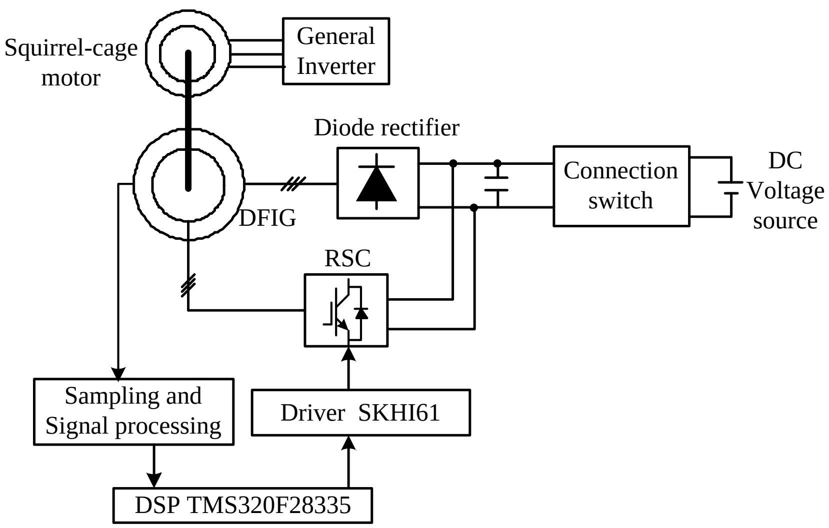

Schematic diagram of the experiment system

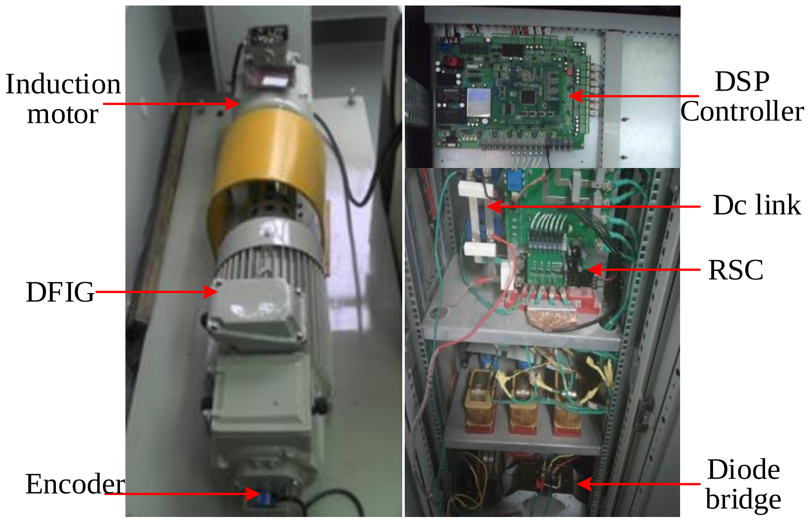

Experimental setup

Stator frequency control of DFIG-DC system

- Experimental results of different frequency control methods

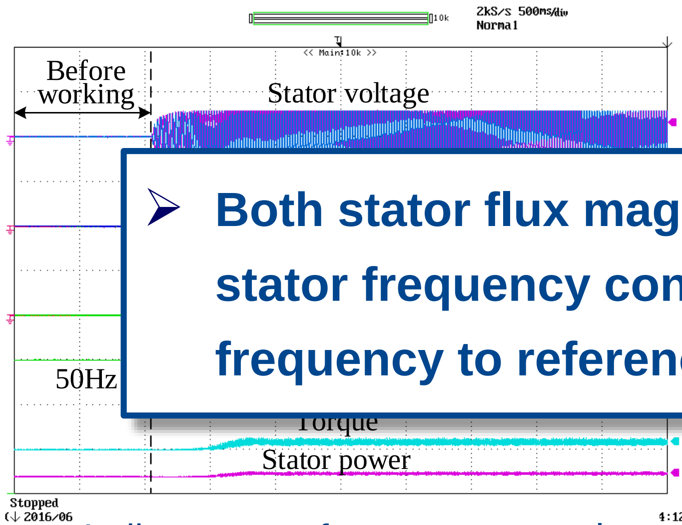

Indirect stator frequency control

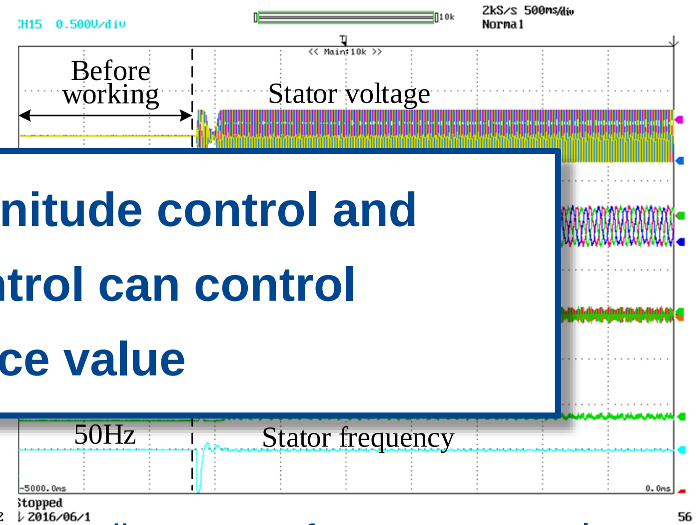

direct stator frequency control

- **Both stator flux magnitude control and stator frequency control can control frequency to reference value**

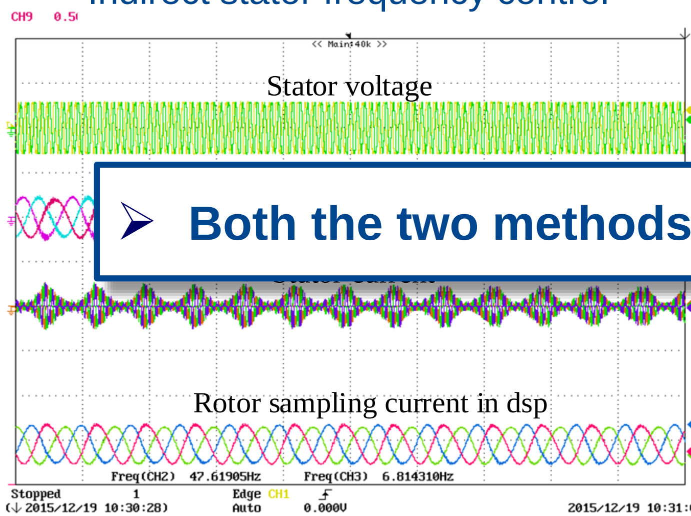

Sampling with dc offset

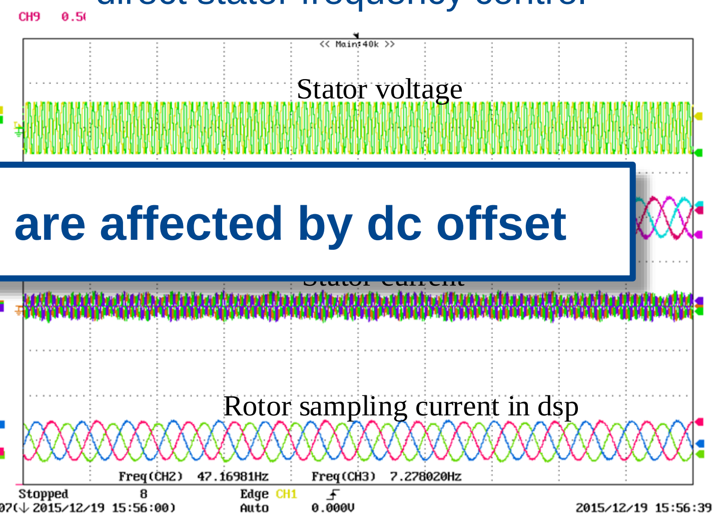

Eleminating the dc offset

- **Both the two methods are affected by dc offset**

Stator frequency control of DFIG-DC system

◆ **Experimental results of different frequency control methods**

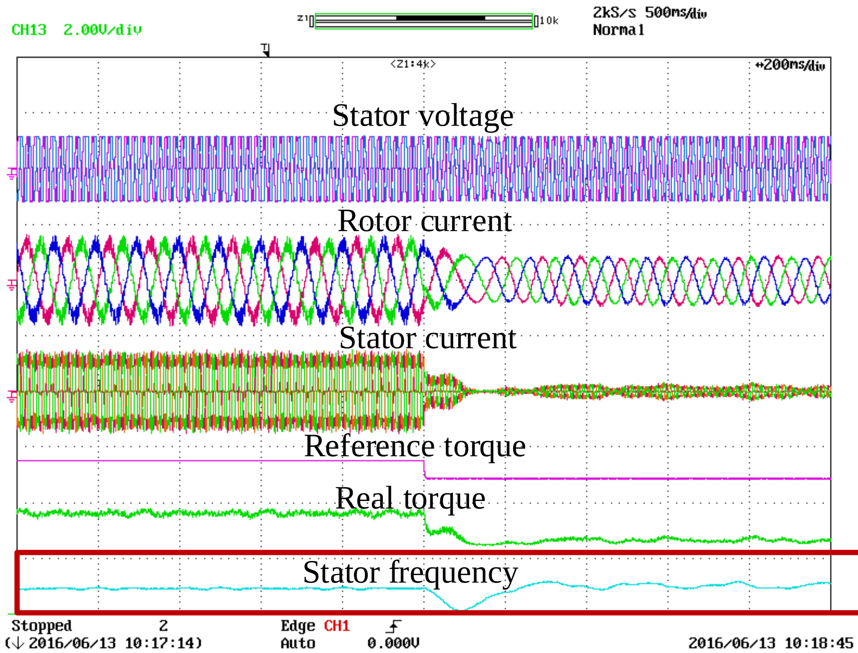

Staor flux magnitude control with power variations

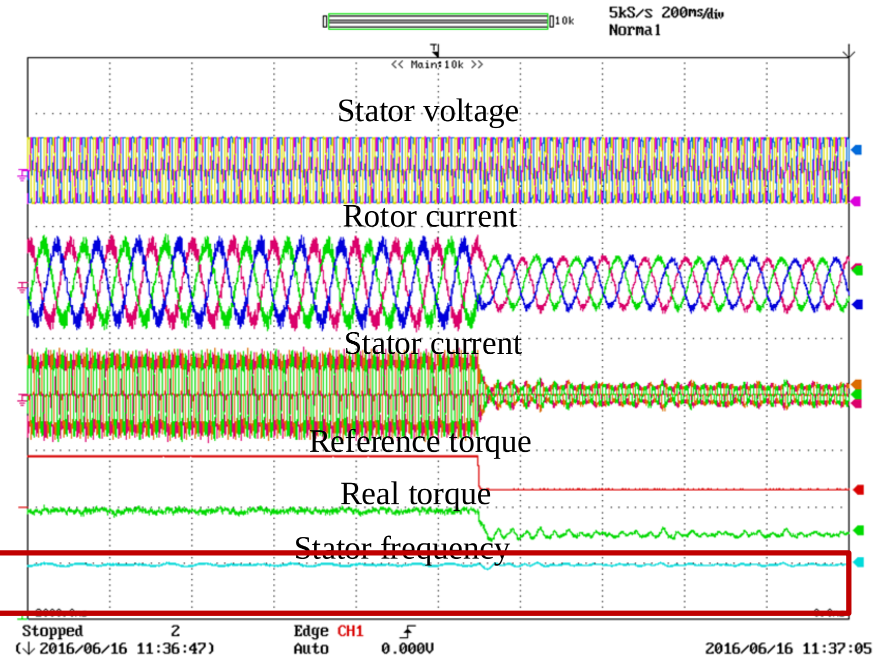

Direct stator frequency control with power varitaions

- ➢ Stator flux magnitude control is affected by power change;
- ➢ Stator frequency control is not affected by power change;

Stator frequency control of DFIG-DC system

◆ **Experimental results of different frequency control methods**

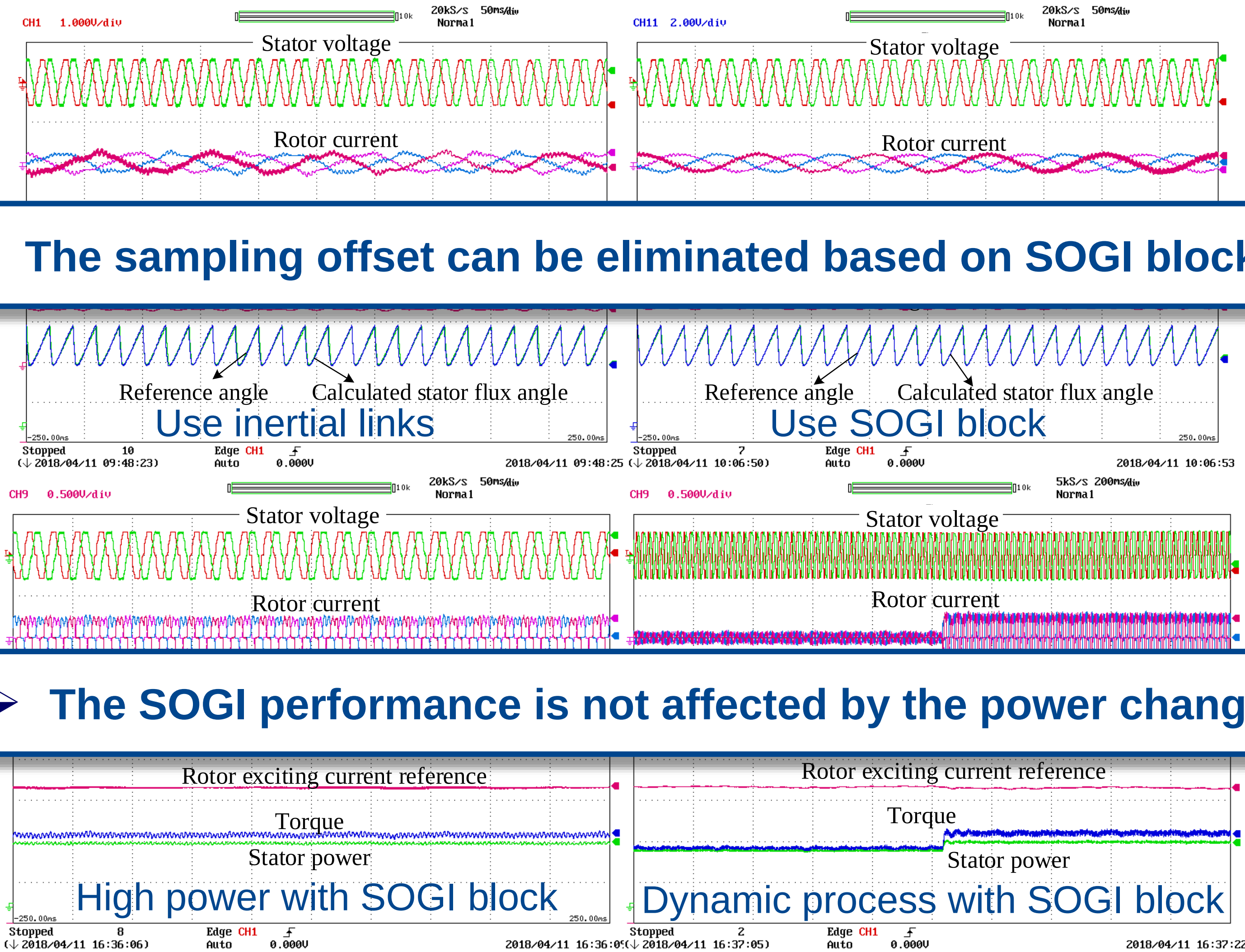

➢ **The sampling offset can be eliminated based on SOGI block**

➢ **The SOGI performance is not affected by the power change**

Stator frequency control of DFIG-DC system

◆ **Performance comparison of different frequency control methods**

	Stator flux magnitude control	Direct stator frequency control	Stator flux angle control
Stator flux model	Current model	Current model	Voltage model
Integral block	No	No	Yes
Ratio between stator and mutual inductance	Yes	Yes	**No**
Sampling offset effect	Yes	Yes	**No**
Power effect	Yes	Yes	**No**

- **The sampling offset can be eliminated by SOGI based stator flux angle control;**
- **Stator flux angle control is not dependent on the ratio between stator and mutual inductance;**

Torque ripple suppression of DFIG-DC system

Torque ripple suppression of DFIG-DC system

◆ **Torque ripple analysis under slightly distorted stator voltage**

Diode bridge 2/3/2 mode

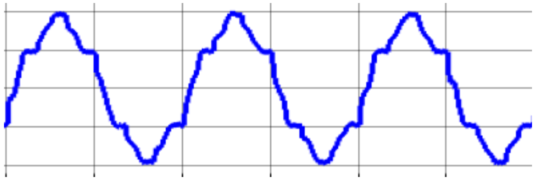

Stator voltage $$\boldsymbol{U}_{sdq} = \boldsymbol{U}_{sdq}^{1} + \boldsymbol{U}_{sdq}^{5} e^{-j6\omega_1 t} + \boldsymbol{U}_{sdq}^{7} e^{j6\omega_1 t}$$

Stator flux $$\boldsymbol{\psi}_{sdq} = \frac{\boldsymbol{U}_{sdq}^{1}}{j\omega_1} - \frac{\boldsymbol{U}_{sdq}^{5}}{j5\omega_1} e^{-j6\omega_1 t} + \frac{\boldsymbol{U}_{sdq}^{7}}{j7\omega_1} e^{j6\omega_1 t}$$

Stator current $$\boldsymbol{I}_{sdq} = \boldsymbol{I}_{sdq}^{1} - \frac{\boldsymbol{U}_{sdq}^{5}}{j\sigma L_s 5\omega_1} e^{-j6\omega_1 t} + \frac{\boldsymbol{U}_{sdq}^{7}}{j\sigma L_s 7\omega_1} e^{j6\omega_1 t}$$

Torque $$T_e = \mathrm{Re}\left(j\boldsymbol{\psi}_{sdq} \boldsymbol{I}_{sdq} \right) = L_m (I_{sq} I_{rd} - I_{sd} I_{rq})$$

Torque ripple $$T_e^{6} = \mathrm{Re}\left[(\boldsymbol{U}_{sdq}^{1} \boldsymbol{I}_{sdq}^{7} - \frac{\boldsymbol{U}_{sdq}^{5} \boldsymbol{I}_{sdq}^{1}}{5}) e^{-j6\omega_1 t} + (\boldsymbol{U}_{sdq}^{1} \boldsymbol{I}_{sdq}^{5} + \frac{\boldsymbol{U}_{sdq}^{7} \boldsymbol{I}_{sdq}^{1}}{7}) e^{j6\omega_1 t} \right]$$

➢ **Torque ripple manily consist of 6th order harmonic——resonant controller**

Torque ripple suppression of DFIG-DC system

- **Direct resonant control under slightly distorted stator voltage**

Pros of direct resonant control

1. Avoid calculate rotor harmonic current
2. Reduce algorithm complexity

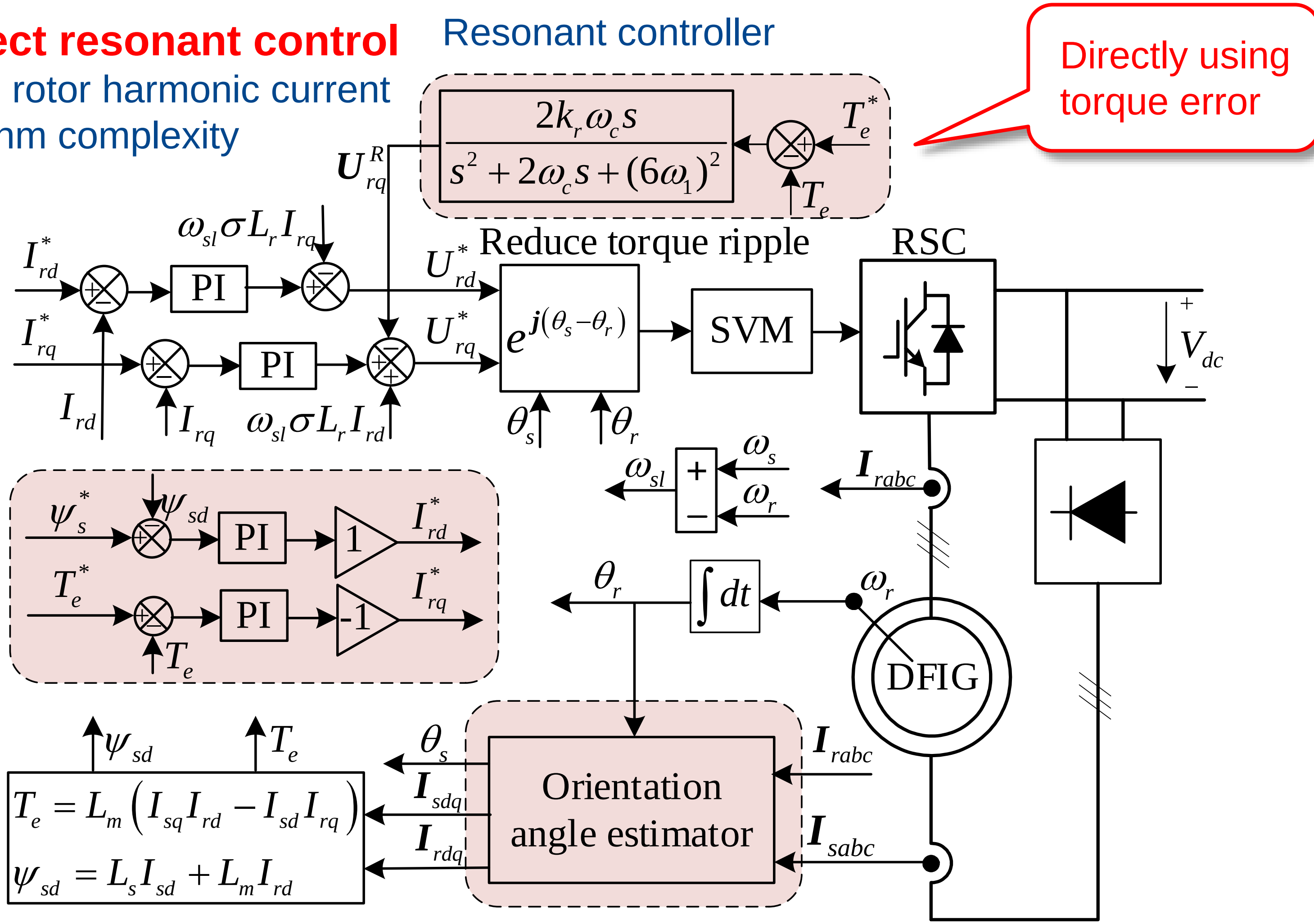

Torque ripple suppression of DFIG-DC system

◆ Experimental results of direct resonant control method

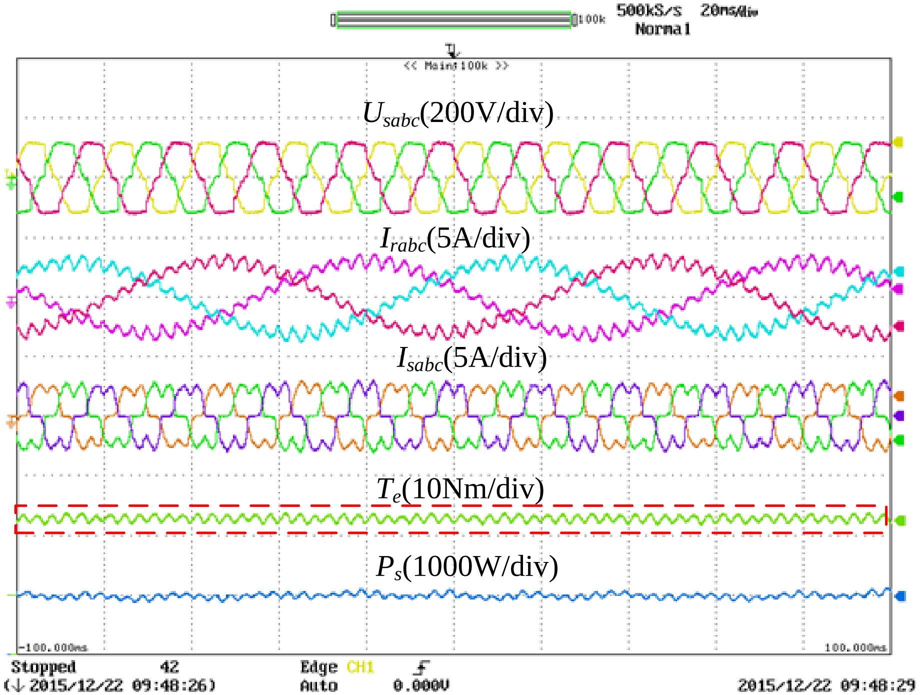

Without using direct resonant control

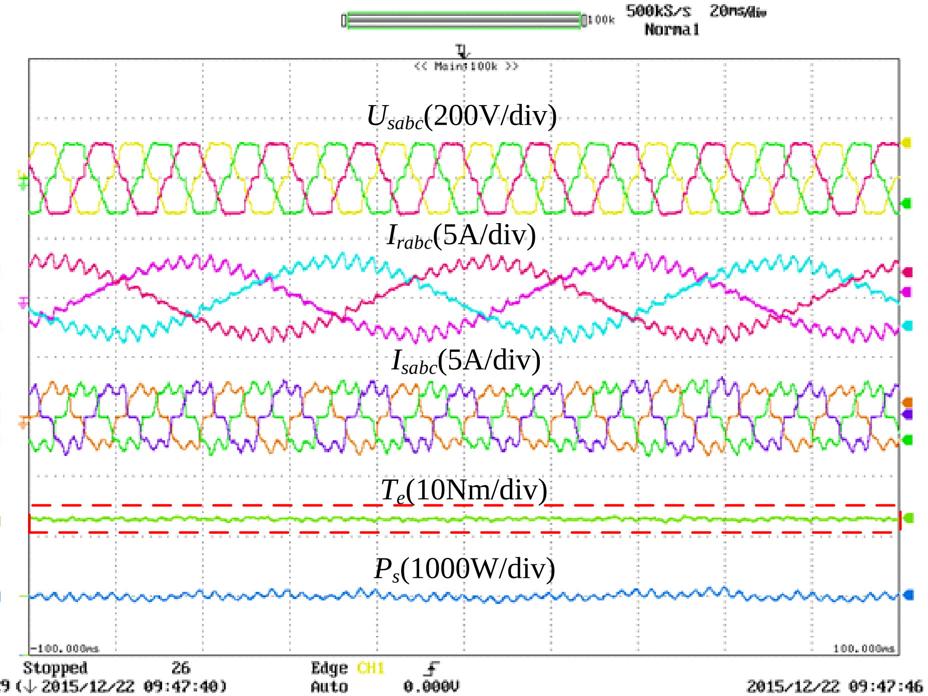

With using direct resonant control

➢ **Direct resonant control can mitigate torque ripple effectively**

Nian Heng, **Wu Chao**, Cheng Peng. Direct resonant control strategy for torque ripple mitigation of DFIG connected to DC link through diode rectifier on stator[J]. IEEE Transactions on Power Electronics, 2017，32(9)：6936-6945.

Torque ripple suppression of DFIG-DC system

◆ **Experimental results of direct resonant control method**

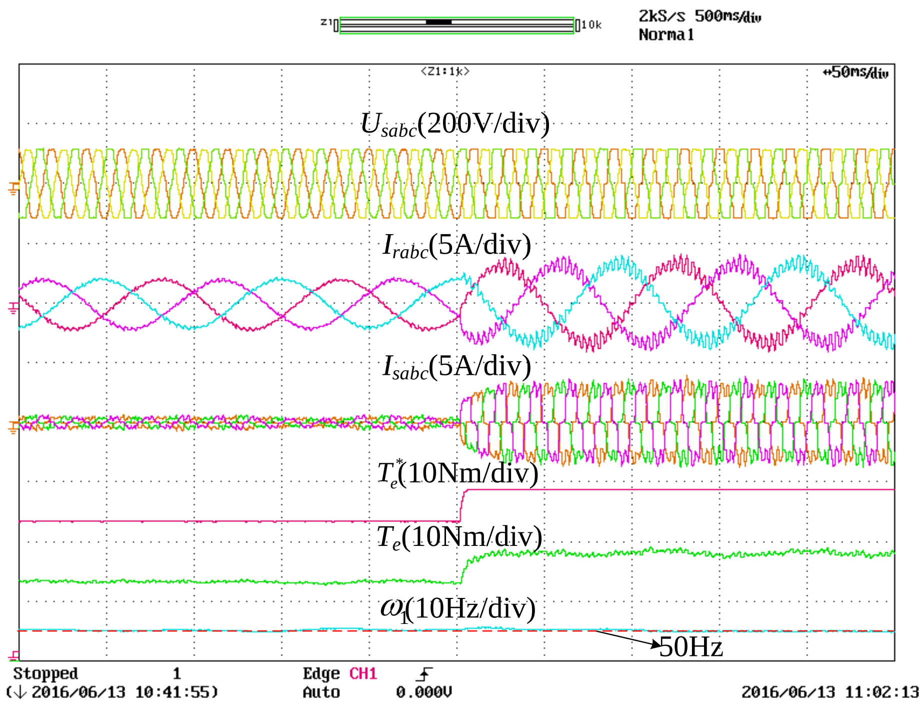

Step response of torque change

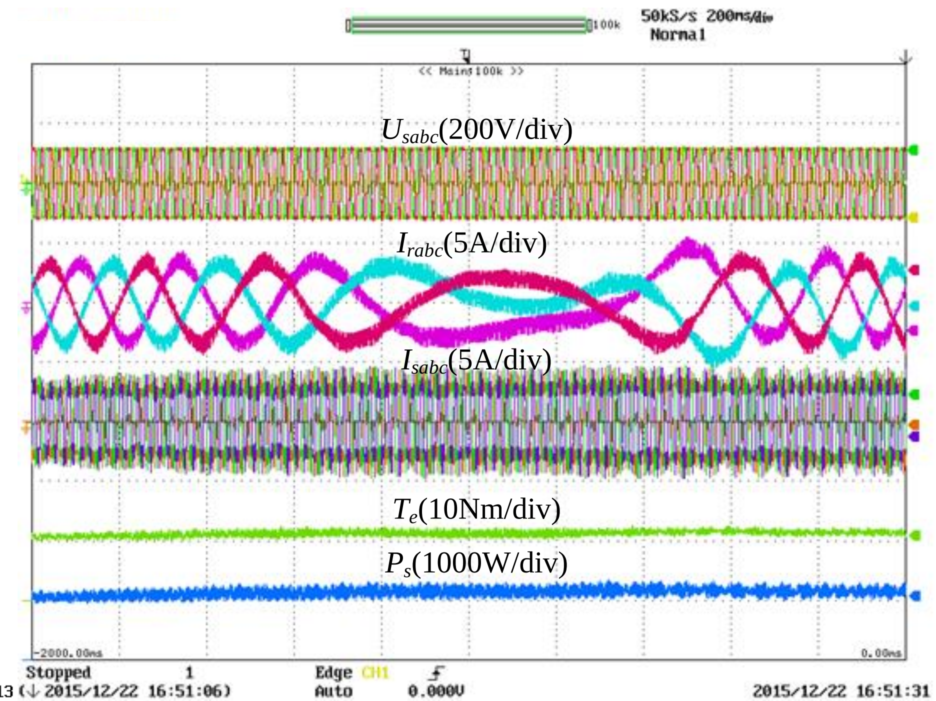

Rotor speed change from 800rpm to 1200rpm

➢ **Direct resonant control can reduce torque ripple in the dynamic process**

Nian Heng, **Wu Chao**, Cheng Peng. Direct resonant control strategy for torque ripple mitigation of DFIG connected to DC link through diode rectifier on stator[J]. IEEE Transactions on Power Electronics, 2017，32(9)：6936-6945.

Torque ripple suppression of DFIG-DC system

- **Torque ripple analysis under highly distorted stator voltage**

Stator voltage

$$U_{sa}(t)=\frac{2}{\pi}V_{dc}\left(\sin\omega_1 t+\sum_{n=1}^{\infty}\left(\frac{\sin(6n-1)\omega_1 t}{6n-1}+\frac{\sin(6n+1)\omega_1 t}{6n+1}\right)\right)$$

$$\boldsymbol{U}_{sdq}=\boldsymbol{U}^{+}_{sdq+}+\sum_{n=1}^{\infty}\left(\boldsymbol{U}^{(6n-1)-}_{sdq(6n-1)-}e^{-j6n\theta_1}+\boldsymbol{U}^{(6n+1)+}_{sdq(6n+1)+}e^{j6n\theta_1}\right)$$

Diode bridge 3/3 mode

Stator flux

$$\boldsymbol{\psi}_{sdq}=\boldsymbol{\psi}^{+}_{sdq+}+\sum_{n=1}^{\infty}\left(\boldsymbol{\psi}^{(6n-1)-}_{sdq(6n-1)-}e^{-j6n\theta_1}+\boldsymbol{\psi}^{(6n+1)+}_{sdq(6n+1)+}e^{j6n\theta_1}\right)$$

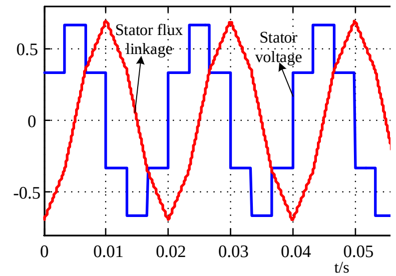

Stator current

$$\boldsymbol{I}_{sdq}=\boldsymbol{I}^{+}_{sdq+}+\sum_{n=1}^{\infty}\left(\boldsymbol{I}^{(6n-1)-}_{sdq(6n-1)-}e^{-j6n\theta_1}+\boldsymbol{I}^{(6n+1)+}_{sdq(6n+1)+}e^{j6n\theta_1}\right)$$

Torque

$$T_e=\mathrm{Re}\left(j\boldsymbol{\psi}_{sdq}\boldsymbol{I}_{sdq}\right)=L_m\left(I_{sq}I_{rd}-I_{sd}I_{rq}\right)=T_{e0}+\sum_{n=1}^{\infty}T_{e6n}$$

Torque ripple

$$T_{e6n}=R_e\left[\left(\boldsymbol{U}^{+}_{sdq+}\boldsymbol{I}^{(6n+1)+}_{sdq(6n+1)+}-\frac{\boldsymbol{U}^{(6n-1)-}_{sdq(6n-1)-}\boldsymbol{I}^{+}_{sdq+}}{6n-1}\right)e^{-j6n\theta_1}+\left(\boldsymbol{U}^{+}_{sdq+}\boldsymbol{I}^{(6n-1)-}_{sdq(6n-1)-}+\frac{\boldsymbol{U}^{(6n+1)+}_{sdq(6n+1)+}\boldsymbol{I}^{+}_{sdq+}}{6n+1}\right)e^{j6n\theta_1}\right]$$

> **Controller should have multi-resonant frequency——repetitive controller**

Torque ripple suppression of DFIG-DC system

◆ **Design of improved repetitive controller**

Conventional repetitive controller (CRC)

$$G_{CRC}(s) = \frac{k_{RC} e^{-T_0 s}}{1 - e^{-T_0 s}}$$

Expand expression

$$G_{CRC}(s) = -\frac{k_{RC}}{2} + \frac{k_{RC}}{T_0 s} + \frac{2k_{RC}}{T_0} \sum_{n=1}^{\infty} \frac{s}{s^2 + (n\omega_0)^2}$$

Without bandwidth

Considering bandwidth

$$G_{BRC}(s) = \frac{k_{RC} Q e^{-T_0 s}}{1 - Q e^{-T_0 s}}$$

$$G_{BRC}(s) = \frac{k_{RC} Q e^{-T_0 s}}{1 - Q e^{-T_0 s}} = -\frac{k_{RC}}{2} + \frac{k_{RC}}{T_0 s + T_0 \omega_c} + \frac{2k_{RC}}{T_0} \sum_{n=1}^{\infty} \frac{s + \omega_c}{s^2 + 2\omega_c s + \omega_c^2 + (n\omega_0)^2}$$

$$\approx -\frac{k_{RC}}{2} + \frac{k_{RC}}{T_0 s + T_0 \omega_c} + \frac{2k_{RC}}{T_0} \sum_{n=1}^{\infty} \frac{s + \omega_c}{s^2 + 2\omega_c s + (n\omega_0)^2}$$

With bandwidth

Torque ripple suppression of DFIG-DC system

- **Design of improved repetitive controller**

Discretization
$$G_{BRC}(z)=\frac{k_{RC}Qz^{-N}}{1-Qz^{-N}} \qquad N=f_s/f_0$$

N is not integer? $$z^{-N}=z^{-N_i-F}$$ How to deal with fractional delay?

$$z^{-F}\approx\sum_{k=0}^{n}A_k z^{-k}, k=0,1,\ldots,n \qquad A_k=\prod_{i=0,i\neq k}^{n}\frac{F-i}{k-i}, \quad k,i=0,1,\ldots,n$$

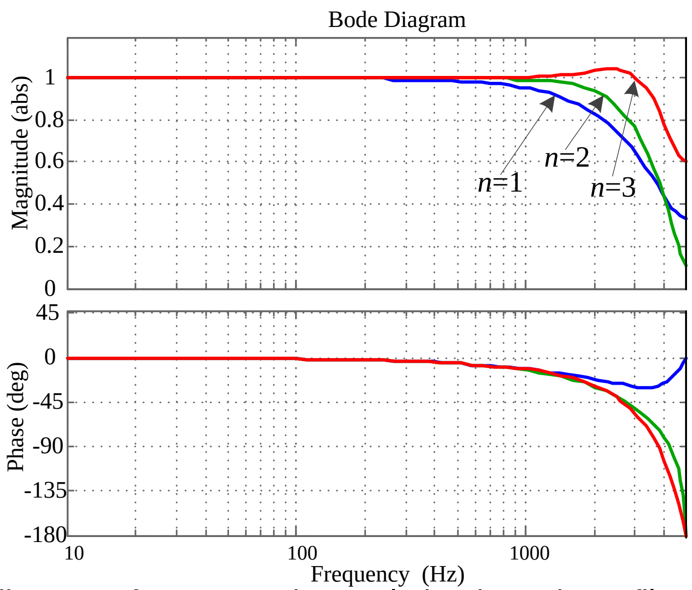

Bode diagram of Lagrange-interpolation-based FIR filter with n=1,2,3

$$z^{-1/3}\approx 0.5556+0.5556z^{-1}-0.1111z^{-2}=F(z)$$

Fractional repetitive controller with bandwidth in the discrete domain

$$G_{BRC}(z)=\frac{k_{RC}Qz^{-N_i}F(z)}{1-Qz^{-N_i}F(z)}$$

Torque ripple suppression of DFIG-DC system

◆ Design of improved repetitive controller

Improved RC

$$G_{IRC}(z) = \frac{k_{RC} Q z^{-N_i} F(z) G_{hp}(z)}{1 - Q z^{-N_i} F(z)} \qquad G_{hp}(z) = \frac{0.955z - 0.955}{z - 0.91}$$

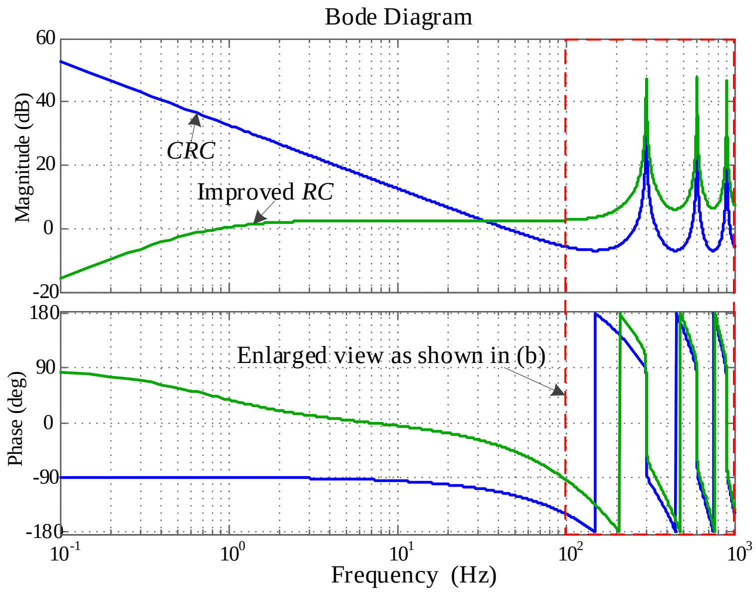

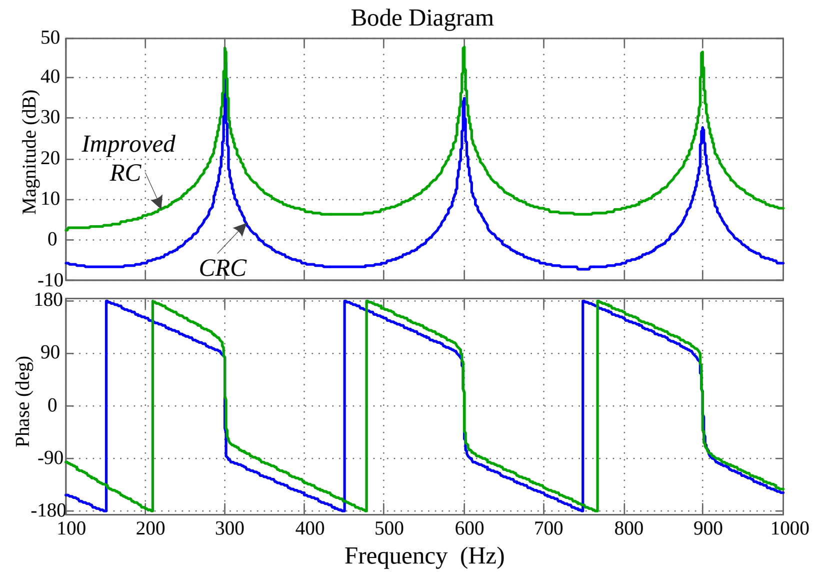

- ➢ **Improved RC has bandwidth and can deal with fractional delay**
- ➢ **Improved RC can deal with the dc offset, which can also be applied in direct resonant control**

Torque ripple suppression of DFIG-DC system

◆ Experimental results with improved repetitive controller

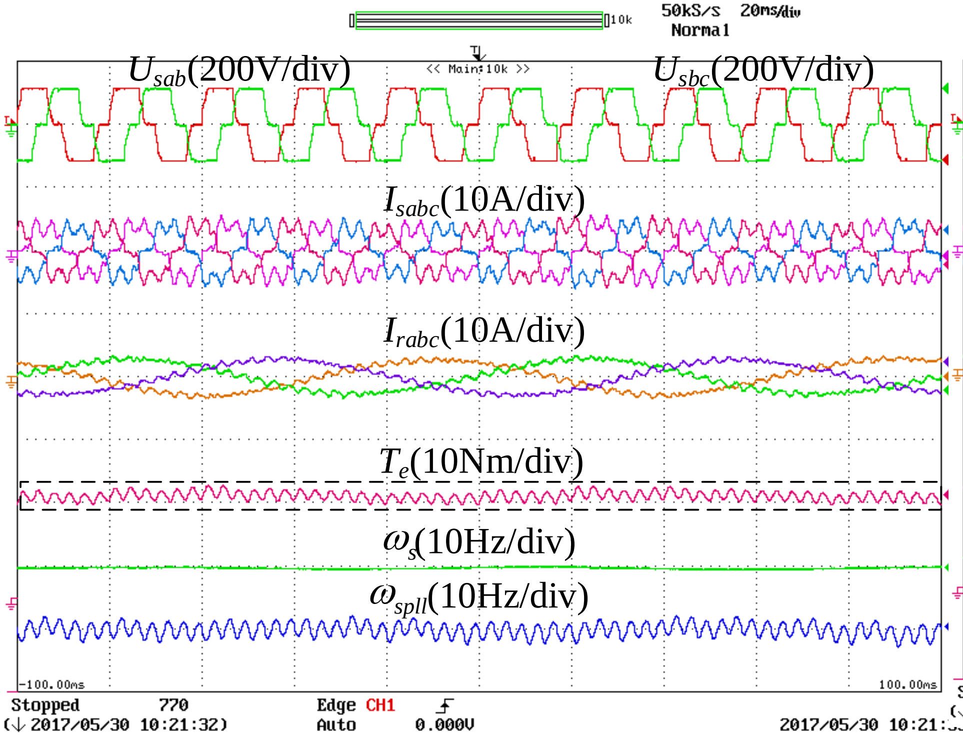

Without applying improved repetitive controller

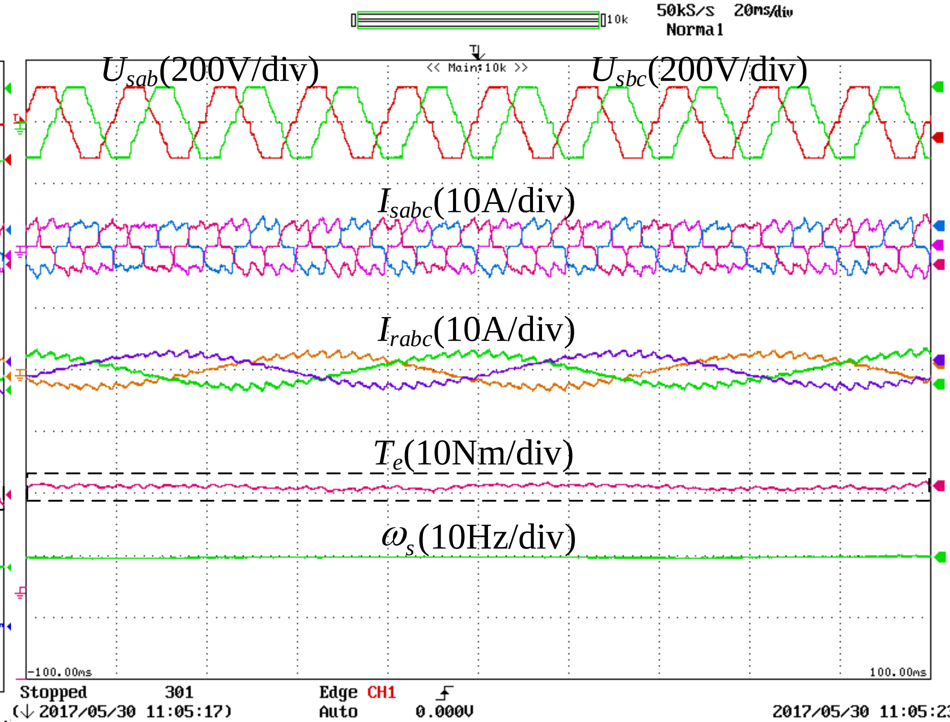

Applying improved repetitive controller

➢ **Improved repetitive controller can suppress the torque ripples**

Wu Chao, Nian Heng. An improved repetitive control of DFIG-DC system for torque ripple suppression[J]. IEEE Transactions on Power Electronics, 2018，33(9)：7634-7644.

Torque ripple suppression of DFIG-DC system

◆ Stator frequency variation for efficiency improvement

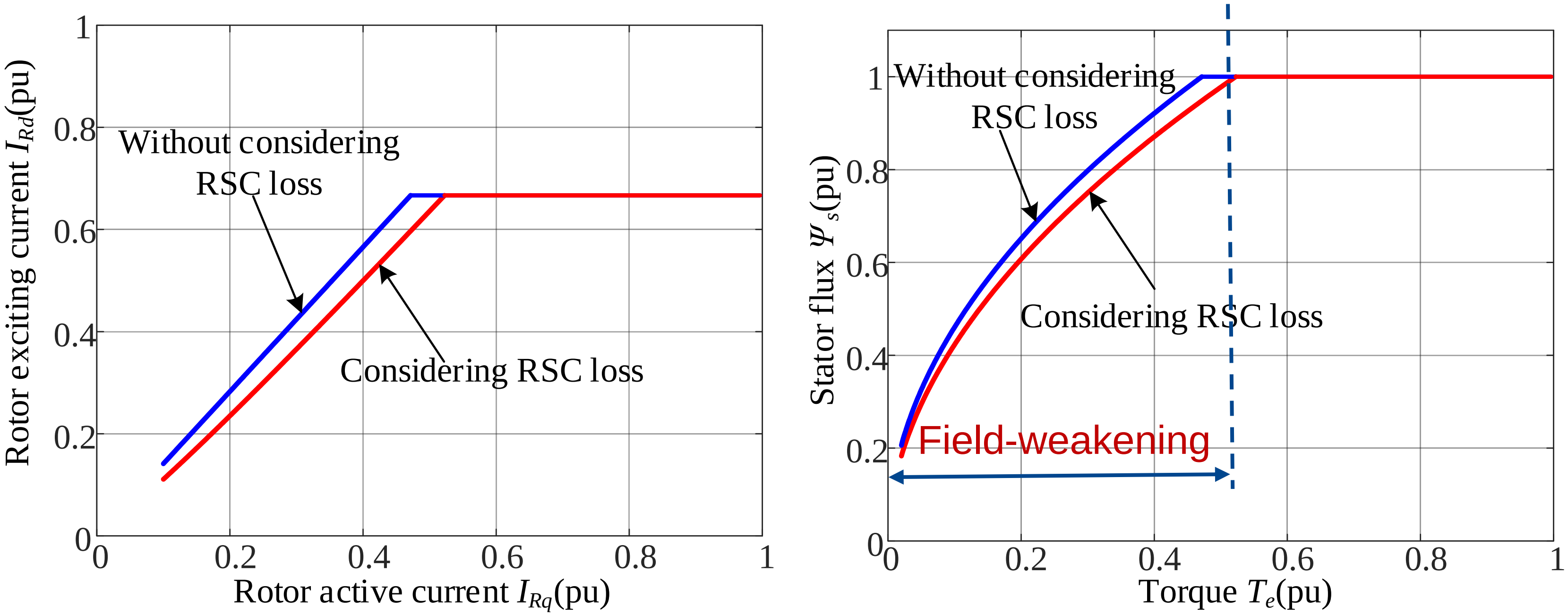

Relationship between rotor current and stator flux with efficiency optimization[1]

- ➢ **Field-weakening for efficiency optimization during low power, stator frequency will increase**
- ➢ **Frequency adaptive repetitive controller is necessary**

[1] Marques G D, Iacchetti M F. Field-weakening control for efficiency optimization in a DFIG connected to a DC-Link[J]. IEEE Transactions on Industrial Electronics, 2016. 63(6): 3409-3419.

Torque ripple suppression of DFIG-DC system

- **Design of adaptive repetitive controller**

$$G_{SOGI_h}(s)=\frac{kh\omega_1 s}{s^2+h^2\omega_1^2}$$

$$A(s)=\frac{U_{s\alpha1}}{U_{s\alpha}}=\frac{G_{SOGI_1}(s)}{1+\sum_{h=0,1,\dots}G_{SOGI_h}(s)}$$

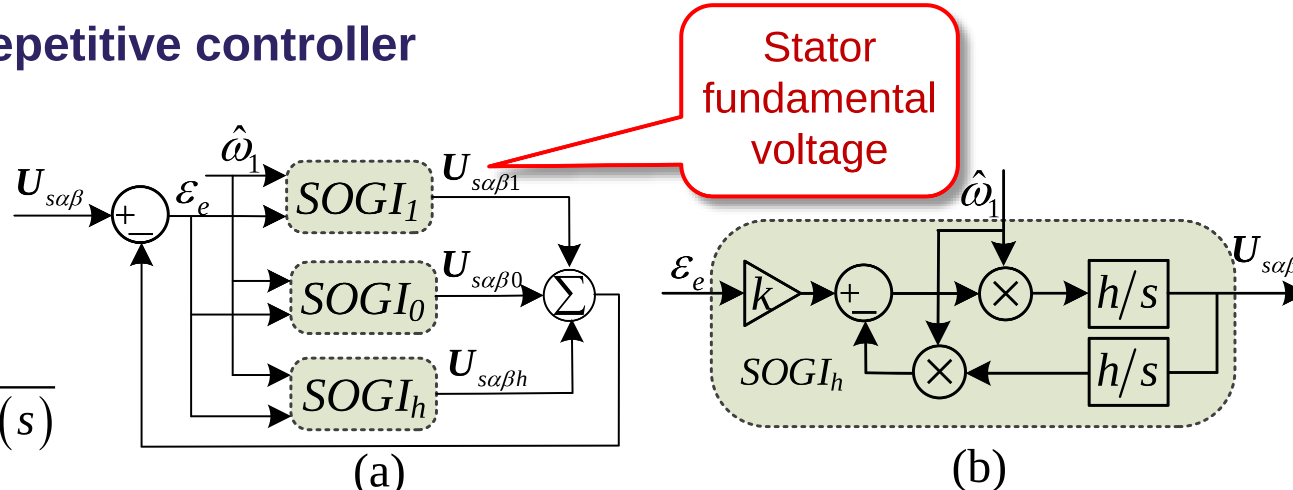

Acquiring stator fundamental voltage

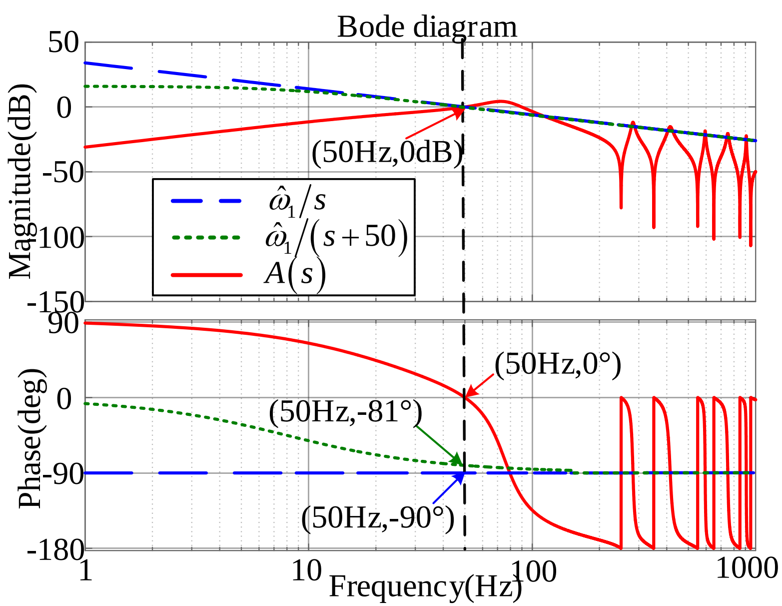

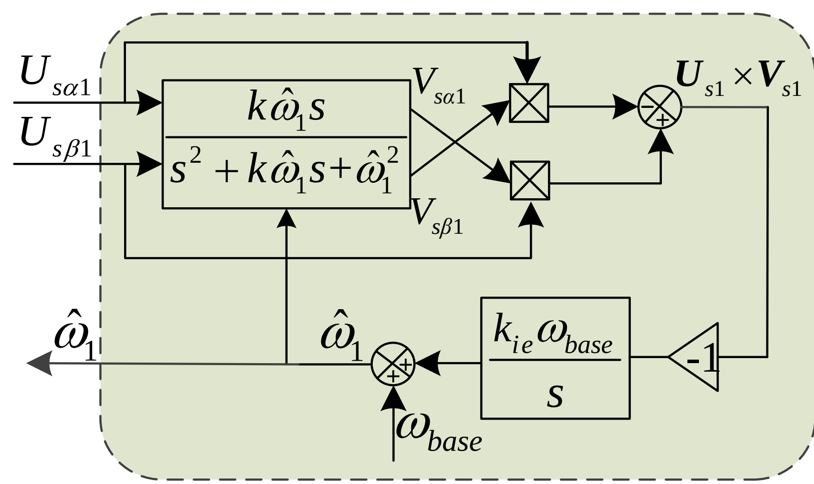

Acquiring stator frequency

Torque ripple suppression of DFIG-DC system

◆ **Design of adaptive repetitive controller**

Adaptitive repetitive controller (ARC)

$$G_{ARC}(z) = k_r \frac{z^{-N_i}\sum_{k=0}^{2} A_k z^{-k} Q(z)}{1 - z^{-N_i}\sum_{k=0}^{2} A_k z^{-k} Q(z)} G_f(z)$$

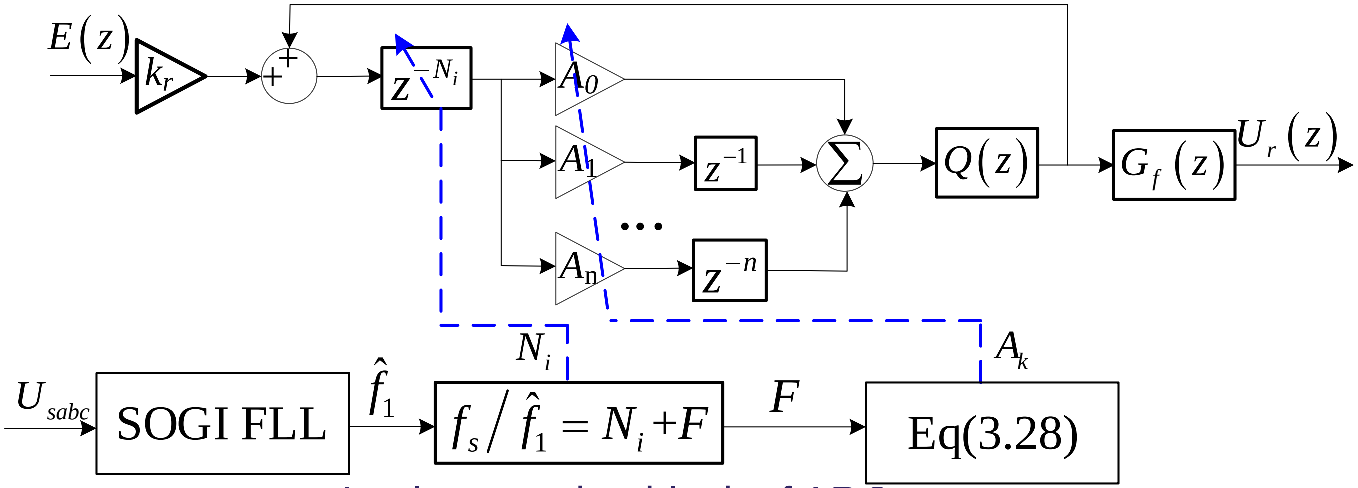

Implementation block of ARC

Output of ARC

$$\boldsymbol{U}_{rdq}^{ARC} = j \frac{z^{-N_i}\sum_{k=0}^{2} A_k z^{-k} Q(z)}{1 - z^{-N_i}\sum_{k=0}^{2} A_k z^{-k} Q(z)} G_f(z)(0 - T_e)$$

Rotor voltage reference

$$\boldsymbol{U}_{rdq}^{*} = \boldsymbol{U}_{rdq}^{PI} - \boldsymbol{U}_{rdq}^{ARC} + j\sigma L_r \omega_{sl} \boldsymbol{I}_{rdq}$$

Chao Wu, Heng Nian, Bo Pang, Peng Cheng. Adaptive repetitive control of DFIG-DC system considering stator frequency variation[J]. IEEE Transactions on Power Electronics，2019，34(4)：3302-3312.

Torque ripple suppression of DFIG-DC system

- **Experimental results with adaptive repetitive controller (ARC)**

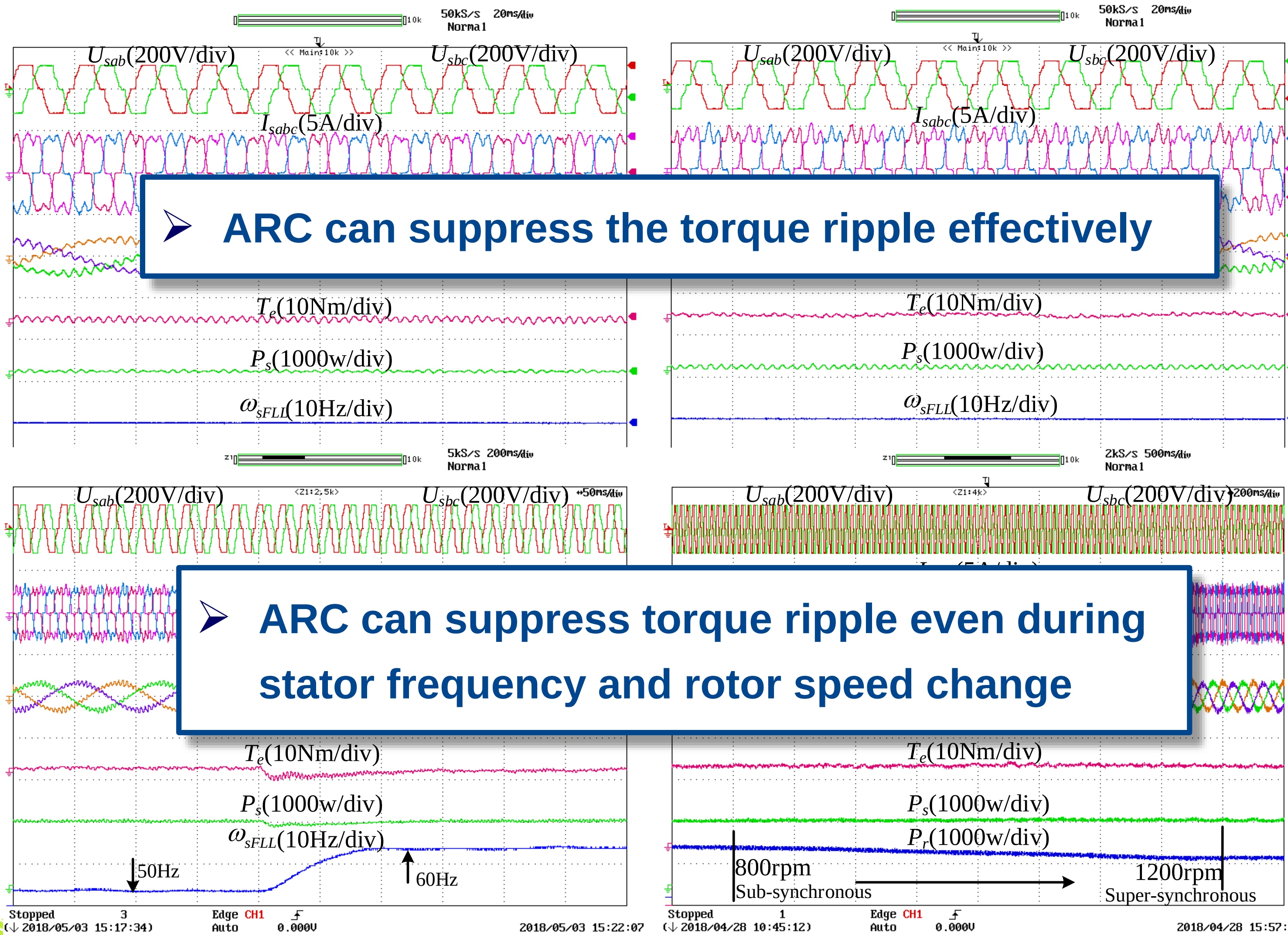

- **ARC can suppress the torque ripple effectively**
- **ARC can suppress torque ripple even during stator frequency and rotor speed change**

Efficiency optimization of DFIG-DC system

Efficiency improvement of DFIG-DC system

◆ Existed efficiency improvement methods

System loss
- Copper loss
- Iron loss

Without considering loss of harmonic currents

$$P_J = R_r I_r^2 + R_s I_s^2 + P_{inv0} I_r$$

$$P_{sh} = P_{sh0}\omega_s \psi_s^2, P_{se} = P_{se0}\omega_s^2 \psi_s^2$$

$$P_{rh} = P_{rh0}\omega_{sr} \psi_s^2, P_{re} = P_{re0}\omega_{sr}^2 \psi_s^2$$

$$EI_{mq} = P_{se} + P_{sh} + P_{re} + P_{rh}$$

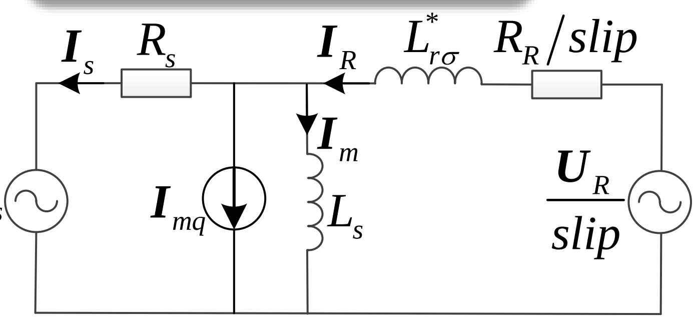

Equivalent circuit of DFIG

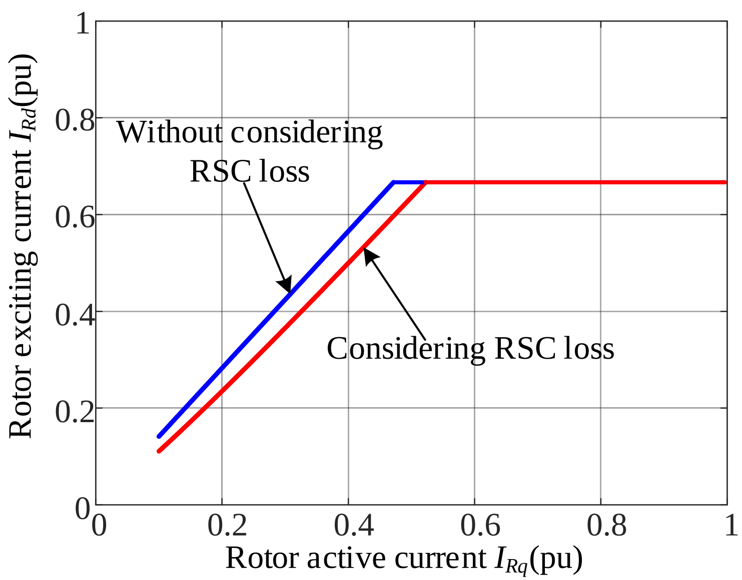

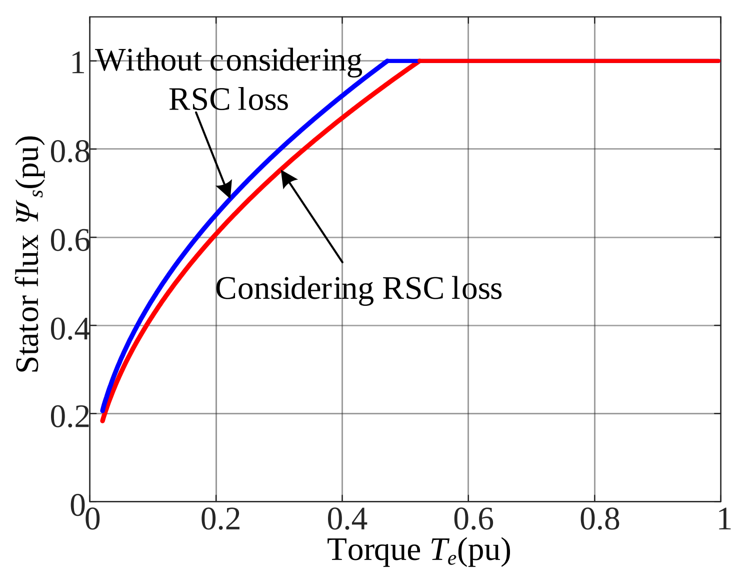

Relationship between rotor current and stator flux with efficiency optimization

Efficiency improvement of DFIG-DC system

◆ **Harmonic current analysis under distorted stator voltage**

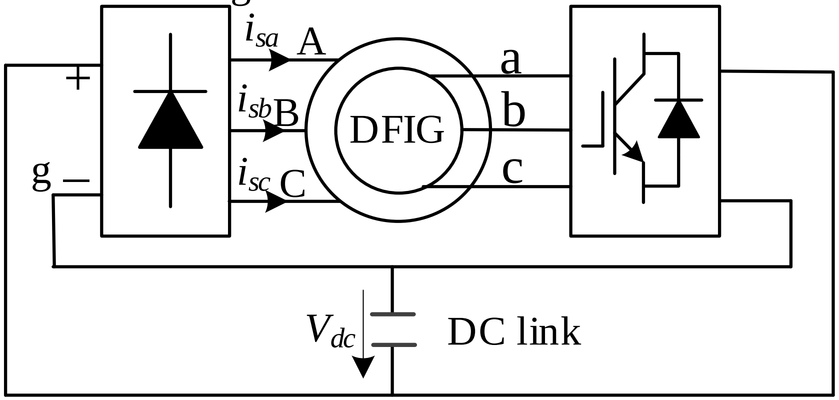

Open winding diagram of DFIG-DC system

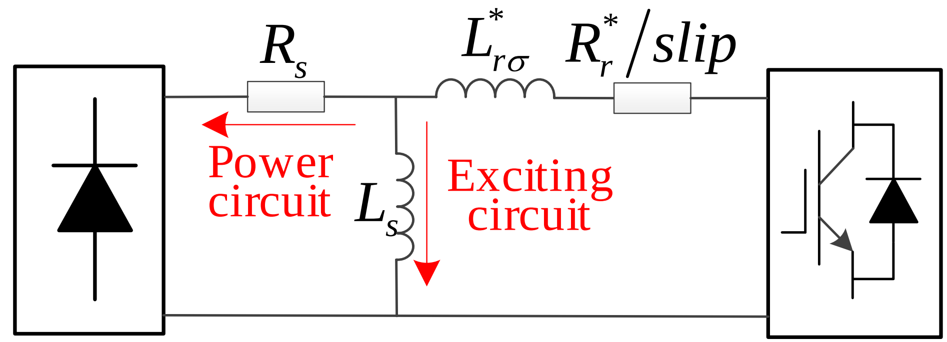

Γ-type equivalent circuit of DFIG

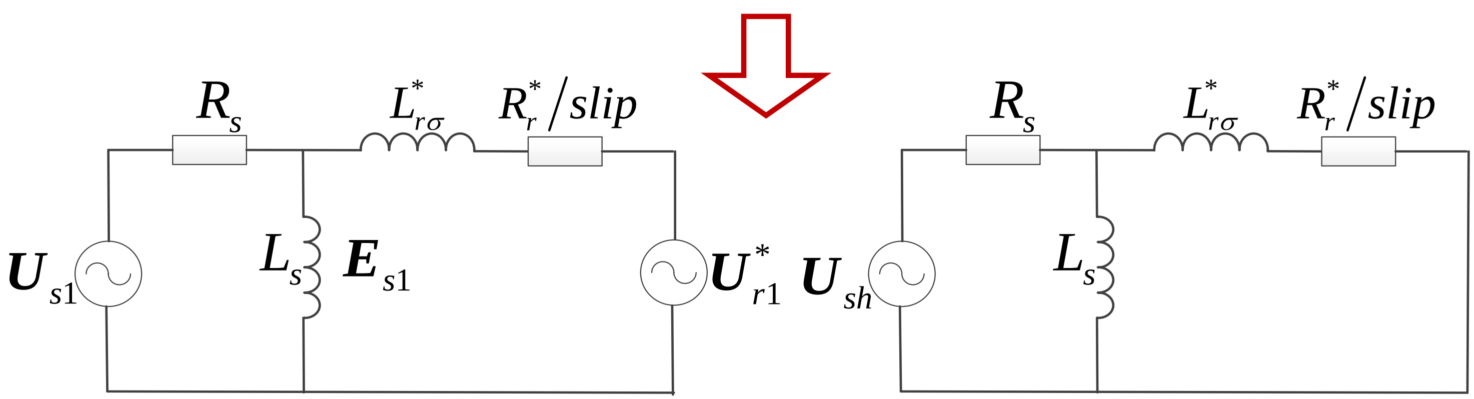

Fundamental current circuit Harmonic current circuit

Equivalent circuit of fundamental and harmonic currents

Efficiency improvement of DFIG-DC system

- **Harmonic current analysis under distorted stator voltage**

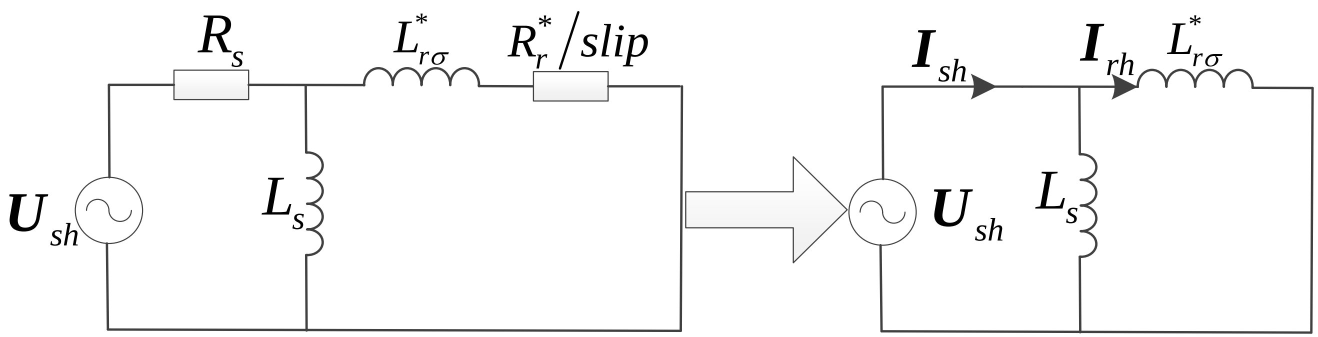

Harmonic current circuit   Simplified harmonic current circuit

When rotor side without injecting harmonic voltage, stator and rotor harmonic current

$$I_{sh} = \frac{U_{sh}}{j\sigma L_s h\omega_1}, \quad I_{rh} = \frac{L_m}{L_r}\frac{U_{sh}}{j\sigma L_s h\omega_1}$$

Where $\sigma = 1 - L_m^2 / L_s L_r$ leakage coefficient, h is harmonic order, ω_1=100π rad/s is stator fundamental freqeuncy

$$I_{shtot} = \frac{|U_{s1}|}{j\sigma L_s \omega_1}\sqrt{\sum_{n=1}^{\infty}\left(\frac{1}{(6n-1)^4}+\frac{1}{(6n+1)^4}\right)}$$

Total stator harmonic currents

$$I_{rhtot} = \frac{L_m}{L_r}\frac{|U_{s1}|}{j\sigma L_s \omega_1}\sqrt{\sum_{n=1}^{\infty}\left(\frac{1}{(6n-1)^4}+\frac{1}{(6n+1)^4}\right)}$$

Total rotor harmonic currents

Efficiency improvement of DFIG-DC system

◆ **Harmonic current analysis under distorted stator voltage**

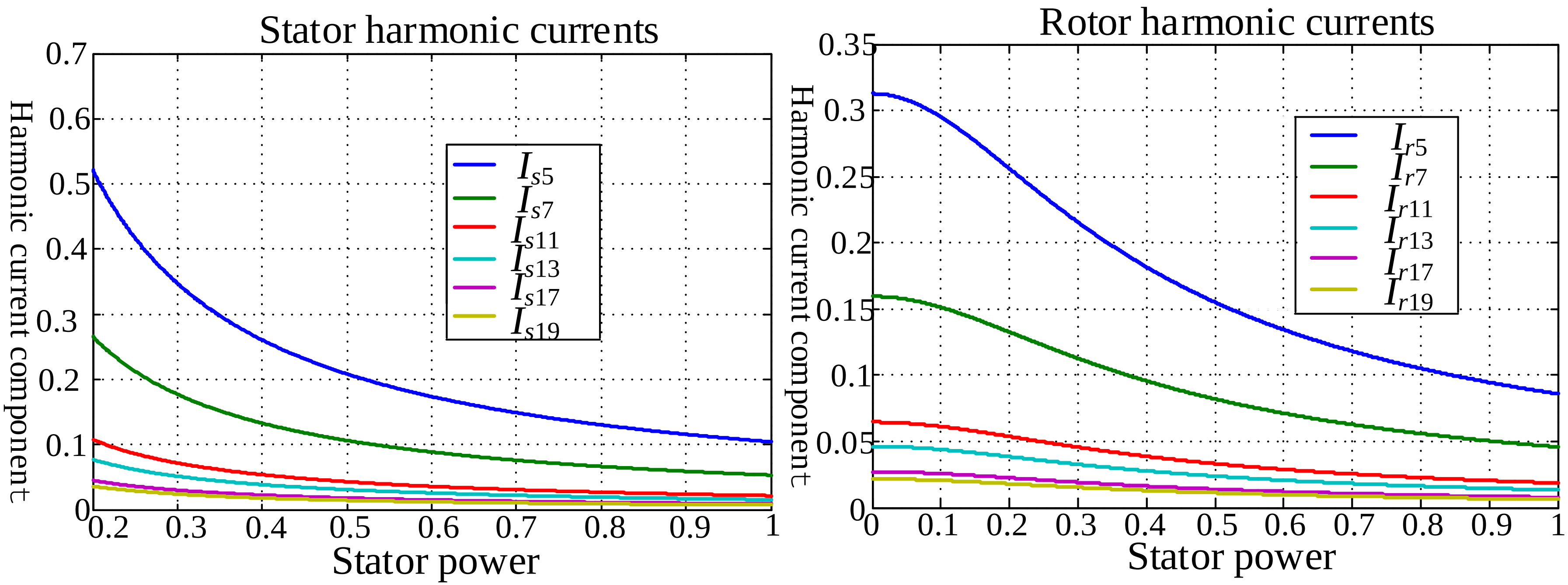

Harmonic currents in stator and rotor without rotor harmonic voltages

- **Both stator and rotor contain large harmonic currents;**
- **It is necessary to suppress the harmonic currents**

Efficiency improvement of DFIG-DC system

◆ Stator sinusoidal current control strategy

Stator harmonic current can be eliminated with appropriate rotor harmonic voltage injection

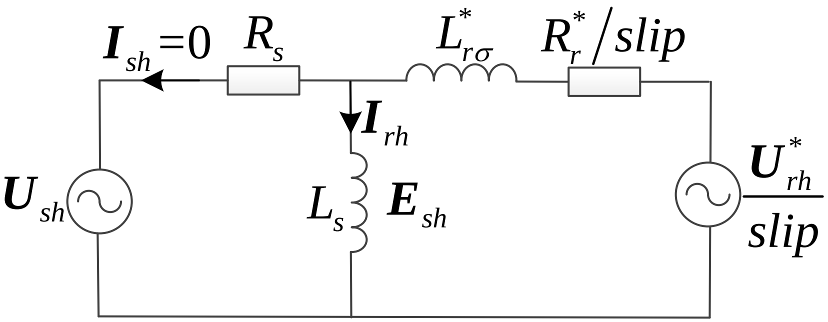

$$\frac{U^*_{rh}}{slip} = \frac{L_s + L^*_{r\sigma}}{L_s} * U_{sh} \qquad slip = \frac{s - j\omega_r}{s}$$

$$U_{rdqh} = \frac{s + j\omega_1 - j\omega_r}{s + j\omega_1} * \frac{L_r}{L_m} U_{sdqh}$$

$$U_{rdqh} = \frac{s^2 + \omega_1\omega_{sl} - j\omega_r s}{s^2 + \omega_1^2} * \frac{L_r}{L_m} U_{sdqh}$$

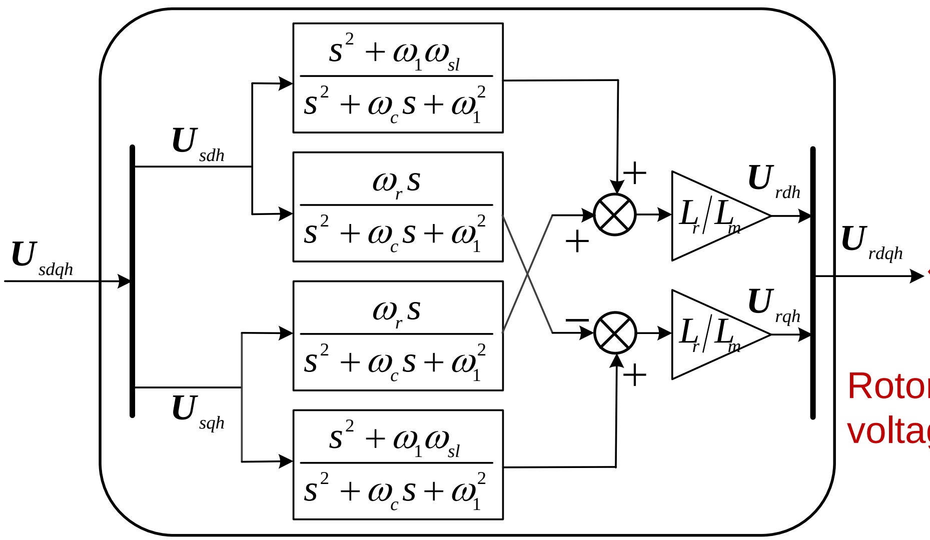

Rotor harmonic
voltage generator

Efficiency improvement of DFIG-DC system

◆ Stator sinusoidal current control strategy

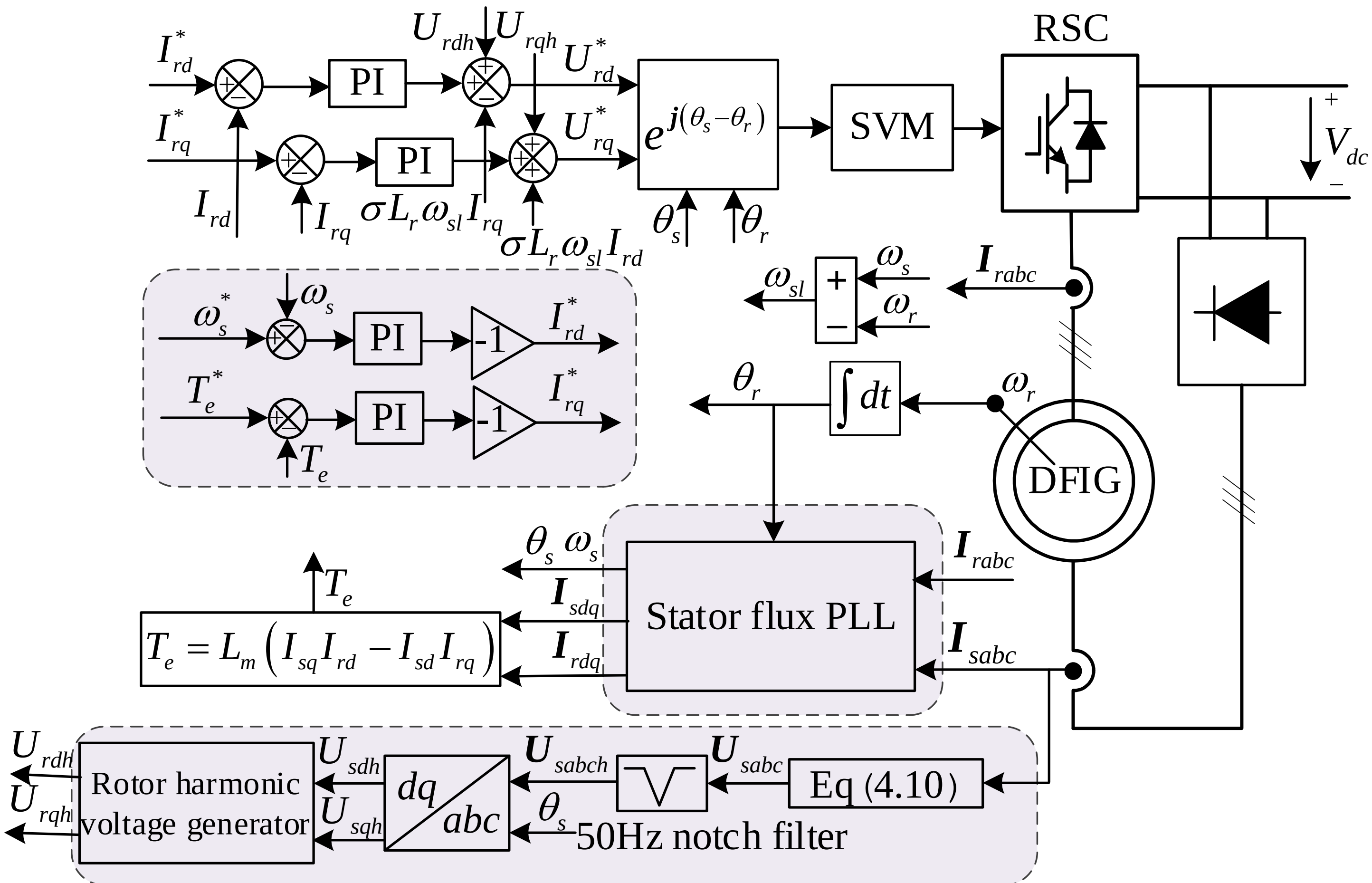

Chao Wu, Heng Nian. Sinusoidal current operation of DFIG-DC system without stator voltage sensors[J]. IEEE Transactions on Industrial Electronics, 2018，65(8)：6250-6258.

Efficiency improvement of DFIG-DC system

◆ **Experimental results of stator sinusoidal current control strategy**

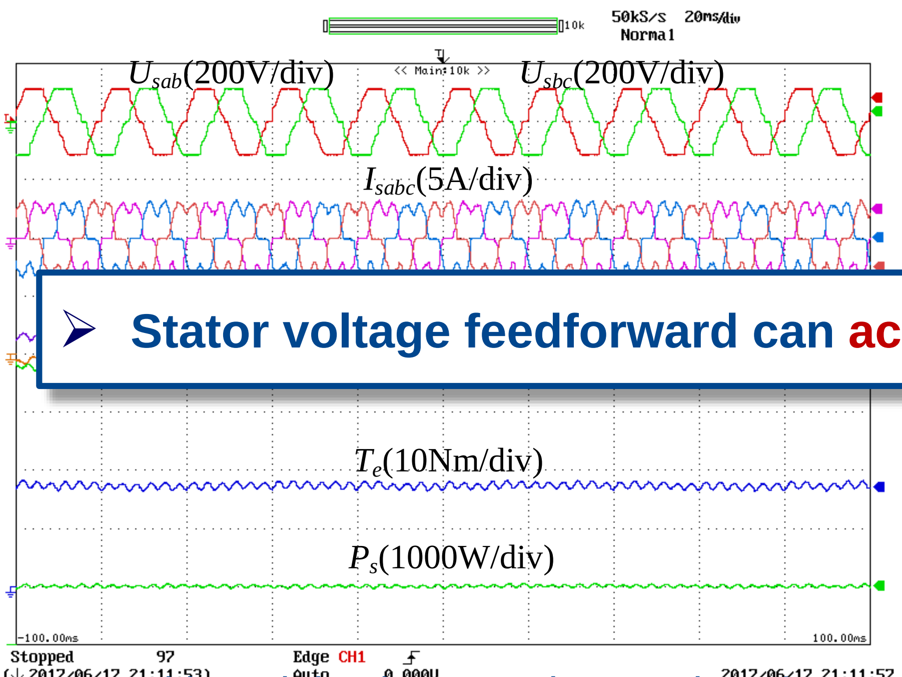

Without injecting rotor harmonic voltages

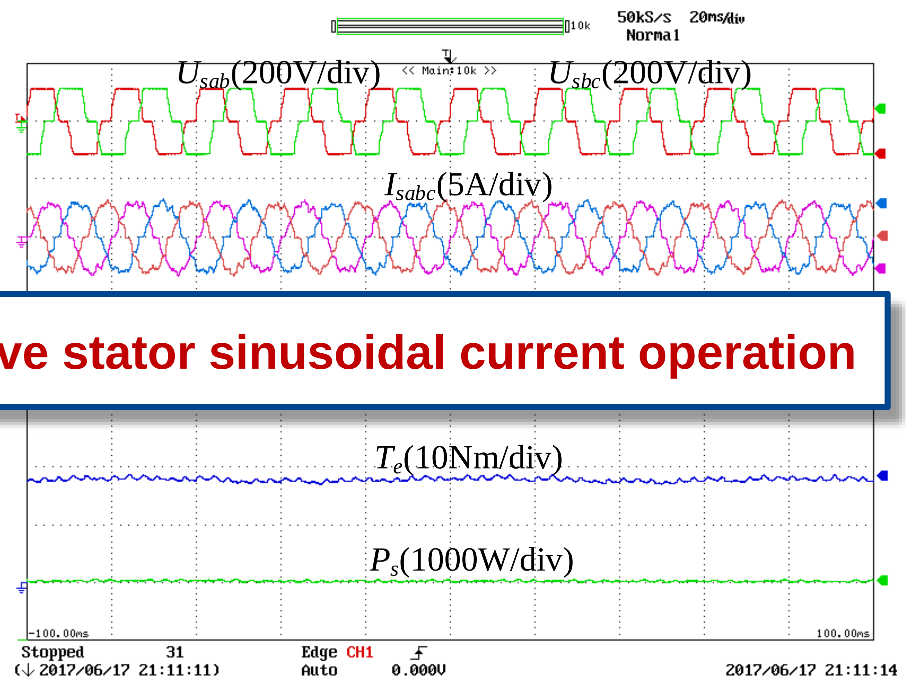

With injecting rotor harmonic voltages

➢ **Stator voltage feedforward can achieve stator sinusoidal current operation**

		5	7	11	13	17	19
Without compensator	I_{sh}/I_{s1}	22.87%	7.18%	5.86%	3.36%	0.98%	1.02%
	I_{rh}/ I_{r1}	14.95%	2.54%	3.40%	2.40%	0.51%	0.59%
With compensator	I_{sh}/I_{s1}	4.38%	2.11%	2.84%	1.65%	0.79%	0.84%
	I_{rh}/I_{r1}	1.40%	1.25%	1.40%	1.26%	0.47%	0.53%

Efficiency improvement of DFIG-DC system

◆ **Experimental results of stator sinusoidal current control strategy**

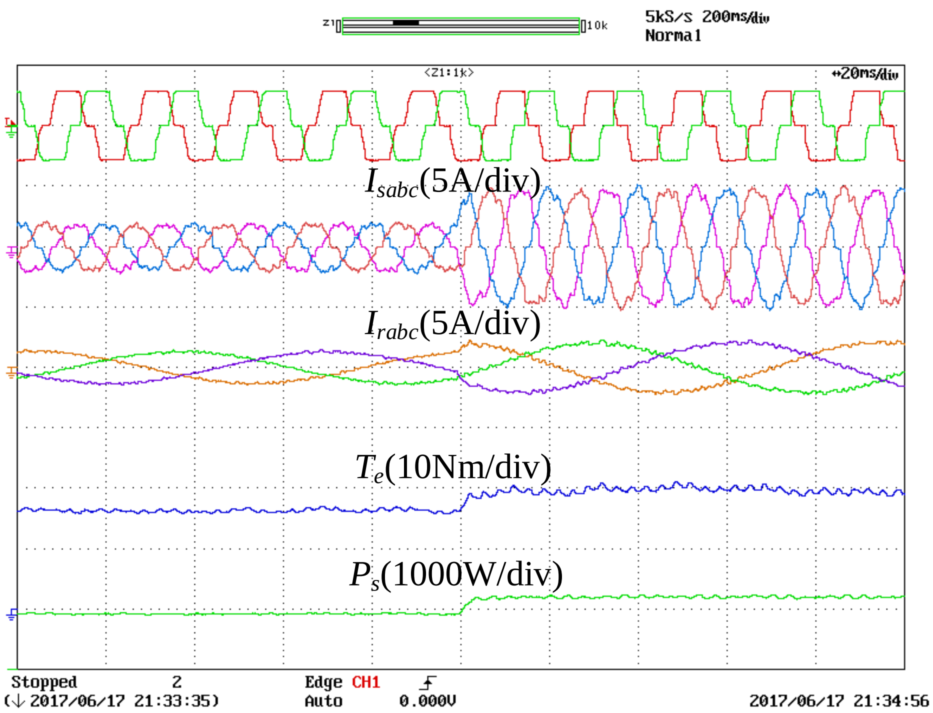

Step response with torque change

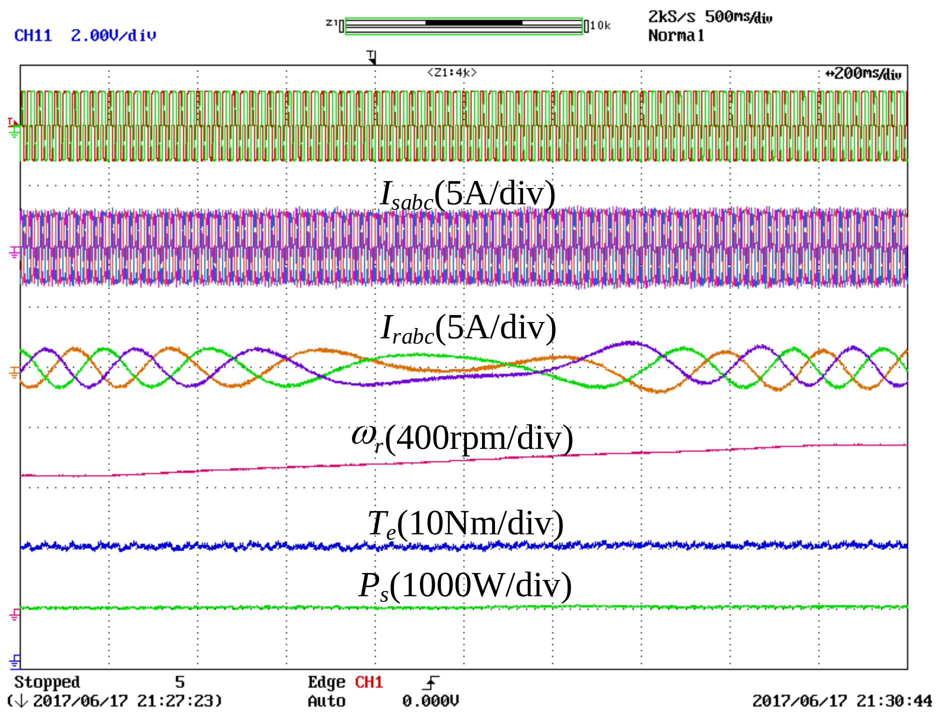

Rotor speed change

➢ **Stator voltage feedforward works well during dynamic process**

Efficiency improvement of DFIG-DC system

◆ Harmonic current analysis with direct torque resonant control

Stator voltage is step wave，torque can be expressed as：

$$T_e = \frac{L_m}{L_s}\left(I_{rd}\psi_{sq} - I_{rq}\psi_{sd}\right) = \left(I_{rd0} + \sum_{n=1}^{\infty} I_{rd6n}\right)\left(\psi_{sq0} + \sum_{n=1}^{\infty}\psi_{sq6n}\right) - \left(I_{rq0} + \sum_{n=1}^{\infty} I_{rq6n}\right)\left(\psi_{sd0} + \sum_{n=1}^{\infty}\psi_{sd6n}\right)$$

Subscript 0 represents dc component，subscript 6*n* represents harmonic component

Stator flux oriented in d-axis，stator q-axis fundamental flux Ψ_{sq0} equal to 0

$$T_e = \frac{L_m}{L_s}\left(-\left(\psi_{sd0} I_{rq0}\right) - \left(\psi_{sd0}\sum_{n=1}^{\infty} I_{rq6n} + I_{rq0}\sum_{n=1}^{\infty}\psi_{sd6n} - I_{rd0}\sum_{n=1}^{\infty}\psi_{sq6n}\right) - \left(\sum_{n=1}^{\infty}\psi_{sd6n}\sum_{n=1}^{\infty} I_{rq6n} - \sum_{n=1}^{\infty}\psi_{sq6n}\sum_{n=1}^{\infty} I_{rd6n}\right)\right)$$

Average torque

Torque ripples at different frequencies

Small terms(ignore)

Torque ripple：

$$T_{eh} = \frac{L_m}{L_s}\left(-\psi_{sd0}\sum_{n=1}^{\infty} I_{rq6n} - I_{rq0}\sum_{n=1}^{\infty}\psi_{sd6n} + I_{rd0}\sum_{n=1}^{\infty}\psi_{sq6n}\right)$$

Operation point

Conclusion：torque ripple is only determined by q-axis harmonic current

Efficiency improvement of DFIG-DC system

◆ **Double-axis direct resonant control strategy**

Relationship between stator and rotor harmonic current：

$$I_{sdh} = -\frac{L_m}{L_s} I_{rdqh} + \frac{1}{L_s}\psi_{sdqh}$$

q-axis(active power axis)for suppressing torque ripple：

$$U_{rq}^{m} = G_{rpc}(s)\left(T_e^{*} - T_e\right)$$

d-axis(reactive power axis)for suppressing d-axis harmonic currents：

$$U_{rd}^{m} = G_{rpc}(s)\left(I_{sdh}^{*} - I_{sdh}\right)$$

Rotor harmonic voltage reference：

$$\boldsymbol{U}_{rdq}^{m} = G_{rpc}(s)\left(I_{sdh}^{*} - I_{sdh}\right) + jG_{rpc}(s)\left(T_e^{*} - T_e\right)$$

Total rotor voltage reference：

$$\boldsymbol{U}_{rdq}^{*} = \boldsymbol{U}_{rdq}^{PI} - \boldsymbol{U}_{rdq}^{m} + j\sigma L_r \omega_{sl} \boldsymbol{I}_{rdq}$$

Efficiency improvement of DFIG-DC system

◆ Double-axis direct resonant control strategy

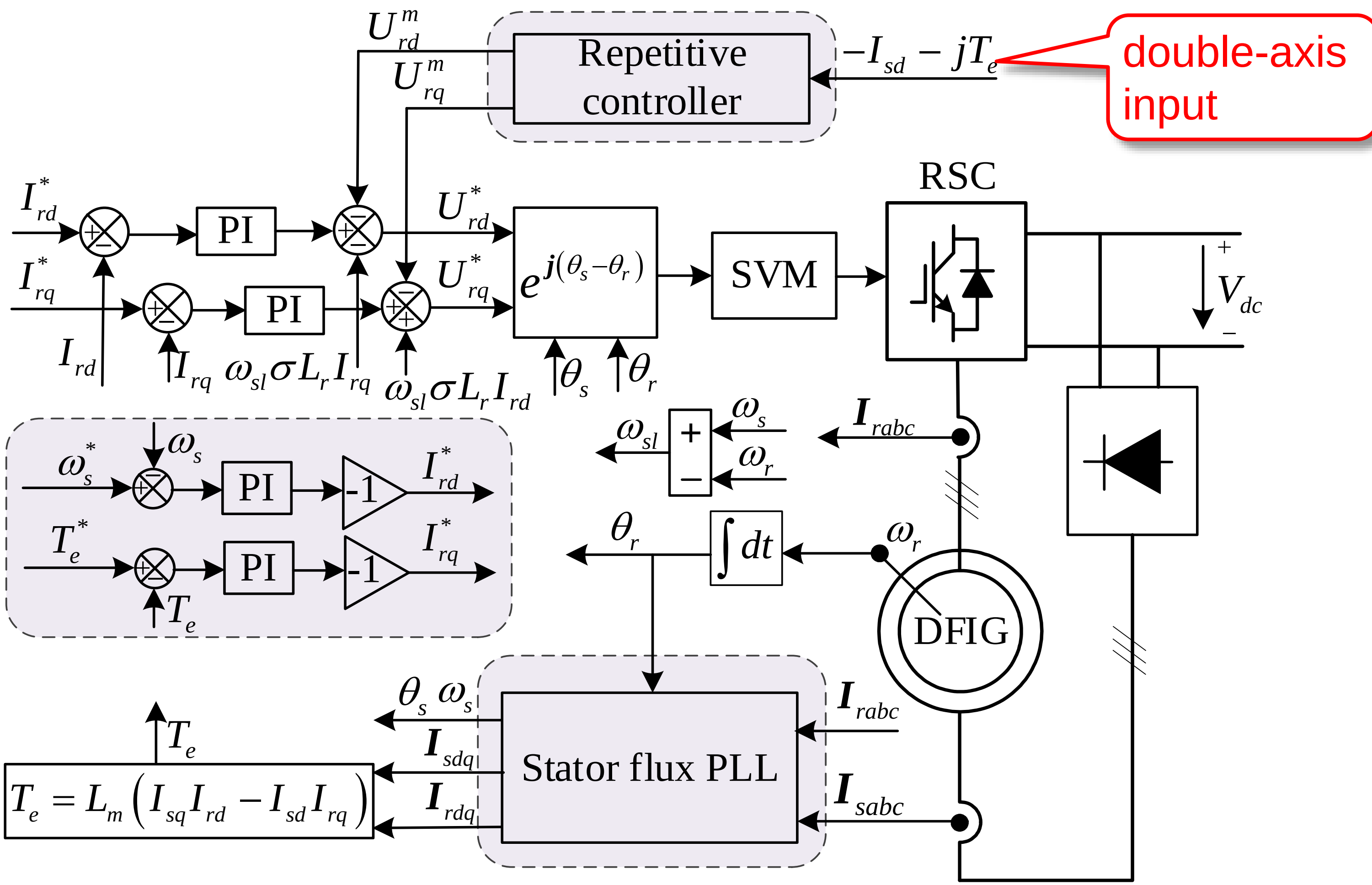

Wu Chao, Nian Heng. Improved direct resonant control for suppressing torque ripple and reducing harmonic current losses of DFIG-DC system[J]. IEEE Transactions on Power Electronics，accepted，2018

Efficiency improvement of DFIG-DC system

◆ Performance analysis of double-axis direct resonant control strategy

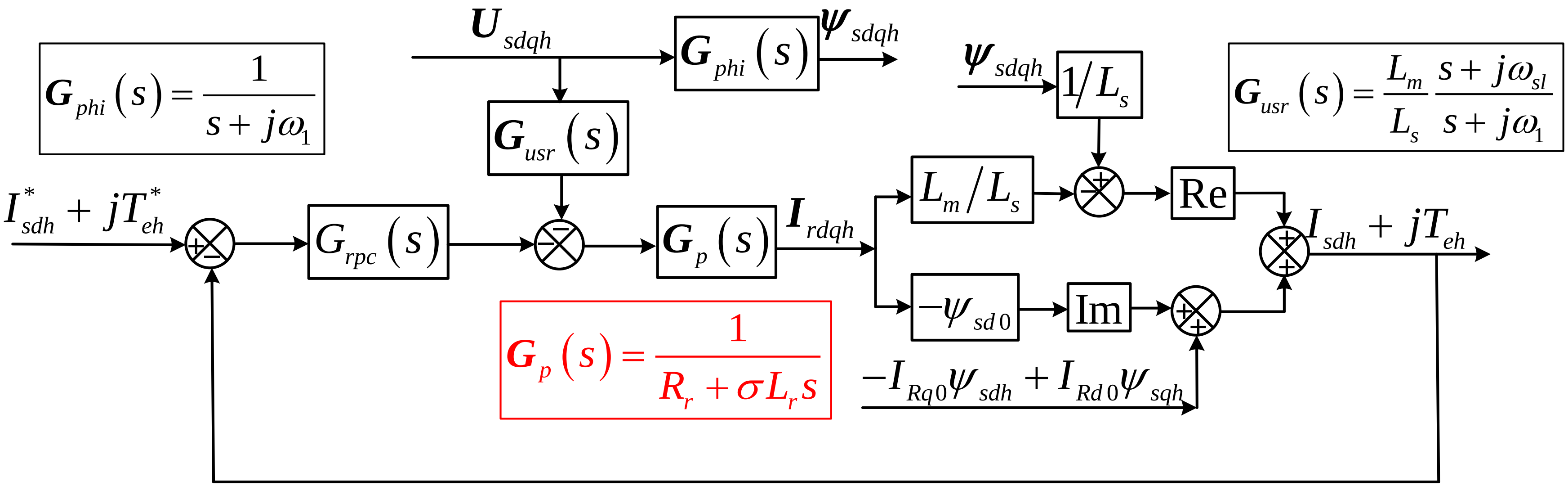

$$I_{sdh}=\mathrm{Re}\left(\frac{L_m}{L_s}\frac{G_{rpc}(s)\boldsymbol{G}_p(s)}{1+G_{rpc}(s)\boldsymbol{G}_p(s)}\left(I^*_{sdh}+jT^*_{eh}\right)+\frac{1/L_s\,\boldsymbol{G}_{phi}(s)+L_m/L_s\,\boldsymbol{G}_{usr}(s)\boldsymbol{G}_p(s)}{1+G_{rpc}(s)\boldsymbol{G}_p(s)}\boldsymbol{U}_{sdqh}\right)$$

$$I_{sdh}=\frac{L_m}{L_s}\frac{G_{rpc}(s)\boldsymbol{G}_p(s)}{1+G_{rpc}(s)\boldsymbol{G}_p(s)}I^*_{sdh}+\mathrm{Re}\left(\frac{1/L_s\,\boldsymbol{G}_{phi}(s)+L_m/L_s\,\boldsymbol{G}_{usr}(s)\boldsymbol{G}_p(s)}{1+G_{rpc}(s)\boldsymbol{G}_p(s)}\boldsymbol{U}_{sdqh}\right)$$

> ➢ **d-axis harmonic current has no relationship with torque ripple**

Efficiency improvement of DFIG-DC system

- **Harmonic currents comparison between different direct resonant control strategies**

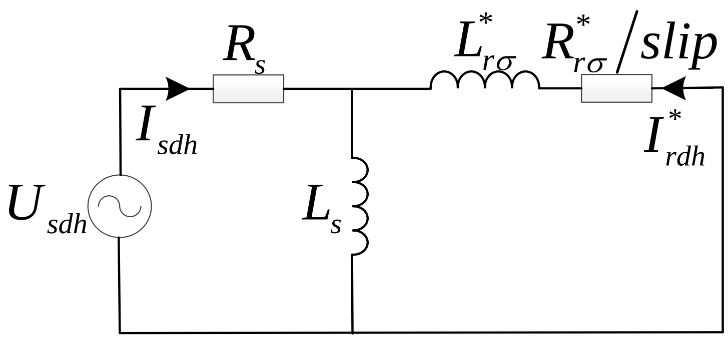

(a)without adding rotor harmonic voltage

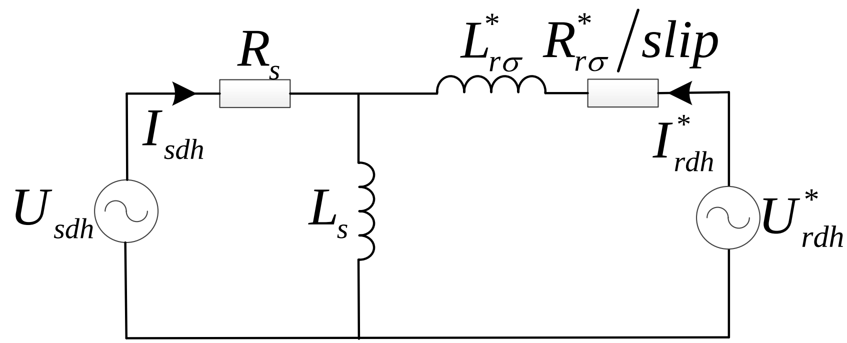

(b)adding rotor harmonic voltage

$$I^*_{rdh} = I_{sdh} = \frac{U_{sqh}}{h\omega_1 L^*_{r\sigma}}$$

Leakage inductance

$$I_{sdh} = 0, \quad I^*_{rdh} = \frac{U_{sqh}}{h\omega_1 L_s}$$

Stator inductance

Stator harmonic voltage

$$U_{sdh} = -\sum_{n=1}^{\infty}\left(\left|u_{s(6n+1)}\right| + \left|u_{s(6n-1)}\right|\right)\sin\left(6\omega_s t\right)$$

$$U_{sqh} = \sum_{n=1}^{\infty}\left(\left|u_{s(6n+1)}\right| - \left|u_{s(6n-1)}\right|\right)\cos\left(6\omega_s t\right)$$

Stator harmonic flux

$$\psi_{sdh} = \sum_{n=1}^{\infty}\frac{\left|u_{s7}\right|}{7\omega_s}\cos\left(6\omega_s t\right) + \frac{\left|u_{s5}\right|}{5\omega_s}\cos\left(6\omega_s t\right)$$

$$\psi_{sqh} = \sum_{n=1}^{\infty}\frac{\left|u_{s7}\right|}{7\omega_s}\sin\left(6\omega_s t\right) - \frac{\left|u_{s5}\right|}{5\omega_s}\sin\left(6\omega_s t\right)$$

Efficiency improvement of DFIG-DC system

- **Harmonic currents comparison between different direct resonant control strategies**

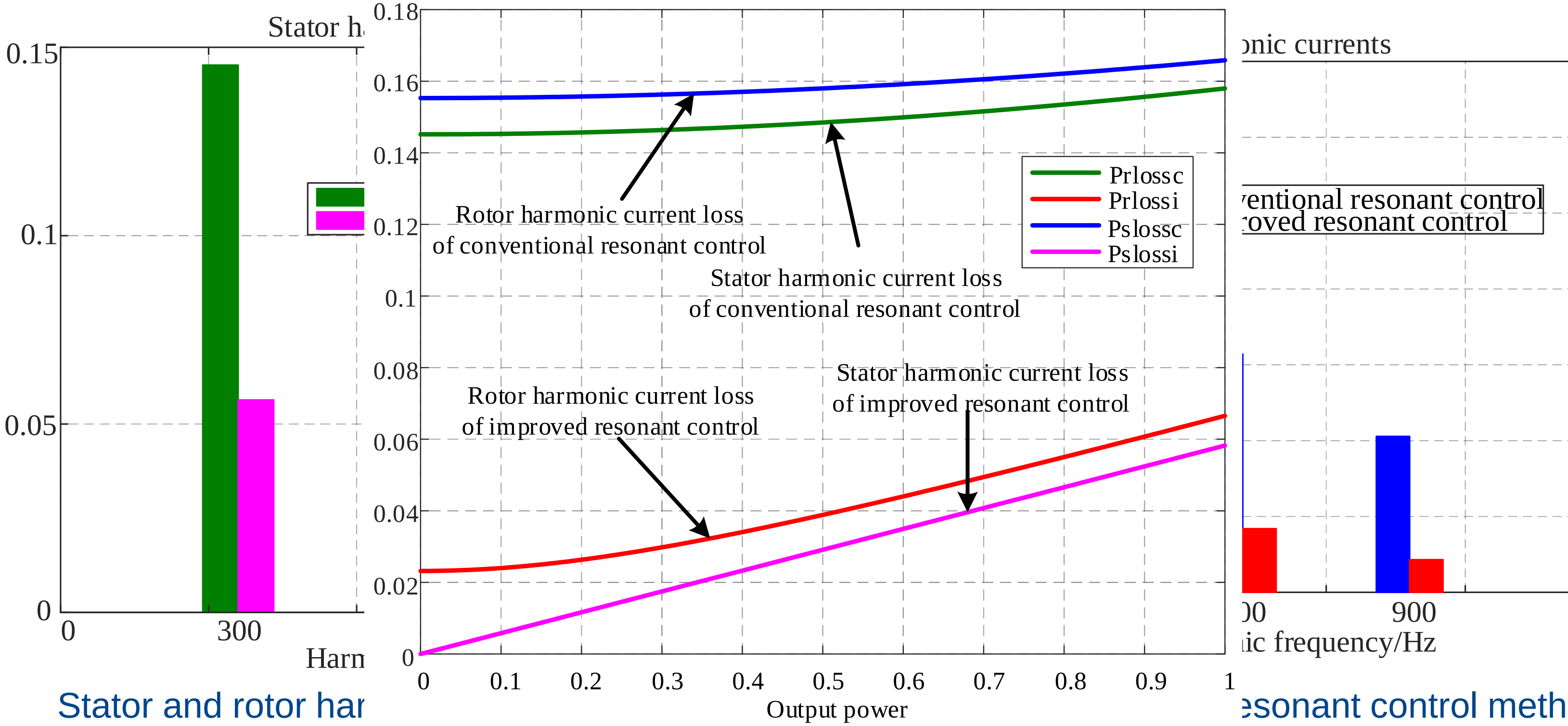

Stator and rotor har… …esonant control methods

> **Double-axis direct resonant control can effectively reduce harmonic currents；**

Efficiency improvement of DFIG-DC system

◆ Comparison between different methods

Performance / Method	torque ripple suppression	parameter dependency	harmonic current mitigation
Indirect resonant control [13]	effective	high	no
Conventional direct resonant control [14]-[16]	effective	low	no
Predictive control [17] [20]	effective	high	no
Double-axis direct resonant control	effective	low	yes

> ➢ **Double-axis direct resoant control can simultaneously suppress torque ripple and reduce harmonic currents**

Chao Wu, Heng Nian. Improved direct resonant control for suppressing torque ripple and reducing harmonic current losses of DFIG-DC system[J]. IEEE Transactions on Power Electronics，vol. 34, no.9, pp. 8739-8748, Sep. 2019.

Efficiency improvement of DFIG-DC system

◆ Experimental results of double-axis direct resonant control strategy

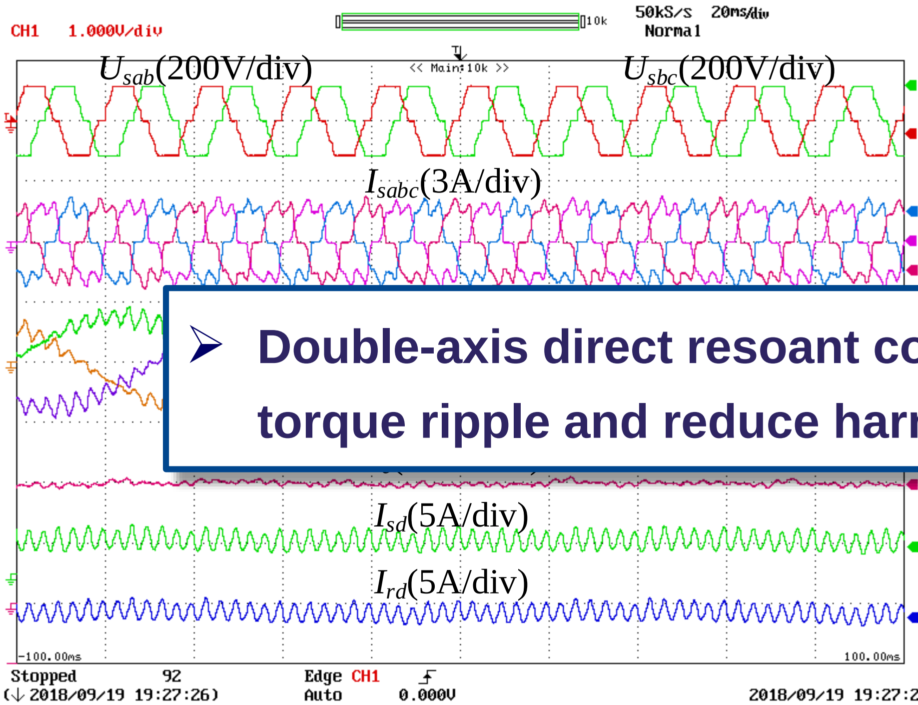

Single-axis direct resonant control

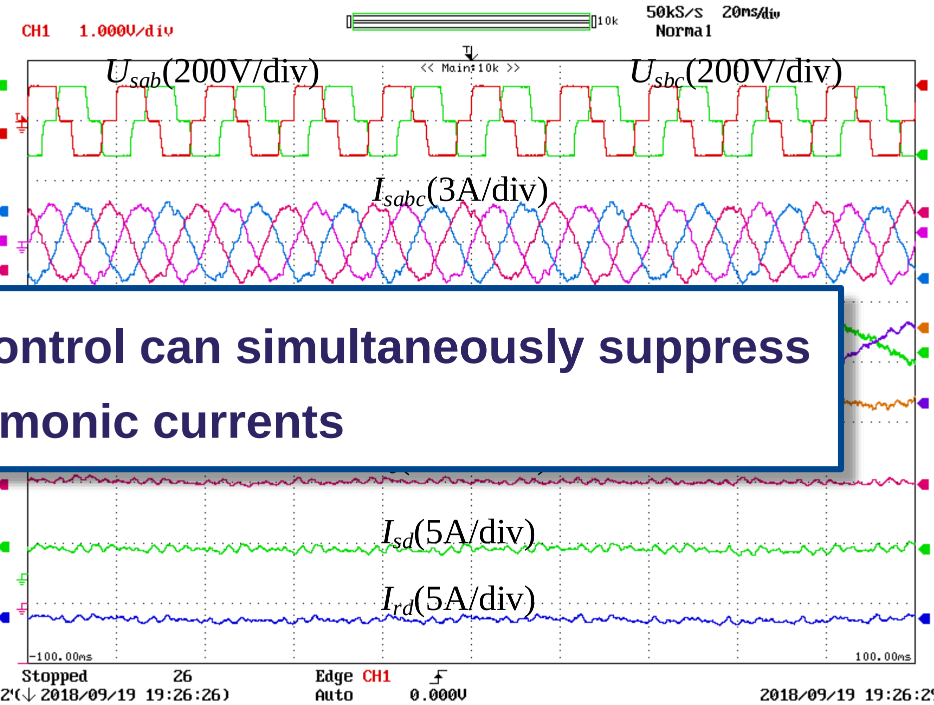

Double-axis direct resonant control

- **Double-axis direct resoant control can simultaneously suppress torque ripple and reduce harmonic currents**

The THD of stator and rotor current and torque with different control methods

THD	Without resonant control	Conventional direct resonant control	Improved direct resonant control
Stator current	24.23%	22.45%	8.44%
Rotor current	16.55%	15.32%	6.35%
Torque	5.86%	0.95%	0.94%

Efficiency improvement of DFIG-DC system

◆ **Experimental results of double-axis direct resonant control strategy**

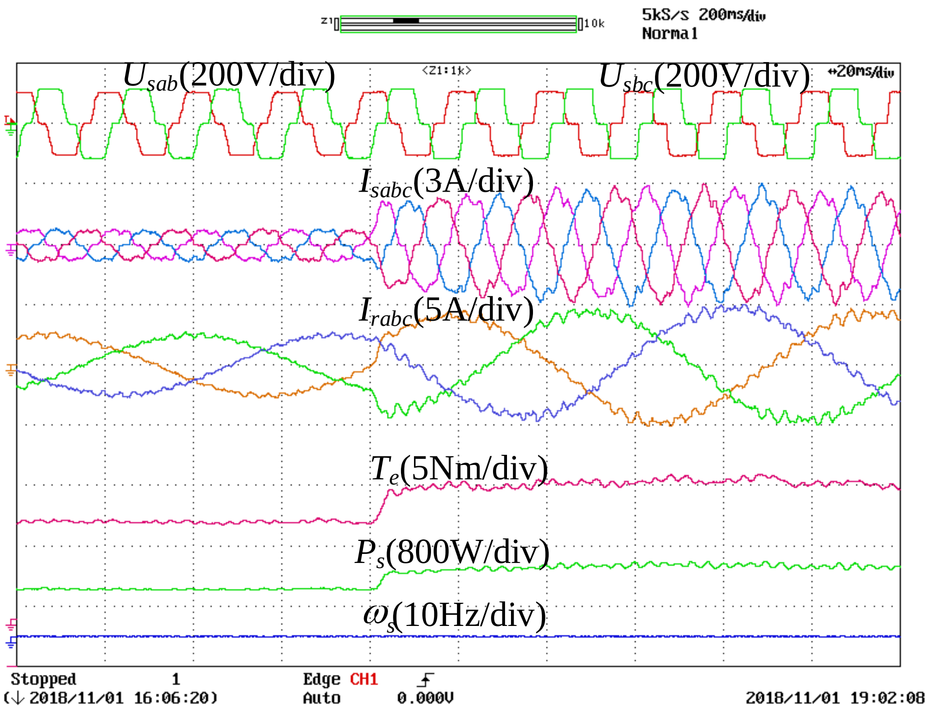

Step response with torque change

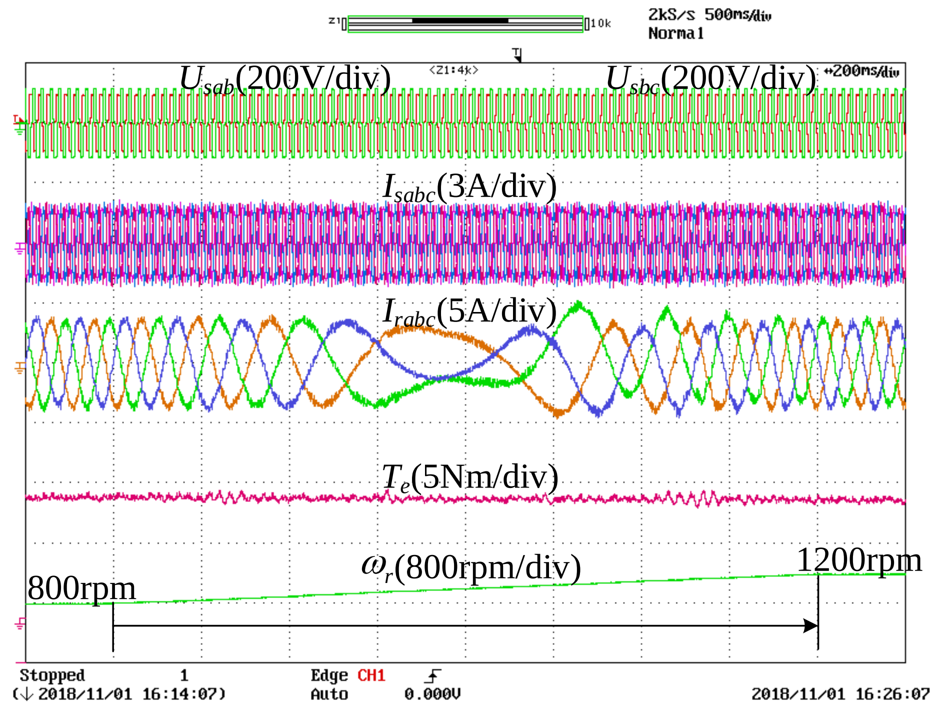

Rotor speed change

➢ **Double-axis direct resonant control method can simultaneously mitigate the torque ripple and harmonic currents during dynamic process**

Robust control of DFIG-DC system

Robust control of DFIG-DC system

◆ Recap of DFIG-DC system

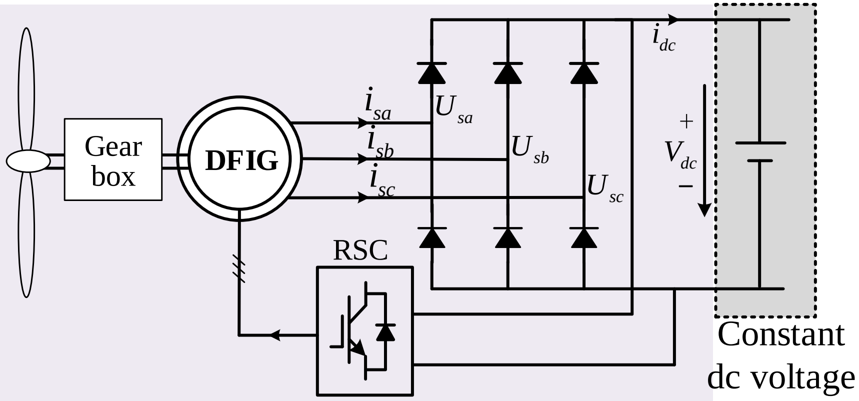

Detailed configuration of DFIG-DC system

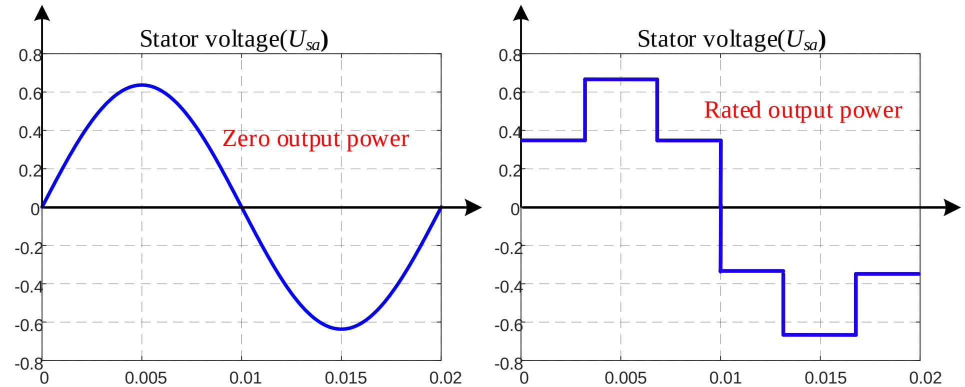

Variation of stator voltage from zero to rated output power

How to deal with the diode bridge?

Is it a problem? ⇒ **Challenges and opportunities coexist**

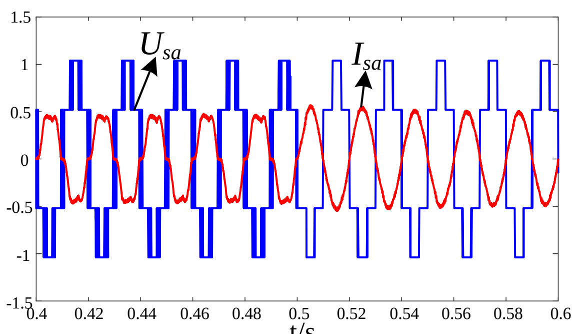

The relationship between stator voltage and current

The potential advantages

1. Stator frequency as a degree of freedom
2. Stator fundamental voltage is constant
3. Stator current and stator voltage are in the same phase

Robust control of DFIG-DC system

◆ Existing methods-Stator Flux Orientated Control

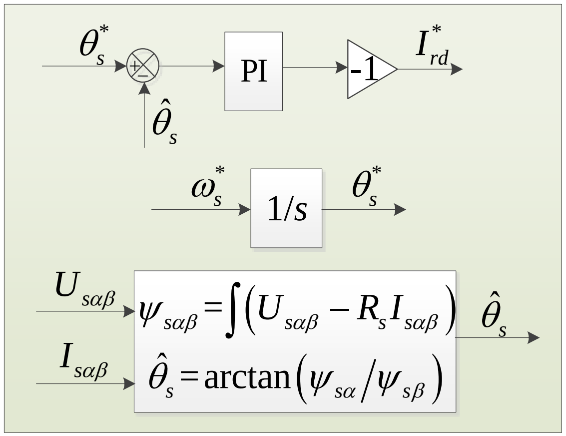

Stator flux angle control [1]

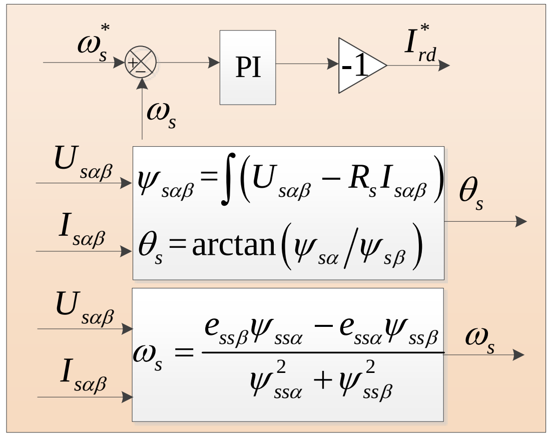

Stator frequency control [2]

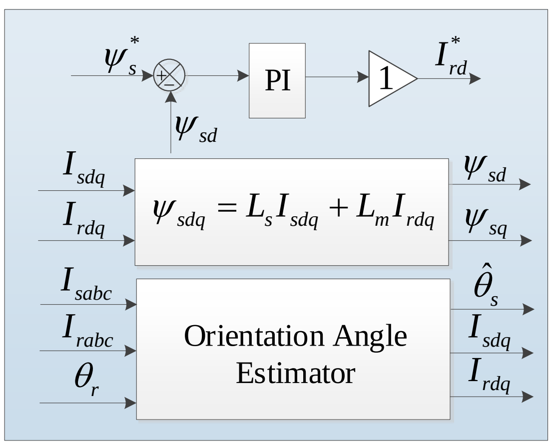

Stator flux magnitude control [3]

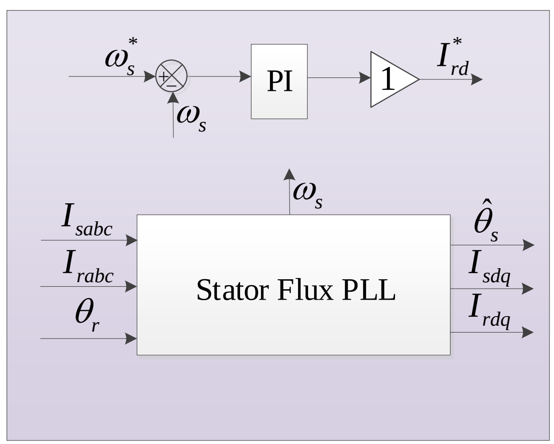

Stator flux PLL [4]

Objectives

- Vector control
- Decoupling control of stator frequency and output power

Drawbacks

- Dc sampling offset
- Parameter dependency
- Stator voltage and current sensors

Reference

[1] G.D. Marques and M.F. Iacchetti, Stator Frequency Regulation in a Field-Oriented Controlled DFIG Connected to a DC Link. *IEEE Transactions on Industrial Electronics*, 2014. 61(11): p. 5930-5939.
[2] M.F. Iacchetti, Marques G.D. and R. Perini, Torque Ripple Reduction in a DFIG-DC System by Resonant Current Controllers. *IEEE Transactions on Power Electronics*, 2015. 30(8): p. 4244-4254.
[3] H. Nian, C. Wu and P. Cheng, Direct Resonant Control Strategy for Torque Ripple Mitigation of DFIG Connected to DC Link through Diode Rectifier on Stator. *IEEE Transactions on Power Electronics*, 2017. 32(9): p. 6936-6945.
[4] C. Wu and H. Nian, An Improved Repetitive Control of DFIG-DC System for Torque Ripple Suppression. *IEEE Transactions on Power Electronics*, 2018. 33(9): p. 7634-7644.

Robust control of DFIG-DC system

Why field orientated control?
Is vector control indispensable? ⇒ **Power-current coupling control**

Mathematical model of DFIG-DC system

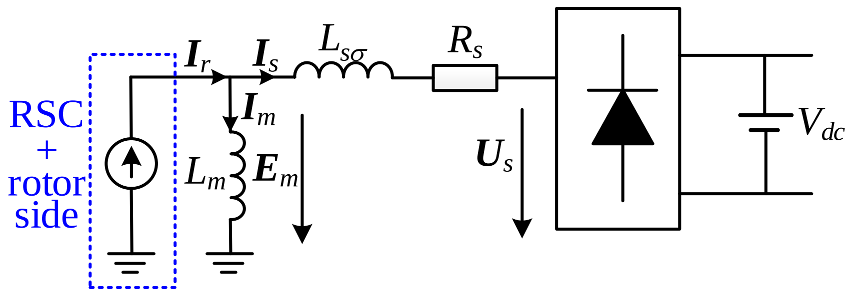

Equivalent circuit of the DFIG-DC system

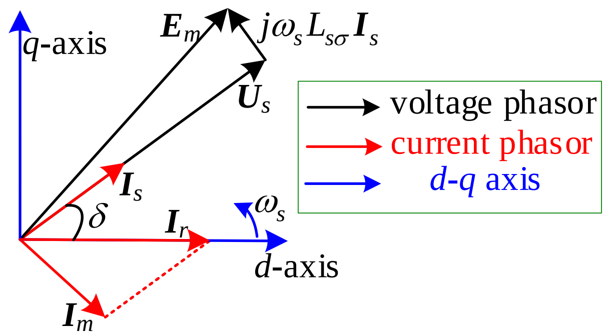

Phasor diagram of DFIG

Stator power $$P_s = \mathrm{Re}\left(\boldsymbol{U}_s \boldsymbol{I}_s\right) = \left|\boldsymbol{U}_s\right|\left|\boldsymbol{I}_s\right| = \frac{L_m}{L_s}\left|\boldsymbol{U}_s\right|\left|\boldsymbol{I}_r\right|\cos\delta$$

Unique characteristics

- The stator power is proportional with the magnitude of rotor current
- The stator power can also be controlled by the angle

Robust control methods

- Stator power-rotor current magnitude control method
- Stator power-rotor current angle control method

Robust control of DFIG-DC system

Power-magnitude control of DFIG-DC system without stator side sensors

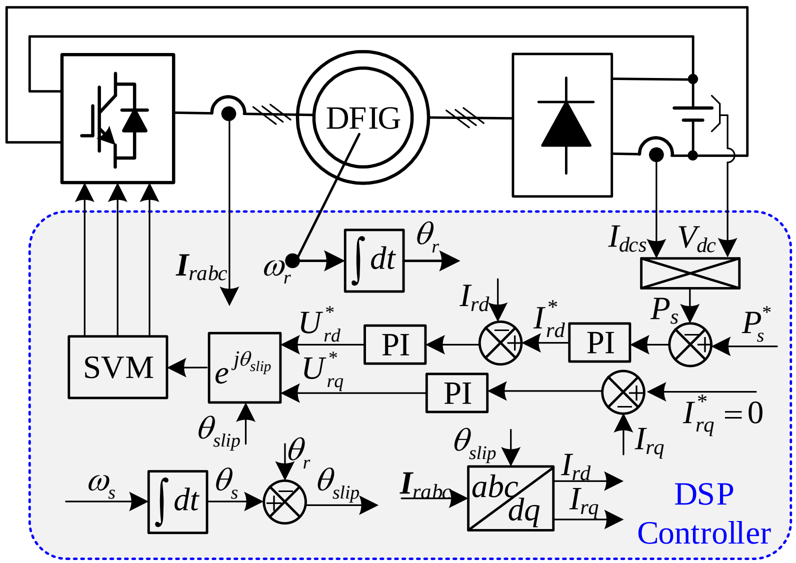

Power-magnitude control scheme of RSC

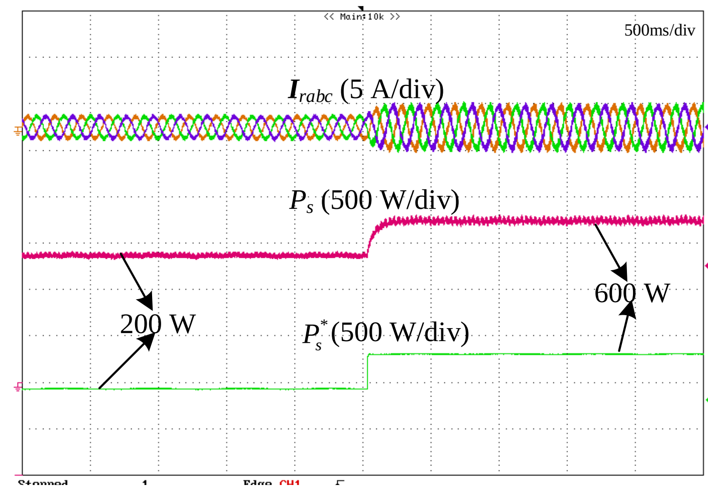

Step response of stator power change

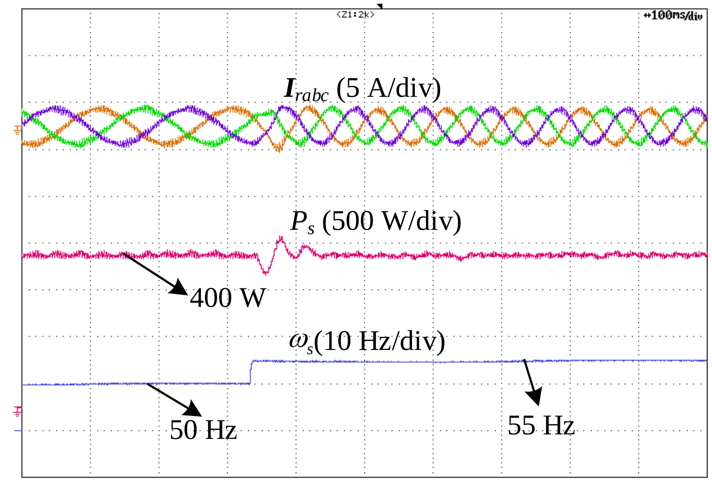

Step response of stator frequency change

Control Methods

- Power-current magnitude control method
- Stator frequency is flexibly given
- Without stator side sensors

C. Wu, Y. Jiao, H. Nian, F. Blaabjerg, "A Simplified Stator Frequency and Power Control Method of DFIG-DC System Without Stator Voltage and Current Sensors", *IEEE Trans. on Power Electron.*, vol. 35, no. 6, pp. 5562-5566, Jun. 2020.

Robust control of DFIG-DC system

Power-angle control of DFIG-DC system without stator side sensors

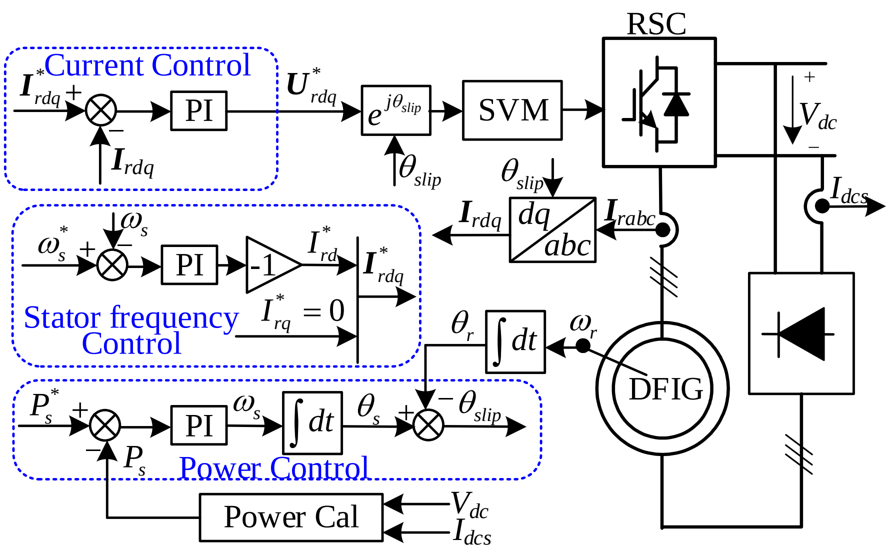

Power-angle control scheme of RSC

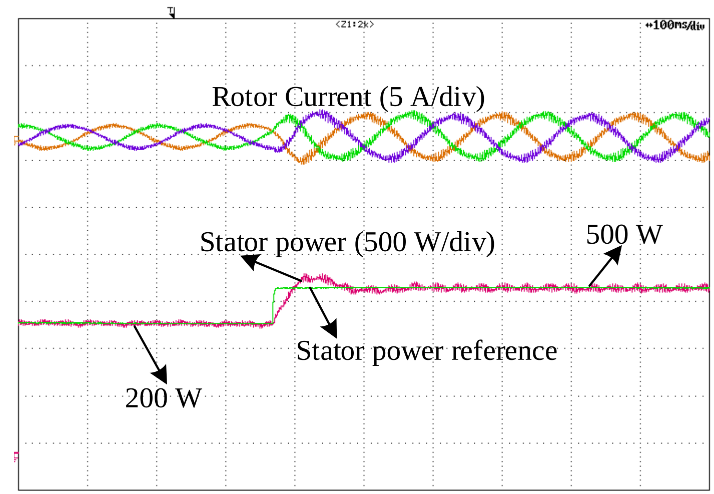

Step response of stator power change

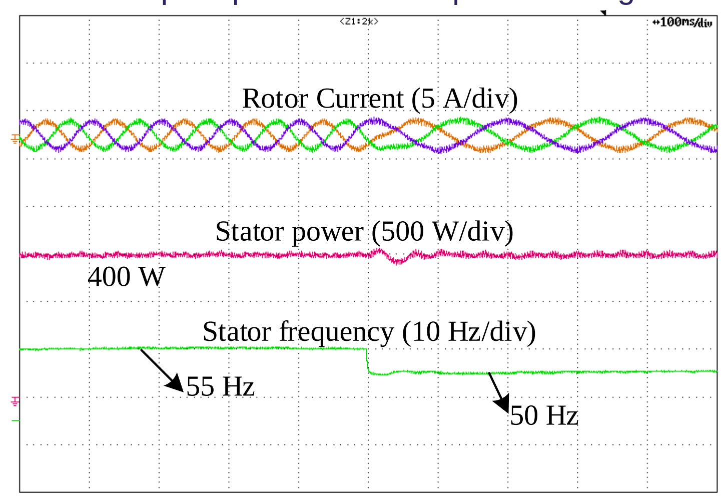

Step response of stator frequency change

Control Methods

- Power-current angle control method
- Acquirng stator frequency through power loop
- Without stator side sensors

C. Wu, P. Cheng, H. Nian and F. Blaabjerg, "Rotor Current Oriented Control Method of DFIG-DC System Without Stator Side Sensors," in IEEE Transactions on Industrial Electronics, vol. 67, no. 11, pp. 9958-9962, Nov. 2020.

Robust control of DFIG-DC system

◆ Unified power control of DFIG-DC system

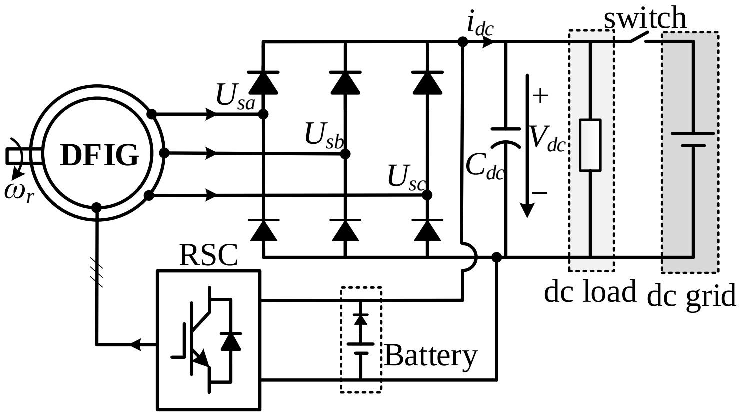

DFIG connected to a DC link using diode rectifier

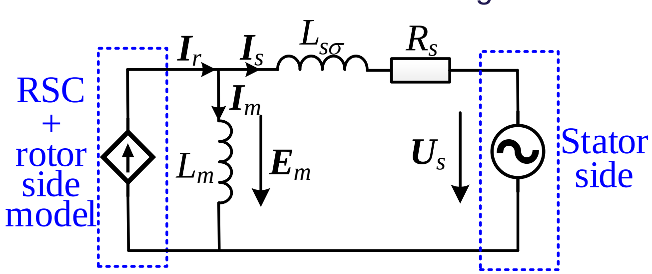

Steady-state equivalent circuit of the DFIG-DC system

❖ Two operation modes

- Grid-connected mode

  Objective: MPPT control

- Stand-alone mode

  Objective: DC voltage control

$$P_s = \mathrm{Re}\left(U_s I_s\right) = \frac{L_m}{L_s}\left|U_s\right|\left|I_r\right|\cos\delta$$

$$V_{dc} = \frac{\pi}{2}\left|U_s\right| = \frac{\pi}{2}\omega_s L_m\left|I_r\right|\sin\delta$$

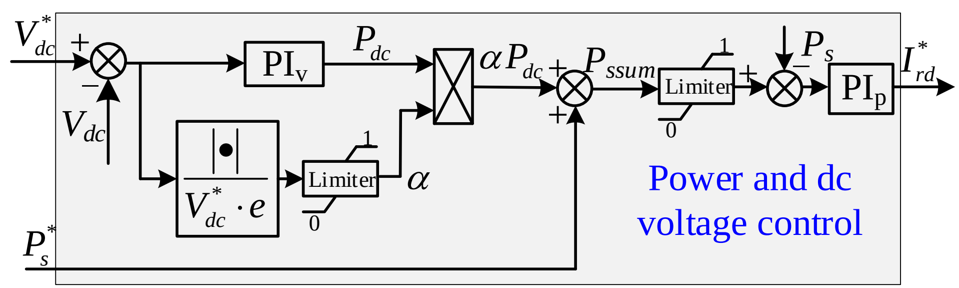

The detailed block diagram of power and dc voltage control

Unified power reference

$$P_{ssum} = \alpha P_{dc} + P_s^* = \alpha \frac{k_{pv}s + k_{iv}}{s}\left(V_{dc}^* - V_{dc}\right) + P_s^*$$

Coefficient related to dc voltage error

$$\alpha = \frac{\left|V_{dc}^* - V_{dc}\right|}{V_{dc}^* \cdot e}$$

Robust control of DFIG-DC system

◆ Unified power control of DFIG-DC system

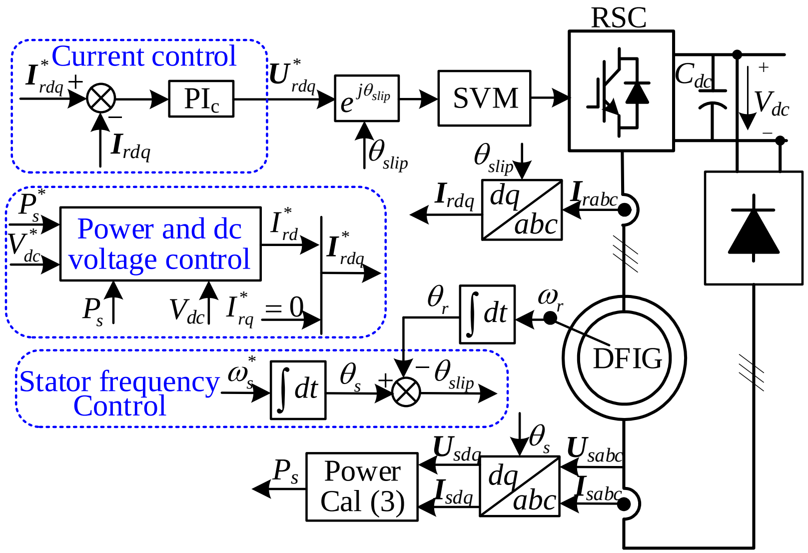

Unified power control method of RSC

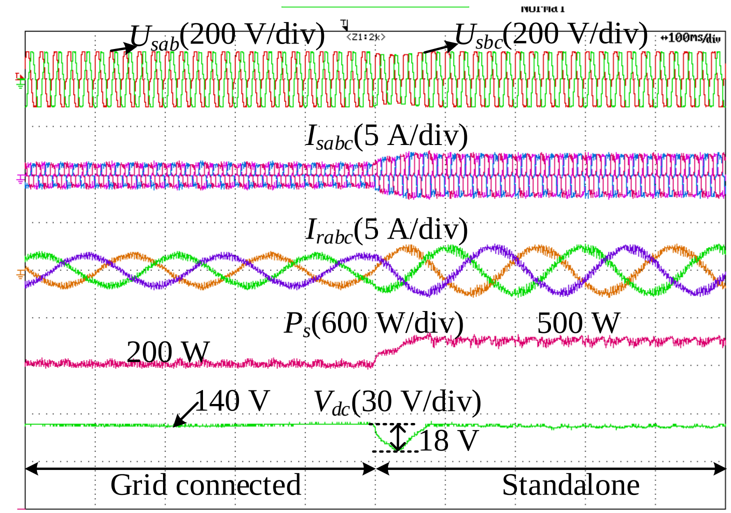

Experimental results of DFIG from grid connected to standalone mode

Control Methods

- Dc voltage and stator power can both be controlled through the unified power.
- Stator frequency is flexibly given.
- Both in grid-connected and stand-alone mode .

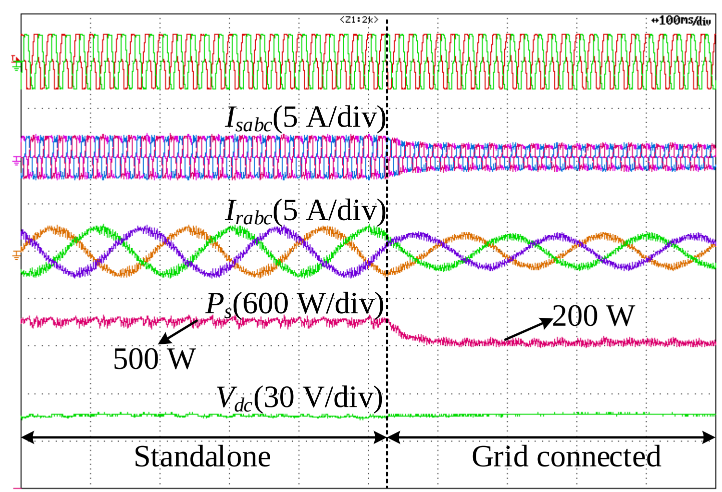

Experimental results of DFIG from standalone to grid connected mode

C. Wu, P. Cheng, Y. Ye and F. Blaabjerg, "A Unified Power Control Method for Standalone and Grid-Connected DFIG-DC System," in IEEE Transactions on Power Electronics, vol. 35, no. 12, pp. 12663-12667, Dec. 2020.

Robust control of DFIG-DC system

◆ Conclusion

- ❑ Due to the stator side diode bridge, the stator voltage and current are almost in same phase, which indicates that there is naturally no reactive power in the stator side of DFIG.
- ❑ The power-magnitude and power-angle control methods are simple and effective, which can avoid the using of stator side sensors.
- ❑ This sensorless control method can improve the robustness and reliability of DFIG-DC system.
- ❑ The unified power control strategy can make the DFIG-DC system works well in both grid-connected mode and stand-alone mode.

References

1. Chao Wu, Dao Zhou and Frede Blaabjerg, “Direct Power Magnitude Control of DFIG-DC System Without Orientation Control”, IEEE Trans. on Ind. Electron., vol. 68, no. 2, pp. 1365-1373, Feb. 2021.
2. Heng Nian, Chao Wu, Peng Cheng, “Direct Resonant Control Strategy for Torque Ripple Mitigation of DFIG Connected to DC Link through Diode Rectifier on Stator”, IEEE Trans. on Power Electron., vol. 32, no. 9, pp. 6936-6945, Sep. 2017.
3. Chao Wu, Dao Zhou, Peng Cheng, Frede Blaabjerg, “A Novel Power-Angle Control Method of DFIG-DC System Based on Regulating Air Gap Flux Vector”, IEEE Trans. on Power Electron., vol. 36, no. 1, pp. 513-521, Jan. 2021.
4. Chao Wu, Peng Cheng, Frede Blaabjerg, “A Unified Power Control Method for Standalone and Grid Connected DFIG-DC System”, IEEE Trans. on Power Electron., vol. 35, no. 12, pp. 12663-12667, Dec. 2020.
5. Chao Wu, Yingzong jiao, Heng Nian, Frede Blaabjerg, “A Simplified Stator Frequency and Power Control Method of DFIG-DC System Without Stator Voltage and Current Sensors”, IEEE Trans. on Power Electron., vol. 35, no. 6, pp. 5562-5566, Jun. 2020.
6. Chao Wu, Peng Cheng, Heng Nian, Frede Blaabjerg. “Rotor Current Oriented Control Method of DFIG-DC System Without Stator Side Sensors”, IEEE Trans. on Ind. Electron., vol. 67, no. 11, pp. 9958-9962, Nov. 2020.
7. Chao Wu, Heng Nian, “Improved direct resonant control for suppressing torque ripple and reducing harmonic current losses of DFIG-DC system”, IEEE Trans. on Power Electron., vol. 34, no.9, pp. 8739-8748, Sep. 2019.
8. Chao Wu, Heng Nian, Bo Pang, Peng Cheng, “Adaptive Repetitive Control of DFIG-DC System Considering Stator Frequency Variation”, IEEE Trans. on Power Electron., vol. 34, no. 4, pp. 3302-3312, Apr. 2019.
9. Chao Wu, Heng Nian, “An Improved Repetitive Control of DFIG-DC System for Torque Ripple Suppression”, IEEE Trans. on Power Electron., vol. 33, no.9, pp. 7634-7644, Sep. 2018.
10. Chao Wu, Heng Nian. “Sinusoidal current operation of DFIG-DC system without stator voltage sensors”, IEEE Trans. on Ind. Electron., vol. 65, no.8, pp. 6250-6258, Aug. 2018.
11. Chao Wu, Heng Nian, “Stator Harmonic Currents Suppression for DFIG Based on Feed-Forward Regulator Under Distorted Grid Voltage”, IEEE Trans. on Power Electron., vol. 33, no. 2, pp. 1211-1224, Feb. 2018

Thank you for your attention!

Questions & Comments ?

Chao Wu

Email: cwu@et.aau.dk